DIGITAL TWIN ANALYTICS; LIFE-CYCLE MODELING OF STRUCTURES FOR PRESENT AND FUTURE CONDITION ASSESSMENT

by

Sara Mohamadi
A Dissertation
Submitted to the
Graduate Faculty
of
George Mason University
in Partial Fulfillment of
The Requirements for the Degree
of
Doctor of Philosophy
Civil Environment and Infrastructure Engineering

Committee:

_____	Dr. David Lattanzi, Dissertation Director
_____	Dr. Girum Urgessa, Committee Member
_____	Dr. Behzad Esmaeili, Committee Member
_____	Dr. Paulo Costa, Committee Member
_____	Dr. Sam Salem, Department Chair
_____	Dr. Kenneth S. Ball, Dean, Volgenau School of Engineering
Date:_____	Spring Semester 2021 George Mason University Fairfax, VA

DIGITAL TWIN ANALYTICS; LIFE-CYCLE MODELING OF STRUCTURES FOR PRESENT AND FUTURE CONDITION ASSESSMENT

A Dissertation submitted in partial fulfillment of the requirements for the degree of Doctor of Philosophy at George Mason University

by

Sara Mohamadi
Master of Science
George Mason university, 2016
Bachelor of Science
University of Mazandaran, 2009

Director: David Lattanzi, Associate Professor
Department of Civil, Environmental and Infrastructure Engineering

Spring Semester 2021
George Mason University
Fairfax, VA

DEDICATION

To

My best friend and dear husband, Yashar

& my lovely daughter, Neelye.

ACKNOWLEDGEMENTS

First and foremost, I would like to express my respect and appreciation to my dissertation adviser, Prof. David Lattanzi, for his guidance, support, patience, understanding, and knowledge. He has set an example of excellence as a researcher, mentor, instructor, and role model.

I would also like to express my gratitude to my doctoral dissertation committee members, Prof. Paulo Costa, Prof. Girum Urgessa, and Prof. Behzad Esmaeili for their priceless technical guidance and feedback.

I would also like to acknowledge and thank professors, staff, and students at the Sid and Reva Dewberry Department of Civil, Environmental, and Infrastructure Engineering for all they did for me during these years. I would like to specifically acknowledge all the members of the Lattanzi Research Group (LRG) for their support and friendship.

TABLE OF CONTENTS

LIST OF TABLES

LIST OF FIGURES

ABSTRACT

DIGITAL TWIN ANALYTICS; LIFE-CYCLE MODELING OF STRUCTURES FOR PRESENT AND FUTURE CONDITION ASSESSMENT

Sara Mohamadi, Ph.D.

George Mason University, 2021

Dissertation Director: Dr. David Lattanzi

The evaluation of structural systems is a necessary task in order to maintain the integrity of structures over time. These assessments are designed to detect damages of structures and ideally help inspectors to estimate the remaining life of structures. Current methodologies for monitoring structural systems, while providing useful information about the current state of the structures, are limited in the monitoring of structural defects over time and linking them to predictive simulation. A digital twin (DT), as defined here, integrates monitoring observations and geometric survey data with numerical simulations in order to provide depictions of life-cycle performance. The objective of this research is to propose an integrated framework that supports digital twin modeling of structures. Two main aspects of DT model are studied in this dissertation. First, tracking the evolution of remotely sensed defects, along with linking them to numerical simulation is studied in order to provide structural performance characteristics over time. Second, integrating

survey information from various data sources is investigated. In the first section, remotely sensed defects are parametrized using feature extraction techniques, and a stochastic dynamic model is then adapted to features to model their evolution over time. Then the future state of defects is predicted through the dynamic model. Later, the Finite Element Model of structural components is linked to the future state of defect for predictive simulation. In the second section, results from multiple non-destructive evaluation (NDE) techniques are integrated and used as input in a machine learning classifier to provide a feature-level data fusion of NDE measurements. This integrated framework supporting the life-cycle modeling of structural defects provides more reliable forecasting capabilities and a more comprehensive understanding of structural performance, which improves decision-making processes for asset management. The accuracy, effectiveness, adaptability, and feasibility of the presented framework was evaluated with sets of synthetic and laboratory scale data.

CHAPTER ONE: INTRODUCTION

Motivation

Structural systems evolve over time and permanent damages can occur. These changes could be due to changes in material property, geometry shape and boundary conditions, all of which affect the performance of structural systems and possibly cause system failure. Unpredicted structural failure can lead to catastrophic, economic, and human loss of life. Structures must therefore undergo assessments to evaluate their condition and integrity. There have been significant studies in recent decades on improving Structural Health Monitoring (SHM) techniques and methods (Sartor Richard R., Culmo Michael P., and DeWolf John T. 1999; Shull 2002). The focus of these studies was on non-destructive structural changes and damage identification, as well as on the reliability and safety of monitored structures (Catbas, Gokce, and Gul 2012; Sohn et al. 2002). These assessments are based either on visual inspection with the combination of advanced sensors to identify global changes in structural properties (Comisu et al. 2017; Klikowicz, Salamak, and Poprawa 2016) or on advanced non-destructive evaluation (NDE) techniques to identify local damages in structures (Clifton and Carino 1982; Hellier 2001; Chang Peter C. and Liu S. Chi 2003). These NDE methods are becoming more popular among researchers and engineers for the rapid evaluation of structures through the development of software technologies (Verma, Bhadauria, and Akhtar 2013). In addition to immediate

structural evaluation, these assessments are designed to detect damage in structures and provide information on their safety and reliability, and ideally help engineers to estimate the remaining life of structures. In the current practices, engineers collect a lot of data during the structural life cycle. The diversity of data collected through these assessments is not easily correlated and there are uncertainties about damage identification or quantification in the NDE results. Most survey data are not structured in a way that explains the structure's life cycle performance and the data sources are usually not consistent during the structure's life cycle. As a result, it is challenging to quantitatively evaluate how survey information evolves over time and perform predictive analysis regarding the future condition of the structure. Developments in life-cycle modeling would provide more accurate and robust information about the condition of structures. This would eventually lead to improved decision-making processes for system asset management, which has apparent safety and financial advantages.

In a variety of fields, the Digital Twin (DT) concept has been studied as means of addressing these challenges, especially in the field of aerospace engineering(Glaessgen and Stargel n.d.; Cerrone et al. 2014; Tuegel et al. 2011). A digital twin of a structure, as defined here, is a virtual model of a structure that incorporates monitoring observations and geometric inspection data with numerical simulations to characterize life-cycle performance. Through digital twin modeling, observed damage patterns such as section loss and cracking could be quantitatively parameterized, so that their evolution can be tracked over time and future states can be predicted. This approach not only provides an

assessment of the current state of the structure, but also evaluates its integrity and improves resilience in the future.

The aim of this research is to develop an integrated framework to support the DT modeling of structures. This dissertation considers two aspects of DT systems: 1) dynamic modeling of defects and predictive finite element modeling (FEM) and 2) fusion of multiple data sources. These two aspects of modeling are simplified and shown in Figure 1.1. First life cycle modeling of remotely sensed defects, which are presented as point cloud data, is studied. Point cloud data that are geometric representation of defects are used because they can serve as a consistent record of the state of a structure at a given inspection interval and provide a basis for finite element analysis, among other uses (Khaloo and Lattanzi 2019; Ghahremani Kasra et al. 2018). These defects are parametrized using feature extraction techniques, and then stochastic dynamic models are adapted to model their evolution over time. The future state of defects is then predicted through the dynamic model. Consequently, a predictive analysis with regard to the future condition of the structure can be carried out by linking the evolution of defects to a numerical simulation, which ultimately helps to provide a complete representation of structural performance and integrity over time.

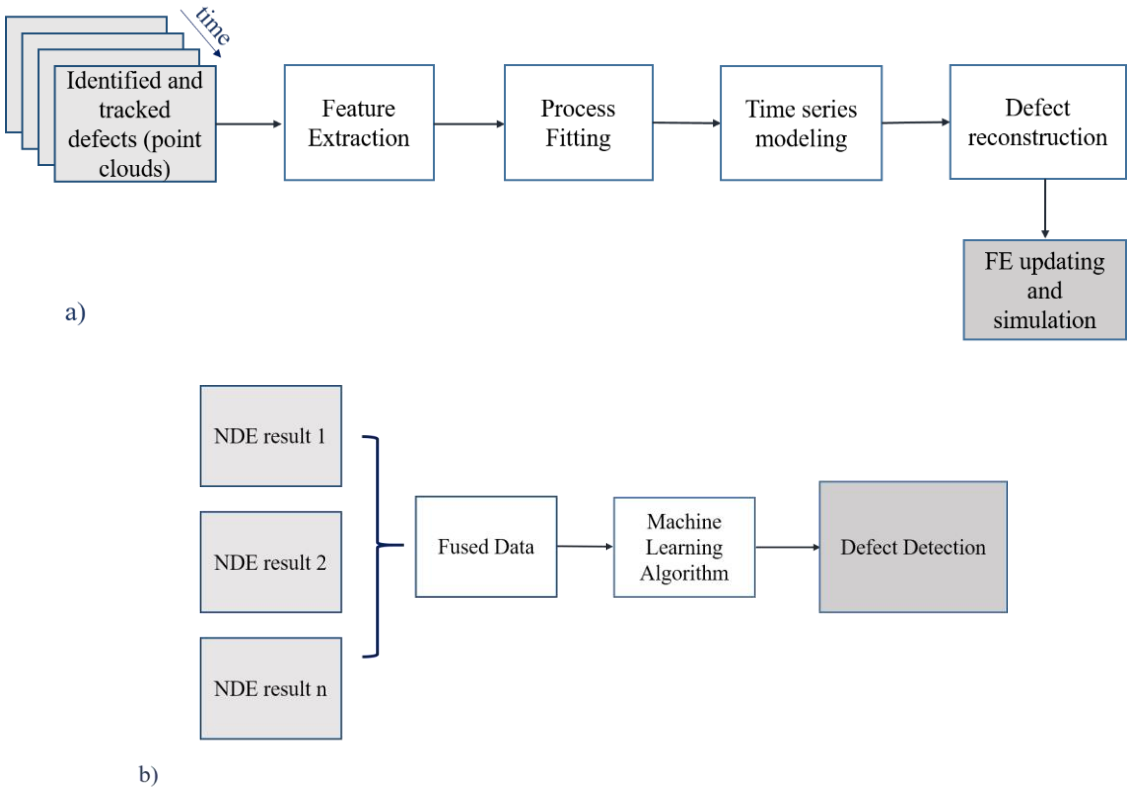

Figure 1.1. The proposed framework for DT modeling: a) life cycle modeling of defect and predictive FE modeling and b) fusion of multiple NDE results.

In the second part, fusion of multiple NDE results are studied. Results from various advanced NDE techniques are fused first to make a combined result, and then the fused results are an input to machine learning algorithm for defect detection.

There are many potential advantages in this integrated framework that support DT modeling. First, it provides engineers with an intuitive and consistent representation of survey information over the life cycle of structures. Remotely sensed defects are numerically parameterized, their evolution are modeled and linked to the remaining structural life cycle. Tracking the evolution of damage in structural performance results in

more reliable forecasting capabilities and a more complete understanding of structural performance, compared to existing NDE techniques, which often do not quantify damage evolution over time. And, by linking the DT model to numerical structural models, the effect of current damage on future conditions and capabilities can be better understood. In addition, fusion of multiple data sources can lead to more accurate defect detection. Features from multiple data sources are extracted and integrated into a combined data set. This combined data set is then an input to machine learning classifier to perform feature fusion and defect detection. Overall, data fusion has a measurable and positive impact on defect detection performance for both corrosion assessment and generalized defect detection in digital twin systems.

Dissertation Organization

Each chapter starts with an introduction and contains some common sections: literature review and research gap, proposed algorithms and methodology, experiments, results and conclusions. It is worth mentioning that the majority of the dissertation contents were peer-reviewed and published in the form of technical journal papers before dissertation submission (Mohamadi and Lattanzi 2019; Mohamadi, Lattanzi, and Azari 2020). The content is as follows:

Chapter Two

Chapter Two begins with a discussion about the current state of structural systems monitoring. It provides a background to modern approaches for evaluating structural integrity and introduces some of the limitations and unaddressed questions in this field. It

presents the research overview and the proposed approach to address the introduced limitations. It also provides the authors contribution to this field.

Chapter Three

Chapter three is a self-contained paper which presents a novel methodology to parameterize remotely sensed defects and model the evolution of such defects over their life cycle. The convex hull parametrization is proposed for characterization of geometrical defects and time-series models are applied for modeling purpose. Through modeling the evolution of defects, their future state is forecasted. The accuracy, completeness, adaptability, and feasibility of the developed method were thoroughly tested through synthetic and laboratory experimental data.

Chapter Four

Chapter four is the draft of self-contained paper which introduces finite element model updating of structural components with regard to their future state of defects. This chapter specifically studies finite element model updating of structural components with regard to their existing crack under fatigue load. An existing crack is identified and its propagation under fatigue load is modeled using the proposed approach in chapter three. Then the future state of crack extension is predicted. The predicted crack extension is then linked to the solid model of component and the numerical model is updated consequently. A core component of the methodology is an approach to evaluate performance of the structural component in the future through linking its finite element model to the crack's evolution. The developed methodology was experimentally validated on experimental fatigue test data and may expand to real-world infrastructure systems in the future.

Chapter Five

Chapter five is a self-contained paper which provides a data fusion of multiple NDE data sources. A wavelet-based approach is used to extract statistically relevant features from NDE Waveforms, and a non-parametric machine learning approach is applied to the fusion of NDE data features. Also, a novel visualization schema is proposed for representing the fused results and measurement uncertainty. The accuracy, adaptability, and feasibility of the developed method were tested using a laboratory experimental dataset from FHWA.

Chapter Six

Chapter six summarizes and outlines the findings and results of the developed frameworks explained. Contributions to the body of knowledge are also identified. Additionally, this chapter provides limitations of the overall research and potential research avenues for future work.

CHAPTER TWO: BACKGROUND AND RESEARCH OVERVIEW

Current Civil Structures Monitoring and Evaluation Challenges

In order to maintain the safety and integrity of structures, it is necessary to develop a reliable and effective non-destructive damage identification techniques. This fact has led researchers to investigate a wide range of NDE techniques and to develop methodologies for evaluating their results in a way that supports decision-making strategies on the integrity of structures. Currently, a wide range of NDE techniques are used for in-situ evaluation of structures and damage identification. Some of these techniques (e.g. sonic testing and magnetic particles) require in field assessments or cannot provide quantitative results (Ryan et al. 2012).

Beside those techniques, survey data can be stored for later analysis and interpretation (e.g. acoustic wave emission, ultrasonic testing). In addition to the development of NDE techniques, there is a growing number of studies on the use of geospatial imaging technologies such as LiDAR or photogrammetry to provide new sources of survey information. These remote sensing technologies have enabled the generation of highly accurate 3D point cloud models, which can be used to measure defects (Khaloo and Lattanzi 2019; Jafari, Khaloo, and Lattanzi 2016; Cabaleiro et al. 2014; Colomina and Molina 2014). Regardless of the monitoring technique, these data must be interpreted for immediate evaluation, characterizing structural defects and eventually helping engineers to estimate the structure's remaining life. ***While current practices***

provide safe operating conditions and immediate assessment of structures, they have a limitation in contributing to the long-term monitoring of structures.

Using state-of-the-art NDE methods, crack can be identified and located using vibration-based methods (Fan and Qiao 2011; Doebling et al. 1996; Gudmundson 1982), large cracks and voids in concrete and corrosion and cracks in steel can be identified and located using ultrasonic tests(Sharma Shruti and Mukherjee Abhijit 2011; Aranguren et al. 2013; Rens Kevin L. and Greimann Lowell F. 1997). Acoustic wave techniques can also be used to identify and locate imperfections such as the initiation of crack and the growth rate of fatigue cracks and corrosion (Sagar and Prasad 2012), to classify crack modes in concrete(Aggelis 2011; Ohno and Ohtsu 2010; Ohtsu et al. 2002) and to quantify the severity of damage(Zaki et al. 2015; Yoon Dong-Jin, Weiss W. Jason, and Shah Surendra P. 2000; Behnia, Chai, and Shiotani 2014). Furthermore, it is possible to detect and locate hidden and subsurface defects using radiographic tests(Nassr Amr A. and El-Dakhakhni Wael W. 2009; McCann and Forde 2001) and electromechanical method such as ground penetration radar(Chen Dar Hao and Wimsatt Andrew 2010). Finally, using remote sensing technologies (i.e. photogrammetry), crack identification and localization(Tsao Stephen et al. 1994; Kaseko Mohamed S., Lo Zhen-Ping, and Ritchie Stephen G. 1994), detected crack quantification(Jahanshahi et al. 2013),(Khaloo and Lattanzi 2019) and surface corrosion detection(Siegel and Gunatilake 1998) are feasible. ***While these studies have demonstrated the ability to identify damages and to assess the condition of structures, they are limited in their long-term contribution to structural assessment. They focus mainly on improving the accuracy of defect measurement from a single survey***

technique, rather than linking it to complete system assessment. To date, efforts have not been made to model these measured changes/defects as time-dependent phenomena.

Another limitation is that there is usually uncertainty in the detection of damage. For example, cracks detected using inspection videos are usually based on one single images (video frame). The detection of cracks in these videos is challenging because there are a large number of small cracks with low contrast and different brightness on the surfaces, and if there is no other data source supporting the existence of cracks in the structure, the result may be inaccurate due to falsely detected cracks (F.-C. Chen et al. 2017). Or for the evaluation of concrete strength by ultrasonic pulse, which is the most commonly used technique, there are intrinsic factors that can interfere with the NDE test results(Jain et al. 2013) such as the concrete mixture of four materials. This complexity highly irregularizes the behavior of ultrasonic waves in concrete, which in turn hinders non-destructive testing.

To address this, recent studies of data fusion techniques for NDE results have been conducted as a tool to reduce uncertainty. Multisource data fusion, which is the integration of the data from various survey sources, can be used to provide a better interpretation of the observed information by reducing the uncertainty present in individual source data(David Lee Hall and McMullen 2004; Klein 1999). Different techniques such as Bayesian probabilistic approaches, Dempster–Shafer (DS) evidence approach and fuzzy reasoning have been most commonly applied to SHM (R.-T. Wu and Jahanshahi 2018). These methods have been used for damage identification, quantification, and system response estimates (D. L. Hall and Llinas 1997; Chair and Varshney 1986; Faouzi, Leung,

and Kurian 2011; Liu et al. 1999; Vanik M. W., Beck J. L., and Au S. K. 2000). For example, a recursive Bayesian framework was used to update the parameters of a crack growth model, as well as the probability distribution of the crack size and crack growth rate (Rabiei and Modarres 2013), and neural network and fuzzy inference were combined to evaluate the structural condition of a cable bridge (Sun, Lee, and Lu 2016). ***Most of these studies used data fusion techniques to investigate whether the captured changes in structures parameters reflect the existence of damage in the structure rather than its application in damage quantification. To the best of the author's knowledge, no effort has been made to integrate the dynamics of survey information sources together to support the modeling of defect evolution and to predict its future status.***

In addition, recent studies have linked survey observations to Finite Element (FE) simulation of structures. The FE model is important for parameter identification, damage detection and structural condition assessment (Hou, Jankowski, and Ou 2015). The theory and application of structural FE model updating have been studied (S. Zhang et al. 2013; W. Wang et al. 2011). The area known as model updating mainly involves updating components of element properties such as stiffness, mass and damping(KABE 1985; S. W. Smith and Beattie 1991) or correction of parameters such as geometry, material and boundary conditions (Modak, Kundra, and Nakra 2002; Q. W. Zhang, Chang, and Chang 2000; Ghahremani Kasra et al. 2018). ***These studies focus mainly on improving the accuracy of updated models, however, are limited in predictive analysis for future structural performance. With tracking defects evolution over time and updating the FE***

model with regard to future state of defects, the future condition of structure and its capability can be better understood.

As summary, the following challenges remain unaddressed:

- Tracking the evolution of geometric changes/defects over the life-cycles of structures
- Integrating different information sources to reduce their uncertainty
- Linking time-dependent survey observations to structural performance

The aim of this research is to develop a framework to support DT modeling of structures that includes life cycle modeling of defects over time and links time-dependent survey information to numerical simulation of structures. The life cycle dynamics of remotely sensed defects detected through photogrammetry techniques is modeled, various information sources are integrated using data fusion techniques to improve the accuracy and robustness of the results and their evolution can be tracked over time. Eventually, these times dependent survey information are linked to numerical simulation of the structure to perform predictive simulation to provide better understanding of structural performance. The following research questions are addressed to investigate the feasibility of the objectives of this research:

1. How to parameterize geometric defects in a way that illustrates their life-cycle dynamics?

2. How to use a stochastic model, such as an autoregressive model, to analyze local defects over time?

3. How to link survey observations to a numerical simulation for structure performance forecasting?

4. How to fuse different survey data to reduce the uncertainty of the DT model?

Answering questions 1 and 2 addressed the first mentioned limitation, which is tracking the evolution of geometric changes/defects over life-cycle of structure. These two questions were examined in chapter three of this dissertation. Question 3 focuses on the third limitation which is linking time-dependent survey observations to structural performance and was studied in chapter four of this document. Finally, question 4 addressed the second current limitation, which is integrating dynamic of survey information sources together to support the modeling of the evolution of defects was investigated in chapter four of this study.

Research Approach

To develop the proposed framework, the methodology presented here consists of several steps (Figure 2.1 & 2.2). For life cycle modeling of remote sensed defects, once they are identified, the defect must be parameterized in a way that can support dynamic modeling of defect evolution over time. Parameterization is done with feature extraction or feature engineering of the defect. Once parameterized, a dynamic model is adapted to the evolution of numerical features to understand the underlying process of evolution and estimate the future state of the defect through out-sample forecasting. In order to model the dynamics of defect evolution, multiple stages of the defect are identified and parameterized, and a process is fit for modeling the spatial movement of features over time. The future state of damage is forecasted using the adapted stochastic model. Then defect

shape is reconstructed by reversing the descriptor vector back to the original variables. Finally, the finite element model of the structure is updated based on the predicted damage shape and performance of the structure is investigated using finite element simulation. These steps are shown in Figure 2.1.

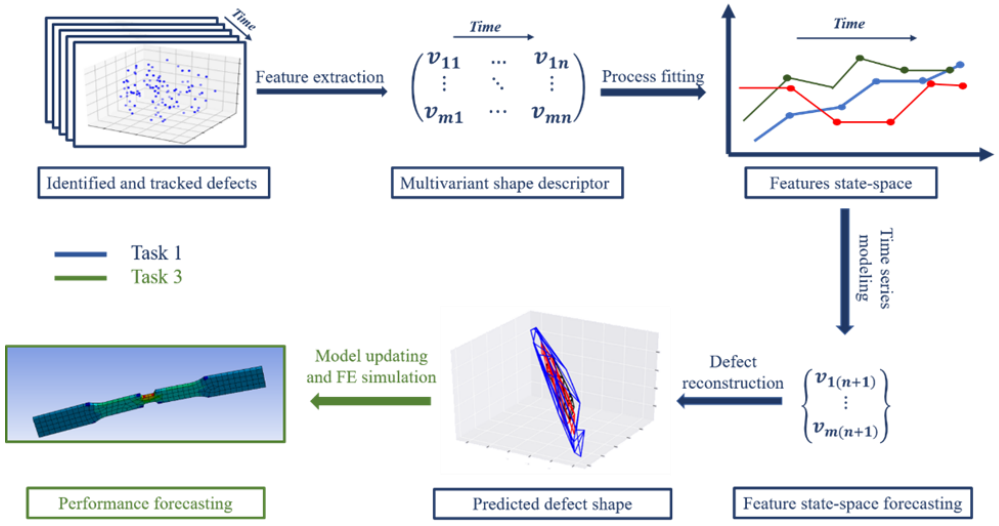

Figure 2.1. Schematic overview of the proposed methodology for life cycle modeling of remote sensed defects and predictive FEM (chapter three and four).

For the fusion of multiple NDE results, various survey information are integrated to make a single combined result and their evolution modeled and tracked over time. For feature-level fusion features, from NDE results are extracted and features are fused to a single feature vector. The probability score of damage in the structural component can be modeled as stochastic process and tracked over time and using time series modeling their

future states can be predicted. Later a dynamic model can be adapted to the evolution of detected defects over time and its future state are forecasted.

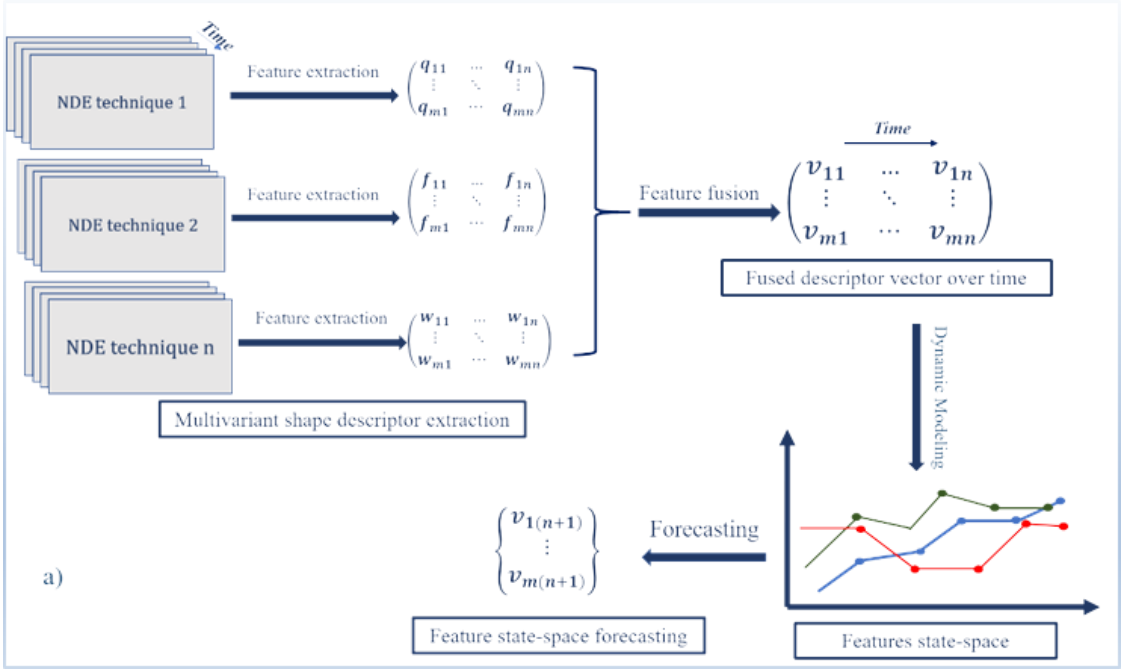

Figure 0.2. Feature-level data fusion (chapter five).

For the study of life cycle modeling of remotely sensed data (i.e. point cloud) in chapter three, synthetic point cloud data with different distribution characteristics representing different flaw shape were generated. Also, different evolution topologies were generated for each flaw shape. Furthermore, fatigue laboratory scale data was used for evaluation of crack propagation modeling. Later, this experimental data was used for evaluation of linking the evolution of time dependent defects to numerical simulation and

performing predictive analysis in chapter four. To investigate NDE data fusion in chapter five, experimental prototype system was created and tested, using FHWA experimental record as a data set.

CHAPTER THREE: LIFE-CYCLE MODELING OF STRUCTURAL DEFECTS VIA COMPUTATIONAL GEOMETRY AND TIME-SERIES FORECASTING

Introduction

This paper presents a method for modeling the time-history evolution of defects quantified through remote sensing technologies such as laser scanning, photogrammetry, or digital imaging. The goal is to expand the use of structural assessment information commonly collected during routine inspections and improve the structural life-cycle assessment process. Conventional structural assessments are typically based on visual inspections, embedded sensor systems, nondestructive evaluation (NDE) techniques, or some combination thereof (Sartor Richard R., Culmo Michael P., and DeWolf John T. 1999; Shull 2002; Comisu et al. 2017; Klikowicz, Salamak, and Poprawa 2016; Clifton and Carino 1982; Hellier 2001; Chang Peter C. and Liu S. Chi 2003). In almost all cases, the goal is the nondestructive detection and identification of structural performance changes and damage, as well as to assess the reliability and safety of monitored structures (Catbas, Gokce, and Gul 2012; Sohn et al. 2002). In addition to immediate structural evaluation, these assessments ideally help engineers to estimate the remaining life of structures. This is commonly done by reviewing historical performance records and holistically identifying temporal trends from the assessment data. However, most assessment data are not structured in a way that explicitly captures the life-cycle performance of a structure, and it is, therefore, challenging to quantitatively evaluate the evolution of inspection data over time and carry out a predictive analysis of the future state

of the structure. Life-cycle data modeling advancements could provide more precise and robust structural information, leading to better system asset management decision making, with apparent safety and financial benefits.

Prior Work

Damage identification, localization, and quantification were extensively studied in the last few decades. Using state-of-the-art NDE methods, cracks can be identified and located using vibration-based methods (Fan and Qiao 2011; Doebling et al. 1996; Gudmundson 1982). These damage identification techniques can be categorized into four main categories based on vibration characteristics: natural frequency-based, mode shape-based, mode shape curvature-based, and techniques using both mode shapes and frequencies. Fan et al. (Fan and Qiao 2011) presented a comprehensive review on these parameter-based methods and discussed their advantages and drawbacks. They also conducted a comparative study of five widely used damage detection algorithms for beam-type structures to assess the validity and effectiveness of the signal processing algorithms. While effective, these methods only focus on damage identification and localization, whereas the development of quantification techniques for damage magnitude is limited. Large cracks and voids in concrete, as well as corrosion and cracks in steel, can be identified and located using ultrasonic tests (Sharma Shruti and Mukherjee Abhijit 2011; Aranguren et al. 2013; Rens Kevin L. and Greimann Lowell F. 1997). Sharma et al. (Sharma Shruti and Mukherjee Abhijit 2011) used ultrasonic guided waves to monitor beams undergoing accelerated impressed current corrosion in the presence of two corrosion mechanism (chloride and oxide). It was found that ultrasonic can successfully detect

corrosion and identify the specific corrosion mechanism. Rens et al. (Rens Kevin L. and Greimann Lowell F. 1997) presented the concept and application of a new indirect inspection technique using ultrasonic spread-spectrum methods to test structural objects. Their laboratory findings show that this new method may be feasible for monitoring and evaluating existing large or complicated structural members. Acoustic wave techniques can also be used to identify and locate imperfections such as the initiation of crack and the growth rate of fatigue cracks and corrosion (Sagar and Prasad 2012), to classify crack modes in concrete (Aggelis 2011; Ohno and Ohtsu 2010; Ohtsu et al. 2002), and to quantify the severity of damage (Zaki et al. 2015; Behnia, Chai, and Shiotani 2014). Ohno and Ohtsu (Ohno and Ohtsu 2010) conducted two crack classification methods and showed that tensile and shear cracks can be distinguished using their criteria. Sagar and Prasad (Sagar and Prasad 2012) used acoustic emission parameterizations to classify the severity of damage into minor, intermediate, and severe damage categories. These prior works show that the acoustic emission techniques are often capable of detecting damage in their early stages, so that an early warning can be given to allow for repair work before a structural element is seriously damaged. Furthermore, it is possible to detect and localize hidden and subsurface defects using radiographic tests (Nassr Amr A. and El-Dakhakhni Wael W. 2009; McCann and Forde 2001) and electromechanical methods such as ground penetration radar (Chen Dar Hao and Wimsatt Andrew 2010). Chen et al. (Chen Dar Hao and Wimsatt Andrew 2010) used ground-coupled penetrating radar (GCPR) to characterize the subsurface conditions of three roadway pavements. The extents of the anomalies in the

horizontal and vertical direction were visible in GCPR images, and this study successfully demonstrated that GCPR is able to identify anomalies and voids.

While these prior studies created the capacity to identify and quantify damage to structures, the emphasis was on improving the accuracy of the detection and measurement of defects. To date, significant efforts were not made to model these measured changes/defects as time-dependent phenomena. Advancements in understanding and modeling of temporal defects will lead to improved decision-making capabilities, as well as expanded use of sensing and monitoring technologies. In addition to the development of NDE and structural health monitoring (SHM) techniques, there are increasing studies on the use of remote sensing and imaging technologies such as LiDAR or photogrammetry to provide new sources of inspection information. These remote sensing technologies provide high-resolution two-dimensional (2D) images or three-dimensional (3D) point cloud models of structures, and can capture the small-scale defects that are critical to understanding structural performance (Khaloo and Lattanzi 2019; Jafari, Khaloo, and Lattanzi 2016; Cabaleiro et al. 2014; Colomina and Molina 2014; Cabaleiro et al. 2015). In complement to the expanding use of these technologies, there are now a variety of methods for isolating and extracting defects from 2D or 3D images (Fleming, Holtmann-Rice, and Bülthoff 2011; Pal and Pal 1993), and advancements in deep machine learning methods portend future improvements (Kalogerakis et al. 2017; Su et al. 2015). A key advantage of these data sources is the direct link between quantified geometric changes and changes in the underlying mechanical performance that can be captured in finite element analysis, as evidenced by a variety of prior work (Ghahremani Kasra et al. 2018;

Fathi, Dai, and Lourakis 2015; Y. Yan, Guldur, and Hajjar 2017). While such capabilities provide valuable tools for structural assessment, they do not explicitly quantify life-cycle dynamics and forecasts of future defect conditions.

The question of the reliability of an engineered system led researchers to investigate the growth of defects such as fatigue cracks and corrosion over the life cycle of the systems. To study fatigue crack growth, model-based estimation methods such as Bayesian methods (Doucet 1998), extended Kalman filtering (Myötyri, Pulkkinen, and Simola 2006), and Monte Carlo sampling (Cadini, Zio, and Avram 2009) were used for quantification of the estimation uncertainty. For corrosion, theoretical models and simulation tools were developed for a better understanding of the nature of the pitting corrosion process, to allow prediction of the temporal evolution of maximum pit depth in corroding structures. In recent studies, stochastic approaches were also applied to simulate corrosion (Valor et al. 2007; Hong 1999; Caleyo et al. 2009; B. H. Zhou and Zhai 2010). All these efforts primarily focus on estimating the reliability of a system given estimates of the current state of a defect, rather than quantifying the future state of the defect in a way that provides support for predictive capacity assessments.

Contribution of This Research

As stated, a critical aspect of long-term structural monitoring is an understanding of detected defects as time-dependent phenomena, and this remains a major outstanding research need. Enhanced temporal modeling of defects would lead to the ability to predict future defect states and, thus, predict the future condition of the structure. While prior studies investigated the temporal behavior of defects from an empirical perspective (Mi,

Michaels, and Michaels 2006; Vu, Stewart, and Mullard 2005), efforts to quantify the dynamics of defect observations captured in remote sensing were, to date, limited. The main objective of this study is to address these limitations for life-cycle modeling of remotely sensed defects using a computational geometry approach to defect parametrization combined with time-series modeling.

Presented in this paper is a novel algorithm to model the life cycle of defects manifested as either 2D or 3D point clouds. Point cloud data are geometric representations of defects that can serve as a consistent record of the state of a structure at a given inspection interval and provide a basis for finite element analysis, among other uses (Khaloo and Lattanzi 2019; Ghahremani Kasra et al. 2018) This algorithm extracts latent features from these defect point clouds through computational geometry, fits a time-series process model to the evolution of those features, and uses a stochastic forecasting model to predict the future state of the defect. Consequently, a predictive analysis with regard to the future condition of the structure could be carried out by linking the modeled evolution of defects to a numerical simulation, ultimately helping to provide a complete representation of structural performance and integrity over time. This paper does not consider the predictive simulation aspect of this process, and the readers are referred to References (Ghahremani Kasra et al. 2018; Fathi, Dai, and Lourakis 2015; Fernandez, Bairán, and Marí 2016) for potential applications in this domain.

The remainder of this paper is structured as follows: firstly, the complete analytical methodology is presented. This is followed by a presentation of synthetic experimental results designed to illustrate the key behavioral aspects of the algorithm. This is followed

by experimental evaluation using fatigue crack propagation data. The paper concludes with an overall assessment of the algorithm and avenues for future work.

Methodology

The methodology presented here consists of several steps (Figure 3.1). Once a defect in the structure is detected, the defect must be parametrized in a way that can support a dynamic modeling of defect evolution over time. Parameterization is achieved with feature extraction from the point cloud through computational geometric modeling of the convex hull of the cloud, resulting in a combination of hull simplexes and vertices. These parameterizations are computed for multiple time steps over the life cycle of the structure. Once parameterized, a time-series model is fit to the sequence of parameterizations in order to capture the underlying process of evolution. This model fitting also enables the estimate the future state of the defect via out-sample forecasting. The defect shape is then reconstructed by reversing the parameterizations back to a geometric point set. While not considered in this work, the methodology presented here can then be used to update a finite element model of the structural component based on the predicted future defect topology, leading to predictive structural assessment.

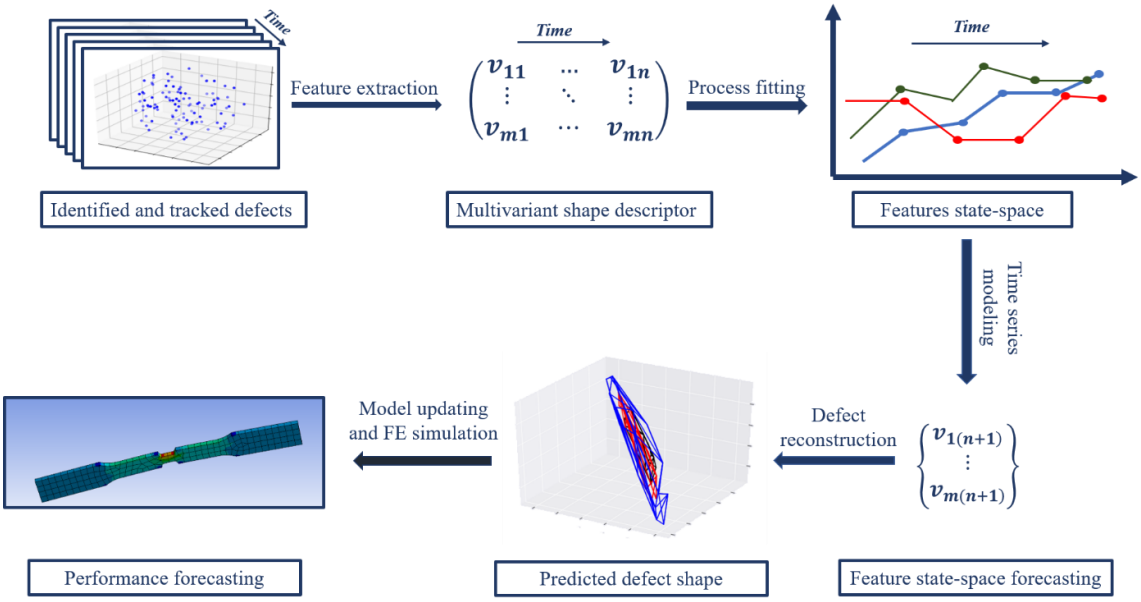

Figure 3.1. Schematic overview of the proposed methodology for life-cycle modeling of remotely sensed defects.

Defect Parameterization

Once a remotely sensed defect in a structural component is detected through computer vision (Ghahremani Kasra et al. 2018), the first step in the modeling process is to parameterize it so that a stochastic dynamic model can be reliably fit the extracted parameters, or a "feature vector" to track the defect evolution over time. The complex nature of point cloud data necessitates this low-dimensional parameterization, as tracking each individual point in a cloud would lead to an intractably high number of time-series model coefficients.

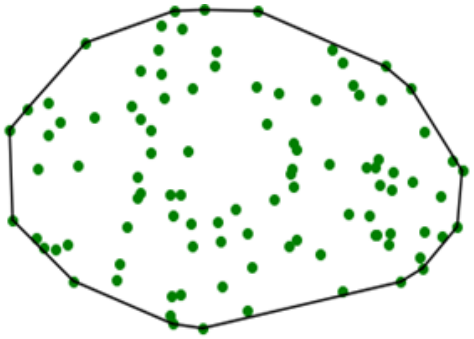

Figure 3.2. Convex hull of a point set in R^2.

Here, we propose that the feature extraction can be done using the concept of a geometric convex hull. The convex hull of a point set is a unique representation of a point set in R^n, defined as the smallest convex polygon that surrounds all points in the point set (Figure 3.2) (Berg 2008). In R^3 or higher-dimensional data spaces, the convex hull is similarly defined as the minimum convex polyhedron of the point set. It should be noted that, while this parameterization reduces the information complexity of the point cloud, the use of a convex hull serves to maintain the dimensionality of the underlying geometric object under observation. This is critical for reconstructing predicted defect states.

The determination of the convex hull is a geometric computation that is useful for many analyses and was successfully applied in domains such as image processing (Rosenfeld 1969) and pattern recognition (Akl and Toussaint 1979). Although a number of alternative feature extraction approaches were considered in this study (Daniels et al. 2007; Pauly, Keiser, and Gross 2003), hull parameterization was used because of its inherent advantages. The description of a defect in terms of its parameterized hull allows for

consistent temporal tracking for predictive purposes, while also reducing the dimension and complexity of the data implicitly. In addition, the convex hull concept can be extended to high-dimensional spaces to support the fusion of multiple sensors and data types, a longer-term goal of this work.

The convex hull of point cloud P is a uniquely defined convex polygon. A natural way to represent a generalized polygon is by listing its vertices in clockwise order, starting with an arbitrary starting point. As such, the problem to be solved is as follows: given a point set $P = \{p1, p2, \dots, pm\}$ in R^n, compute a list that contains those points from P that are the vertices of the convex hull, CH(P). To find those vertices, the algorithm sorts all points through a "divide and conquer" approach (Barber et al. 1996). The convex hull algorithm finds two points with maximum and minimum spatial coordinates in a single dimension and computes a line joining these two points. This line divides the whole set into two halves. For a given half it finds the points with a maximum distance from the dividing line, forming a triangle defined by minimum and maximum point distances. Those points inside the triangle are determined to not be part of convex hull. Then, these steps are iteratively repeated to search for points with maximum distance from the separating line, until there is no point left outside of the computed triangles. The points selected at this step constitutes the convex hull. The convex hull results in a vector containing the Cartesian coordinates of the hull vertices. This extracted vector of vertices is the numerical descriptor that is later fit to a stochastic process model (Figure 3.3).

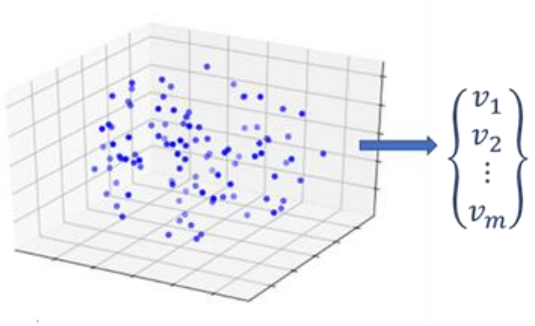

Figure 3.3. Feature extraction of convex hull vertices from a three-dimensional (3D) point cloud.

Hull Registration and Structuring for Time-Series Modeling

Once the hull vertices are extracted, the data must be structured and compiled for time history modeling. Firstly, point clouds from each time step are aligned and registered in a common reference frame. In this work, manual registration was sufficient; however, automatic registration approaches such as the iterative closest point (ICP) algorithm, or by determining the 2D or 3D homography between point sets via feature-based computer vision methods, may be necessary (Figure 3.4) (Besl and McKay 1992; Z. Zhang 1994). The registered defect point clouds are then parameterized using the convex hull computation, resulting in individual $2 \times n$ arrays of vertex coordinates. Each vertex at $t = t_1$ is then spatially tracked across the temporal sequence of vertex arrays. The vertices of a hull in stage 1 (hull_1) are matched to their nearest neighbor (NN) vertices in $hull_2$ and, likewise, those are matched to their NN vertices in hull3, and so on (Kleinberg 1997). The assumed movement of one of the vertices is shown in Figure 3.5. The nearest neighbor is found based on the smallest Euclidean distance between vertex sets. Equation (3.1) shows

the nearest neighbor search in $Hull(Q):\{q_1, q_2, .., q_n\}$ from $p_1 \in Hull(P):\{p_1, p_2, .., p_m\}$ in 2D space (*Hull*(*Q*) and *Hull*(*P*) are two consecutive descriptor vectors).

Equation 3.1

$$d(p_1, q_i) = \sqrt{(q_{ix} - p_{1x})^2 + (q_{iy} - p_{1y})^2}$$

At each time step, the NN of vertices in two time-steps are determined, and the change in magnitude and orientation between matched vertices is computed and compiled for the complete temporal sequence (Figure 3.5). This resulting dataset consists of the distances and orientations of vertex changes between subsequent hull stages throughout a time series. This dataset is illustrated for the identified and aligned multiple stage of a defect with a polygon shape in Figures 3.4 and 3.5.

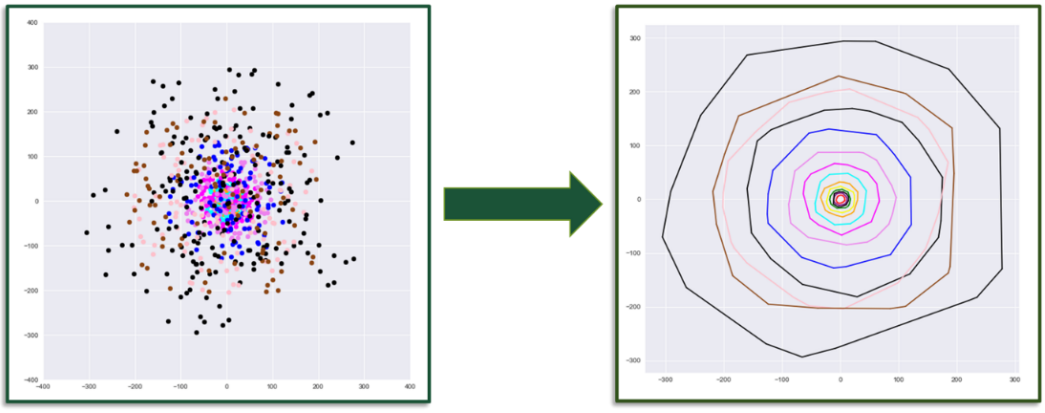

Figure 3.4. Aligning and registering hulls/clouds into a common spatial reference frame.

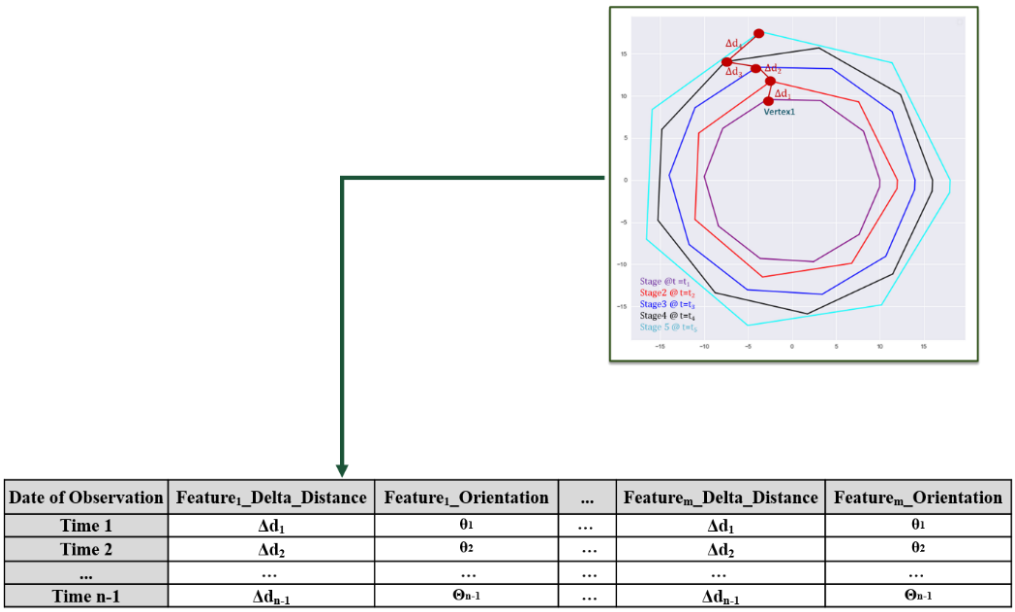

Date of Observation	$Feature_1$_Delta_Distance	$Feature_1$_Orientation	...	$Feature_m$_Delta_Distance	$Feature_m$_Orientation
Time 1	Δd_1	θ_1	…	Δd_1	θ_1
Time 2	Δd_2	θ_2	…	Δd_2	θ_2
...	…	…	…	…	…
Time n-1	Δd_{n-1}	Θ_{n-1}	…	Δd_{n-1}	Θ_{n-1}

Figure 3.5. Dataset representing the extracted vertices for a time-series evolution of an arbitrary polygonal defect.

Time-Series Modeling

The overall approach to time-series modeling is illustrated in Figure 3.6 and presented here. Once the dataset representing the evolution of defects is constructed, a stochastic model can be fit to the dataset to model the dynamics of defect evolution. Each column of this dataset is a time series that represents the evolution of each feature over time. Time-series forecasting is performed in order to capture the underlying long-term life-cycle trends in inspection data. The model can then be used to extrapolate the time series into the future. This modeling approach is particularly useful when the temporal behavior is stochastic, as opposed to understood deterministic evolution, and where the relationship between parameterization variables is not well understood (G. P. Zhang 2003).

For example, in the problem presented later in this paper, there is no knowledge available on the boundary conditions (i.e., applied load and support reactions) of the tested structural component, and there is no established deterministic model for the propagation of fatigue cracks.

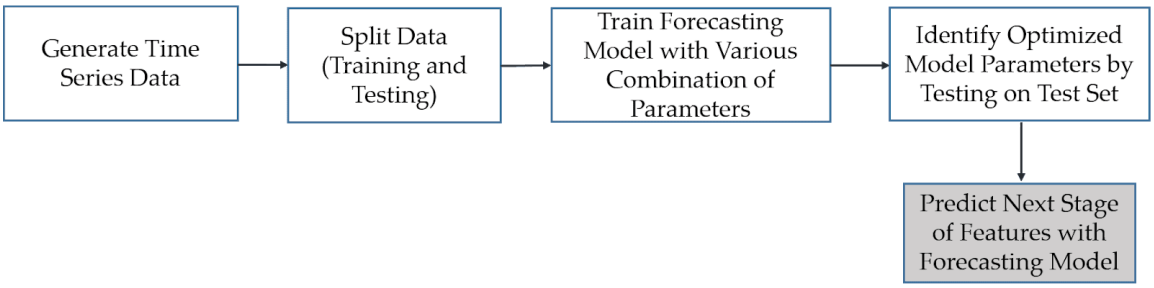

Figure 3.6. Overall time-series modeling methodology.

There are several common approaches to time-series modeling, including autoregression, moving average, exponential smoothing, autoregressive integrated moving average (ARIMA), and multivariate time-series vectorized autoregression (VAR). All of these models are linear, meaning that their predictions of the future values are constrained to be linear functions of past observations. Because of their effectiveness and ease of implementation, linear models are the main research focus for time-series modelers, as is the case in this study. Nonlinear modeling approaches such as recurrent neural networks were not considered here due to the limited training data available for observing defect evolution.

From the available time-series models, ARIMA and VAR models were selected for this study, and their performances were compared against each other. The autoregressive integrated moving average model (ARIMA) methodology developed by Box and Jenkins (George E. P. Box and Jenkins 1976) is able to handle non-stationary time series, in other words, scenarios where the statistical properties of the time series measurements do not remain constant over time. As such, it relaxes the requirement that time-series data be covariance-stationary prior to modeling, and it is well suited to the challenging variations in field conditions that impact remote sensing-based inspection practices (George Edward Pelham Box and Jenkins 1990). With ARIMA, the future value of a variable is assumed to be a linear function of several past observations and random errors. An ARIMA model contains two sub-processes (autoregressive, moving average process) and explicitly includes differencing in the formulation to account for the non-stationarity of the data. ARIMA gained enormous popularity in many areas, and research practice confirmed its power and flexibility (Pankratz 1983; McDowall 1980; Vandaele 1983). A generalized form of the ARIMA time-series model is shown in Equation (3.2).

Equation 3.2

$$Y_{(t)} = \phi_0 + \phi_1 \times Y_{(t-1)} + \phi_2 \times Y_{(t-2)} + \ldots + \phi_p \times Y_{(t-p)} + \varepsilon_t + \theta_1 \times \varepsilon_{(t-1)} - \theta_2 \times \varepsilon_{(t-2)} - \ldots - \theta_q \times \varepsilon_{(t-q)}$$

Where $Y_{(t)}$ and ε_t are the actual value and random error at time t, respectively. ϕ_i (i=1, 2, …, p) and θ_j (j=0,1,2, …, q) are the vectorized model coefficients. p and q are integers and often referred to as orders of the model.

As an alternative, vector autoregressive (VAR) models are effective for multivariant time-series data where there is a potential dependency between model variables. Therefore, unlike an ARIMA model that estimates the present value of a variable based only on its past values, VAR models consider past values of other variables as well. This model was used here to study the dependency and effect of the movement of convex hull vertices on other vertices. The VAR model (Lütkepohl 2005) was used for damage detection studies previously (Yao and Pakzad 2012; Figueiredo et al. 2010), but there was no effort to model the life cycle of a defect to date. The general form of the autoregressive model is shown in Equation (3.3). Similar to ARIMA, the VAR model relates the current value of a variable to its past values.

Equation 3.3

$$Y_{(t)} = \phi_0 + \phi_1 \times Y_{(t-1)} + \phi_2 \times Y_{(t-2)} + \ldots + \varepsilon_t$$

Where ε_t is random error (random shock) and ϕ_i are constants. And similarly, VAR model relates current value of a vector to its past values and each variable depends not only on its own past values but on these of other variables as well in which is K×1 random vector, ϕ_i are fixed (K×K) coefficient matrices and $\varepsilon_t = (\varepsilon_{1t}, \ldots, \varepsilon_{kt})$ is K-dimensional random error (Lütkepohl 2005). To summarize, the power of ARIMA modeling stems from its ability to handle non-stationary time series with non-constant statistical properties over time. On the other hand, VAR is suitable for analyzing stationary multivariant time series with constant statistical properties and dependency among variables.

Model Parameter Identification

Prior to fitting the coefficients of the time-series model, the model order must be optimized. The ARIMA model contains three components for which an order must be determined: autoregressive (AR), integrated (I), and moving average (MA) (Equation (3.2)). The AR component uses the dependent relationship between an observation and some number of lagged observations. The order of the AR component (*p*) is the number of lag observation included in the model. The integrated component (I) employs differencing of raw observation data in order to make the time series stationary, and its order (*d*) is the number of times that the raw observation is differenced. The MA component uses the dependency between an observation and a residual error, and its order (*q*) is the size of the moving average window. In this study, ARIMA model orders (*p*, *d*, and *q*) were evaluated based on a mean squared error. A prototyping dataset was divided into train and test sets, and the optimized combination of model orders was chosen such that they produced the least mean squared error in the test set. For the VAR model, the model order, *p*, was selected based on Hannan–Quinn information criterion (HQIC) (Hannan and Quinn 1979). This criterion was applied because this is used to consistently estimate the order under fairly general conditions (Hamilton 1994). The criterion is shown in Equation (3.4).

Equation 3.4

$$HQIC = -2\ln(L_{\max}) + 2k\ln(\ln(n))$$

where n is the number of observations, k is the number of parameters to be estimated (e.g. the Normal distribution has mu and sigma) and L_{max} is the maximized value of the log-

Likelihood for the estimated model. The coefficients for *k* indicate the level to which the number of model parameters is being penalized. The objective is to find the model order of the selected information criterion with the lowest value HQIC value.

Forecasting and Defect Reconstruction

Once a model is fitted to a sequence of defect observations, the future state of the convex hull parameterizations can be predicted by the forecasting model. Once predicted, the future defect shape can then be reconstructed by converting the feature vector into a hull shape. A complication is that the number of extracted features may be inconsistent at different time steps, and this discrepancy in the length of the vectors in some cases leads to an inaccurate defect prediction. This case will happen when the number of features extracted by convex hull computation at early time steps is significantly smaller than that in the later time steps. To handle this issue, a statistical assumption is employed. For features that were not fit to a model and, therefore, their values were not predicted by dynamic modeling, the arithmetic mean of other features can be used as their expected value.

The pseudocode for the complete algorithmic methodology is shown in Figure 3.7. Upon reconstruction of the predicted geometric configuration of a defect, it is then possible to update a numerical simulation to account for the predicted change in the structure's geometry due to the defect. This updating process is not tested here, but such capabilities were developed in prior related work, including efforts by the authors (Ghahremani Kasra et al. 2018; Fathi, Dai, and Lourakis 2015; Y. Yan, Guldur, and Hajjar 2017).

```
start

    #input: Point cloud of defects in time order
    #outout: The shape of defect in the next time step

    Align all point clouds and register into a common spatial reference
    For each point cloud
        Compute convex hull
        Extract vertices of hull as feature descriptors
    For each feature in feature descriptor vector at t = t0
        Search for nearest neighbor from feature vector(@t=t1) based on smallest Euclidean distance
        Store distance and angle between each pair of features
    Track those found nearest neighbors over time based on their Euclidean distance from the consequitive features vectors
    Build dataset from stored magnitude and orientation of spatial movement of features
    For each column of dataset determine model orders for timeseries model based on chosen criteria
    Build time series model with determined model order and fit the model to timeseries dataset
    Forecast variable/feature values in next time step
    Check the consistency between first and last feature vector:
        If they are consistent
            Do nothing
        Else
            Apply arithmetic mean of all predicted features as expected value of those not predicted
    Reverse the predicted features to a discrete point set and reconstruct shape of defect in next time step

end
```

Figure 3.7. Pseudocode for the proposed methodology.

Experimental Validation

This section presents and discusses the results of experiments designed to evaluate the developed methodology. Two series of tests are presented. The first tests involve a set of experiments performed on synthetic datasets. These datasets were designed to highlight key aspects of the modeling approach and provide insight into algorithm behaviors. The second tests are derived from laboratory-scale tests of fatigue crack propagation in aluminum tensile specimens, in order to illustrate the behavior of the modeling approach in a realistic use case.

Synthetic Dataset

To initially test the accuracy and robustness of the presented methodology, synthetic 2D point clouds analogous to data derived from remote sensing (e.g., laser scanning or photogrammetry) were generated over simulated defect life cycles. Synthetic point clouds with distribution characteristics representing different flaw topologies (e.g.,

rectangle, circle, and generalized polygon) were generated. Additionally, varying evolution time histories were generated synthetically, representing a variety of stochastic processes (e.g., linear, quadratic, random Gaussian, and random uniform). For every combination of defect shape and stochastic process, a set of 20 defect time steps was generated. White noise was also introduced into the point clouds for each time step, in order to simulate more realistic measurements. Finally, uniform and non-uniform feature evolution were considered. Uniform feature evolution refers to a case where all vertices of the convex hull (features in the extracted descriptor vector) have the same expansion magnitude regardless of the trend of evolution. Cases where vertices were allowed to expand at varying magnitudes over a life-cycle simulation were considered non-uniform.

Time-Series Stationarity Assessment

Time series are stationary if the statistics calculated on the time series (e.g., the mean or variance of the observations) are consistent over time. Most statistical modeling methods assume, or require, the time series to be stationary to be effective. There are many methods to check whether a time series is stationary or non-stationary, such as reviewing a time-series plot, reviewing the summary statistics for time series, or using statistical tests. The augmented Dickey–Fuller test (Dickey and Fuller 1981), one of the more widely used, was used in this study. It uses an autoregressive model and optimizes an information criterion across multiple different lag values. The null hypothesis (H0) of the test is that the time series can be represented by a unit root that it is not stationary (i.e., it has some time-dependent structure). The alternate hypothesis (rejecting the null hypothesis) is that the time series is stationary.

Table 3.1. The p-values from Augmented Dickey-Fuller test stationary test.

Defect Shape / Defect Evolution	**Triangle**	**Rectangle**	**Circle**	**Polygon**
Uniform				
Linear	0.002	0.002	0.020	0.030
Quadratic	1.000	1.000	1.000	1.000
Random Uniform	0.950	0.950	0.390	0.940
Random Gauss	0.960	0.960	0.990	0.950
Non-uniform				
Random Uniform	0.950	0.950	0.96	0.990

Table 3.1 shows the average *p*-values of each generated time series, which is used in the augmented Dickey–Fuller test to evaluate stationarity for various defect shapes and evolutions. A *p*-value above 0.05 suggests that a test fails to reject the null hypothesis (H0), and it is concluded that such time-series models are non-stationary. This analysis shows that all of the generated time-series simulations, with the exception of the simplest linear evolution process, are non-stationary. As such, it was anticipated that the ARIMA approach would perform better than the VAR approach for the synthetic datasets.

Time-series modeling

After the synthetic datasets were generated, ARIMA and VAR model orders were selected prior to fitting to time series. For the VAR models, all extracted feature vectors were input as a matrix at once, and the model order (*p*) was set as the same for all features, whereas, for the ARIMA model, each feature vector was considered individually, and model orders suitable to each time series were chosen based on least mean squared error. Models were then fit to the time series.

Metrics

The key metric for evaluating the time-series model behavior was defect reconstruction accuracy. To evaluate the results, the predicted defect shape for a future time step was compared against an established ground truth for each scenario. Two geometric metrics were computed: the percentage difference between the area of two shapes and their overlap area percentage. These two metrics were necessary in order to identify scenarios where the predicted and ground truth defect sizes were similar, but where there was a divergence in the geometric topology. Measuring point clouds directly on a point-wise basis using the raw data was not considered, as the randomly sampled nature of point cloud data inhibits such measurements, and the focus of this effort was on the accuracy of the predicted convex hulls.

Results and discussion

Table 3.2 and 3.3 show the comparison of predicted defect shapes for both the ARIMA and VAR models against the ground truth. The time series generated from linear, quadratic expansion models are defined as deterministic time series, as their future value can be exactly computed by a mathematical function. These mathematical functions are $y_t = \theta t^0$ for linear expansion, and $y_t = \theta \times d^{(t-1)}$ for quadratic expansion (θ and d are both constants). As expected, the predicted feature state from both models completely matched with the ground truth, regardless of the defect shape. The ability to forecast such a simple deterministic process is inherent to both ARIMA and VAR modeling approaches and was used to validate basic model performance.

Table 3.2. Comparison of predicted defect shape using ARIMA model against ground truth.

Defect Shape / Defect Evolution	Triangle		Rectangle		Circle		Polygon	
Metrics	Overlap (%)	Area_Diff (%)	Overlap (%)	Area_Diff (%)	Overlap (%)	Area_Diff (%)	Overlap (%)	Area_Diff (%)
Uniform								
Linear	100	0	100	0	100	0	100	0
Quadratic	100	0	100	0	100	0	100	0
Random Uniform	100	15	100	10	100	19	89	15
Random Gauss	100	4	100	5	100	8	92	11
Non-uniform Random Uniform	95	7	96	5	98	4.5	87	17

Table 3.3. Comparison of predicted defect shape using VAR model against ground truth.

Defect Shape / Defect Evolution		**Triangle**		**Rectangle**		**Circle**		**Polygon**	
Metrics		**Overlap (%)**	**Area_Diff (%)**	**Overlap (%)**	**Area_Diff (%)**	**Overlap (%)**	**Area_ Diff (%)**	**Overlap (%)**	**Area_Diff (%)**
Uniform	Linear	100	0	100	0	100	0	100	0
	Quadratic	100	0	100	0	100	0	100	0
	Random Uniform	100	16	100	19	100	19	87	16.5
	Random Gauss	100	6	100	7.5	100	9	91	19
Non-Uniform	Random Uniform	92	8	94	21	95	9	85	25

More interesting results can be seen for the Gaussian and uniform random stochastic time series, which are more realistic representations of defect life-cycle dynamics in practical problems. Such stochastic processes are more challenging for any predictive model. As can be seen, ARIMA models provide relatively better prediction, although the results show many similarities. The reason for the difference in predictive accuracy is the capability of ARIMA in handling nonstationary time series, as well as the assumptions of variable dependencies in VAR. Also, results show that both models can

predict a defect with a Gaussian underlying process better than those with a uniform random evolution. The reason lies in the difference between the statistical properties of the two processes. Gaussian processes have a single most likely value in the distribution (the mean), whereas, in uniform distributions, every allowable value is equally likely, degrading predictive capabilities. Overall, the results of these synthetic experiments indicated that the convex hull parameterization approach and time-series modeling provides reliable and accurate representations of defect evolution across a range of defect topologies and is reasonably robust to noisy measurements. As anticipated, ARIMA provided higher prediction accuracy as stationarity assumptions became increasingly unrealistic.

Experimental Dataset

To further evaluate the methodology under more realistic conditions, a dataset from prior experimental testing was repurposed. In these laboratory tests, aluminum tensile coupons were tested to observe fatigue crack growth under cyclic fatigue loading. Marine-grade aluminum 5052-H32 with a nominal thickness of 2.29 mm was used. The specimen had a machined elliptical flaw in the center, and increasing load caused initiation and growth of cracks on both the right and left sides of this notch. Cycling tension loading was performed over 80,000 cycles, and the state of crack growth was captured at 30 intermediate intervals during the test, using an inspection microscope connected to a digital camera. The captured images were then segmented to isolate the crack, and the crack patterns were transformed from pixels into point clouds through binarization and spatial

point sampling (Figure 3.8). This resulted in 2D point clouds with between 6000 and 12,000 points, depending on the size of the crack.

The convex hulls of these point clouds were computed, and feature evolutions were exported as time series, as per the methodology delineated in methodology section. An analysis of the datasets yielded an average *p*-value of 0.35, indicating that the statistical uncertainty of the experimental measurements was non-stationary. Three different tests are presented in this section to evaluate the performance of the proposed methodology including single-step prediction, multiple-step prediction, and prediction during nonlinear system dynamical behavior.

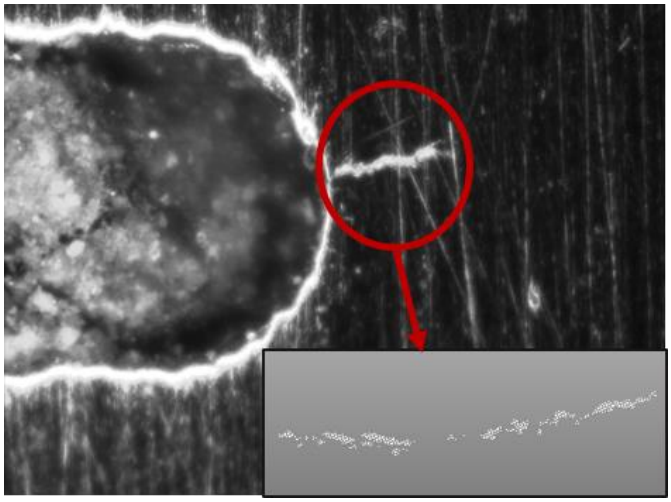

Figure 3.8. Extracted point cloud from the captured image.

Single-step prediction

Performance of the proposed algorithm for predicting a single future step is evaluated in this section. Both ARIMA and VAR model were used to find the pattern of crack growth and predict the future state of crack. The convex hulls of the right and left cracks at a load of 80,000 cycles were computed and held out as the ground truth for one single-step prediction. Results are shown in Table 3.4 and Figure 3.9. Since the performance of the ARIMA and VAR model was almost identical, the predicted shape from both models had overlap, and only the ARIMA model can be seen in the Figure 9.

Table 3.4. Comparison of predicted crack shape from ARIMA and VAR against ground truth.

	ARIMA		**VAR**	
Metric	Overlap (%)	Area_Diff (%)	Overlap (%)	Area_Diff (%)
Right Crack	100.0	7.0	100.0	7.0
Left Crack	99.0	5.0	96.0	5.0

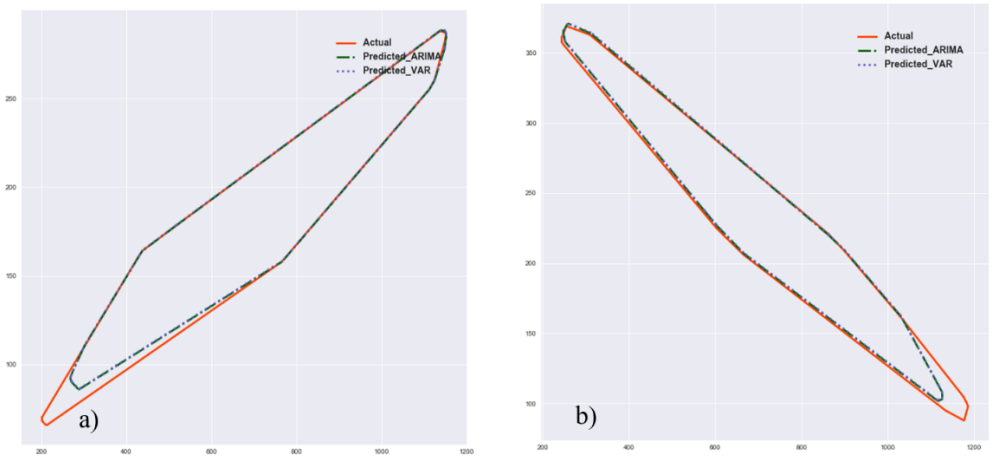

Figure 3.9. Comparison of the predicted crack shape against the ground truth for (**a**) right and (**b**) left cracks.

Multiple-step prediction

To evaluate the capability of the proposed algorithm for prediction of multiple steps, 20 steps of the right-side crack, corresponding to approximately 40,000 loading intervals, were used to fit to the ARIMA and VAR models based on the HQIC criterion. The true convex hulls of the crack at time steps 21–30 were then computed and held out as the ground truth. Then, prediction of 1–10 time steps into the future were computed and evaluated. Table 3.5 shows the results from the ARIMA model. Since the performance of ARIMA and VAR was very similar for this specific problem, only ARIMA is shown here. What these results reflect is, in part, the sensitivity of the time-series modeling process to the number of time-series data points or lags, used in predictive computation. For the results shown using 20 lags, predictive accuracy begins to degrade at future time steps approximately 25% the length of the total lag, in this case, five steps. Similar results were observed for models with varying numbers of lags. When fewer than 10 lags were used to fit the model, predictive accuracy was deemed unacceptable.

Table 3.5. Comparison of predicted crack shape from ARIMA against ground truth.

	1-step	**2-steps**	**3-steps**	**4-steps**	**5-steps**
Overlap (%)	100	100	99	98	96
Area_Diff (%)	1	1	4	3	4
	6-steps	**7-steps**	**8-steps**	**9-steps**	**10-steps**
Overlap (%)	95	94	93	92	91
Area_Diff (%)	3	6	5	3	3

Prediction during nonlinear system behavior

The goal of this study was to evaluate the performance of the model during a geometric nonlinearity in the evolution of a defect over time. For the crack fatigue problem studied here, there was a sudden change in the direction of crack growth after 48,000 load cycles. Of course, the predictive time-series models could not accurately forecast the convex hull immediately after this event. Rather, the question here was how long it would take the time-series models to correct for this nonlinearity in the dynamic evolution. The results for both ARIMA and VAR models are shown in Tables 3.6 and 3.7. As can be seen, the ARIMA model quickly adapted after only two load steps (at 50,000 load cycles). The VAR model struggled to adjust for far longer, only regaining consistent predictive accuracy after 60,000 load cycles, equivalent to an additional four model time steps.

Table 3.6. Comparison of the predicted crack shape from ARIMA model against ground truth.

Load	**48k**	**50k**	**52k**	**54k**	**58k**
Overlap (%)	83	96	95	99	95
Area_Diff (%)	8	14	17	15	3

Table 3.7. Comparison of predicted crack shape from VAR model against ground truth.

Load	**48k**	**50k**	**52k**	**54k**	**58k**	**60k**	**62k**	**64k**
Overlap (%)	63	70	66	92	70	95	87	97
Area_Diff (%)	8	14	17	15	16	5	2	6

Results and discussion

Table 3.4 shows the comparison of predicted crack shape from the ARIMA and VAR models against the ground truth for cracks at the left- and right-hand sides of the notch. Figure 3.7 shows the predicted hull shape from both models against ground truth.

Results reflect that ARIMA and VAR models both provide an accurate prediction of the future state of the crack, and the presented method is able to match the convex hull of the ground truth with high accuracy. Also, the results shown in Table 3.5 suggest that ARIMA and VAR models are able to predict hull shape of the crack even 10 times steps ahead with reasonable, although slightly degraded, accuracy. However, the approach is not able to mimic the true shape of the crack. Unlike the analysis performed on synthetic point clouds in the prior section, the crack shape cannot be reasonably defined by a convex polygon and, therefore, convex hull parametrization cannot represent the true shape of this polygon. However, it does predict the extremis of the visible crack tip. The evaluation of the nonlinear system dynamic prediction (Tables 3.6 and 3.7) shows that the ARIMA model has much better performance in adapting to a nonlinear change in defect evolution and suggests that ARIMA approaches are more robust compared to VAR methods.

Limitations of the method

While the developed approach was shown to be effective under the experimental conditions described here, it is important to recognize the limitations of this approach. These tests were performed under controlled laboratory conditions and were not subject to the distortions and increased measurement uncertainty that arise due to environmental variations. How this measurement approach performs under unpredictable, and likely nonlinear, loading and thermal conditions remains an unstudied problem, but such conditions will undoubtedly have a negative impact on predictive performance. Field conditions are likely to degrade both the quality of generated point clouds and the

predictive accuracy of any autoregressive tracking method. Furthermore, more complex material behavior, for example, highly random cracking in heterogeneous materials such as concrete, will degrade the accuracy of the autoregressive model. In general, increases in the stochasticity and nonlinearity of the underlying degradation process will result in a significant reduction in algorithm accuracy.

Conclusions and Future Work

In this work, a methodology to parametrize and model the dynamics of defect evolution based on convex hull parametrization and time-series modeling was introduced. Using convex hull parametrization, 2D synthetic and experimental point clouds representing various defect shapes and stochastic evolutions were parametrized, and their evolutions were modeled using time-series forecasting models. The future state of defects was then forecasted and evaluated against ground truth. The results indicate that this convex hull approach provides consistent and accurate representations of defect evolution across a range of defect topologies and is reasonably robust to noisy measurements; however, the behavior of the underlying dynamical process plays a significant role in predictive accuracy. Predictive accuracy degrades for both ARIMA and VAR models as defect evolution becomes increasingly nonlinear, although ARIMA is slightly more robust under such conditions.

The proposed methodology has a number of advantages over current practices. Firstly, it provides engineers with an intuitive and consistent representation of remotely sensed information over a structure's life cycle through the reduced-dimension convex hull

representation. Tracking the evolution of damages and their connections to structural performance also results in more reliable forecasting capabilities and a more complete understanding of structural performance, particularly compared to existing NDE techniques that often do not quantify damage evolution through time. This process also does not require extrapolation from other datasets for prediction; rather, it builds up a time-series representation based solely on the observed evolution of a given defect.

This study was part of an ongoing research program, and various parts of the presented methodology are being considered for further improvement. The limitations discussed in limitation section highlight potential avenues for future work. The behavior of the algorithm under higher degrees of statistical uncertainty and material variability should be investigated. More datasets from other crack scenarios should also be considered, for instance, concrete cracking in civil infrastructure. Such studies may provide insight into how particular algorithmic aspects, such as the nearest neighbor matching aspects of hull tracking, behave under complex material phenomena such as crazing or alkali–silica reactions in concrete. In such cases, the cracks may branch and split, creating unforeseen modeling challenges.

The parametrizations and hull modeling are being studied for temporal tracking of non-geometric changes such as color change in structures. The hull parametrization method is also being extended to high-dimensional feature space analyses, supporting the fusion of multiple sensors and survey information for holistic life-cycle modeling. As was presented in the methodology description, the results of this work will ultimately be used to support finite element model updating for predictive analysis of structural capacity. One notable

avenue for future work is to adapt the algorithm to more realistically parameterize defect shapes using a combination of a convex and concave hull algorithm (Ebert, Belz, and Nelles 2014). Such an approach would allow for more accurate depiction of complex geometric topologies similar to the fatigue cracks evaluated in this work. In addition, nonlinear time-series modeling methods such as recurrent neural networks may be studied for more complex defect evolutions; however, such machine-learning-driven approaches need much larger datasets to be employed.

CHAPTER FOUR: PREDICTIVE FINITE ELEMENT MODEL OF FATIGUE CRACK SIMULATION FOR STRUCTURE PERFORMANCE FORECASTING VIA COMPUTER VISION TECHNIQUE

Introduction

This paper presents a method for updating the Finite Element (FE) model of structural components under fatigue load based on the future state of existing crack. The goal is to conduct a predictive analysis for structure capacity and evaluate the integrity of such structures under cyclic loading. Cyclic loading can initiate a crack in a structurally weak area of a component and the crack can then grow due to fatigue. The growth of a crack throughout the volume of a component can result in catastrophic fracture. Many structures are exposed to repeated loading over their life cycles, and fatigue may lead to the failure of various types of structures, including bridges. Therefore, it is essential to accurately predict the crack extension over its life cycle and make decisions about effective maintenance and retrofitting. There are, however, different types of uncertainty factors such as material properties, geometric properties, boundary conditions and load conditions that contribute to the modeling of a structure (Aghagholizadeh and Catbas 2015).

The FE model updating method emerged in the 1990s as an important subject for mechanical and aerospace structures (He, Yu, and Chen 2008; D. L. Hall and Llinas 1997). FE model updating is a procedure that provides an effective way to obtain a precise model whose numerical predictions agree with the measured results from a real structure. Model updating can provide a consistent and reliable benchmark corresponding to the real structure (Mottershead and Friswell 1993; S. Zhang et al. 2013). Theory and application of

structural FE model updating have been extensively studied (Ding et al. 2012; Y. Wang et al. 2013; S. Zhang et al. 2013). Most of these studies mainly focus on identification, localization and quantification of structural damage through a model-updating procedure and are limited in predictive analysis for future structural performance. Evaluation of structural integrity in the future could provide more precise and robust structural information, leading to better system asset management decision-making, with apparent safety and financial benefits.

Prior Studies

There are mainly two procedures involved in FE model updating: matrix updating and parameter correction. Matrix updating involves directly updating the components of element matrices such as stiffness, mass, and damping (KABE 1985, 198; S. W. Smith and Beattie 1991). Parameter correction (Modak, Kundra, and Nakra 2002; Q. W. Zhang, Chang, and Chang 2000; Ren and De Roeck 2002) corrects the structural design parameters such as geometry, materials, and boundary conditions. Parameter updating is widely applied in practice, since the explicit physical meaning of the parameters is clear (Teughels and De Roeck 2005). The purpose of these methods is to update the parameters of a finite element model corresponding to the undamaged structure in order to match the measured data from the damaged structure. In this way, identification, localization and quantification of structural damage can be achieved (Perera, Fang, and Huerta 2009). Most of the approaches use the modal data of a structure before damage occurs as baseline data, and all subsequent tests are compared to it. Any deviation in the modal properties from this

baseline data is used to estimate the crack size and location (Mottershead and Friswell 1993).

Along with FE model updating studies, extensive research has been done on FE simulation of fracture mechanics as the presence of cracks can significantly decrease structural strength and reliability. Fracture mechanics is divided into two main categories: linear elastic fracture mechanics (LEFM) in which it is assumed that materials show only linear elastic behavior under operating conditions and elastic plastic fracture mechanics (EPFM). LEFM has been extensively studied and successfully used to model the fatigue crack growth behavior (X. Yan 2007; Banks-Sills 1991; Atkinson 1977; Pak 1992; Pan 1997). However, it was found that many engineering materials show some inelastic behavior under operating conditions and EPFM has been studied to address LEFM limitations. Cohesive zone model originally proposed by Barenblatt (Barenblatt 1962) and Dugdale (Dugdale 1960) to investigate materials exhibiting plasticity. Since then cohesive fracture modeling was applied in several areas, such as concrete (Mosalam and Paulino 1997; S. H. Song, Paulino, and Buttlar 2006; S. Song, Paulino, and Buttlar 2008), dynamic crack growth (Siegmund, Fleck, and Needleman 1997; G. Ruiz, Pandolfi, and Ortiz 2001) and viscoelasticity (Rahulkumar et al. 2000).

To reduce the shortcomings of the FE method for modeling the propagation of various discontinuities such as cracks ,the extended finite element method (XFEM) was presented by Belytschko and Black (Belytschko and Black 1999). The main goal was enriching finite element approximations to solve the crack growth problems with minimal re-meshing. The technique allows modeling the entire crack geometry independent of the

mesh and completely avoids the need to re-mesh as the crack grows. The XFEM was applied in various aspects of crack problems, including LEFM crack growth (Tarancón et al. 2009), crack growth with frictional contact (X.-P. Zhou, Chen, and Berto 2020), cohesive crack propagation (Grogan, Ó Brádaigh, and Leen 2015; Feng and Gray 2019), quasi-static crack growth (Sukumar and Prévost 2003), fatigue crack propagation (Golewski, Golewski, and Sadowski 2012; Irani, Mehri, and Seifollahi 2014), stationary and growing cracks (Lee and Martin 2016) and three-dimensional crack propagation (Baydoun and Fries 2012).

These studies mainly focus on improving the accuracy of numerical models, however, are limited in predictive analysis for future structural performance. With linking the FE model with the future state of cracks, the future condition of structure and its capability can be better understood.

There has been an increasing interest in studies about the use of remote sensing and imaging technologies to develop methods and techniques to reliably identify different visual defects, including concrete cracks, fatigue cracks, and asphalt cracks.(Spencer, Hoskere, and Narazaki 2019; Jahanshahi and Masri 2012; Jahanshahi et al. 2009; Tsao Stephen et al. 1994; Kaseko Mohamed S., Lo Zhen-Ping, and Ritchie Stephen G. 1994; Abdel-Qader Ikhlas, Abudayyeh Osama, and Kelly Michael E. 2003; F. Chen and Jahanshahi 2018). In complement to the expanding use of these methods, there are now a variety of methods for isolating and extracting cracks from 2D or 3D images as three-dimensional point cloud models(Jafari, Khaloo, and Lattanzi 2016; Khaloo and Lattanzi

2019; Cabaleiro et al. 2015; Colomina and Molina 2014; Fleming, Holtmann-Rice, and Bülthoff 2011; Pal and Pal 1993).

A key advantage of these data sources is the direct link between quantified geometric changes and changes in the underlying mechanical performance that can be captured in finite element analysis, as evidenced by a variety of prior work (Ghahremani Kasra et al. 2018; Fathi, Dai, and Lourakis 2015; X. Yan 2007). However, to the best of authors' knowledge, there is no study to use these identified cracks for FE model updating. Linking the identified and quantified cracks to the FE models of structures is computationally cost effective for capability of locally updating the model rather than global updating. Also, unlike the common crack modeling approaches, which simulates the crack in the element by reducing local stiffness, this method involves the crack size and location directly to the model (Friswell and Penny 2002; Dimarogonas 1996; Ostachowicz and Krawczuk 2001; Brandon 1998; Kisa and JA 2000).

Contribution of This Research

The authors developed an approach for damage detection and FE model updating of structural components through computer vision techniques (Ghahremani Kasra et al. 2018). They studied the proposed approach on section loss damages and the results showed that the proposed approach will enable engineers to use the updated structural model to determine the reserve capacity and remaining service life of structural elements. The authors also in another study (Mohamadi and Lattanzi 2019) developed an approach to parameterize and model the dynamic evolution of the remotely sensed damages (e.g. cracks) in structures and successfully predicted their future state.

The main objective of this study is to link the numerical model of structures to the future state of crack extension and conduct a predictive analysis for structures capacity. Updating the numerical model involves the solid model updating for which the authors' previously developed approach is applied (Ghahremani Kasra et al. 2018). To compute the future state of the crack, above mentioned parameterization and modeling approach is used(Mohamadi and Lattanzi 2019). Here, to address some limitations of previous work in reconstructing the crack shape (see Methodology section), the authors proposed an additional step to update the structural components' solid model. First, the point cloud of an identified crack at one of the primary loading cycles is used to update the solid model of the structural component via a computer vision technique. Then point clouds at various load cycles are parameterized, and the future crack extension is forecasted via stochastic modeling. Once again, the solid model is updated with regard to the predicted crack extension and fracture simulation is conducted. As a result, the crack propagation can be modeled, and the future capacity of the structure can be predicted.

A new approach presented here overcomes the shortcoming of the convex hull representation in the previous study and enables to update the solid model based on the predicted crack extension while mimicking the crack shape.

To the best of the authors' knowledge, no research has studied FE model updating based on the future state of crack or linked the FE model to remotely sensed cracks. A predictive analysis with regard to the future condition of the remotely sensed cracks through linking the modeled evolution of cracks to a numerical simulation ultimately helps

provide a complete representation of structural performance and integrity over time. It also results in more reliable forecasting capabilities.

The remainder of this paper is structured as follows: First, the complete analytical methodology is presented. This is followed by experimental evaluation of the proposed approach using fatigue crack propagation data. Sources of error and limitation of the proposed approach are discussed in the next section. The paper concludes with an overall assessment of the FE model updating approach and avenues for future work.

Methodology

The overall methodology (Figure 4.1) consists of two main steps: First extension of the crack in the future load cycle is predicted and second, FE model is updated with regard to the predicted crack extension for predictive simulation. In the first step, once cracks in the structure are identified and represented as point clouds, the cracks are parametrized in a way that can support a dynamic modeling of defect evolution over time. Convex hull computation is an approach to parameterization and feature extraction that is proposed by the authors in their previous study (Mohamadi and Lattanzi 2019). Convex hull computation is used to parameterize the cracks and hull vertices are extracted as unique features which their evolution over time is modeled. Once features are extracted, a time-series model is fit to the sequence of features in order to capture the underlying process of the crack evolution. This model fitting also enables the estimation of the future state of the crack via out-sample forecasting. The crack shape is then reconstructed by reversing the extracted features back to a geometric point set. Once the crack shape is reconstructed, the crack extension (i.e. length and orientation) can subsequently be computed by calculating

the distance and angle between the predicted crack extremes. The next step is to update the FE model with regard to the predicted crack extension. The authors' previous study showed that the proposed hull parameterization method while has good accuracy of crack length prediction has some limitations for mimicking the crack shape. Therefore, the predicted hull cannot be used to update the solid model. To overcome the hull parameterization limitation the FE model updating includes two steps: First the solid model is updated with regard to the identified crack at one of the primary loading cycles which mimic the actual crack shape. In this step, the identified crack represented as a point cloud is converted to a solid model and subtracted from the baseline or uncracked component. Second, the predicted crack extension is used to update the geometry of the model once again. In this step the only parameter to update is the crack tip location which is predicted through time-series forecasting model. Crack size and consequently the solid model is updated with changing the crack tip location.

Once the solid model is updated, it is imported into the FE program and fatigue simulation is conducted. The integrity of the structural component is evaluated under cyclic loading. The complete FE model updating process is evaluated through an experimental fatigue tensile test.

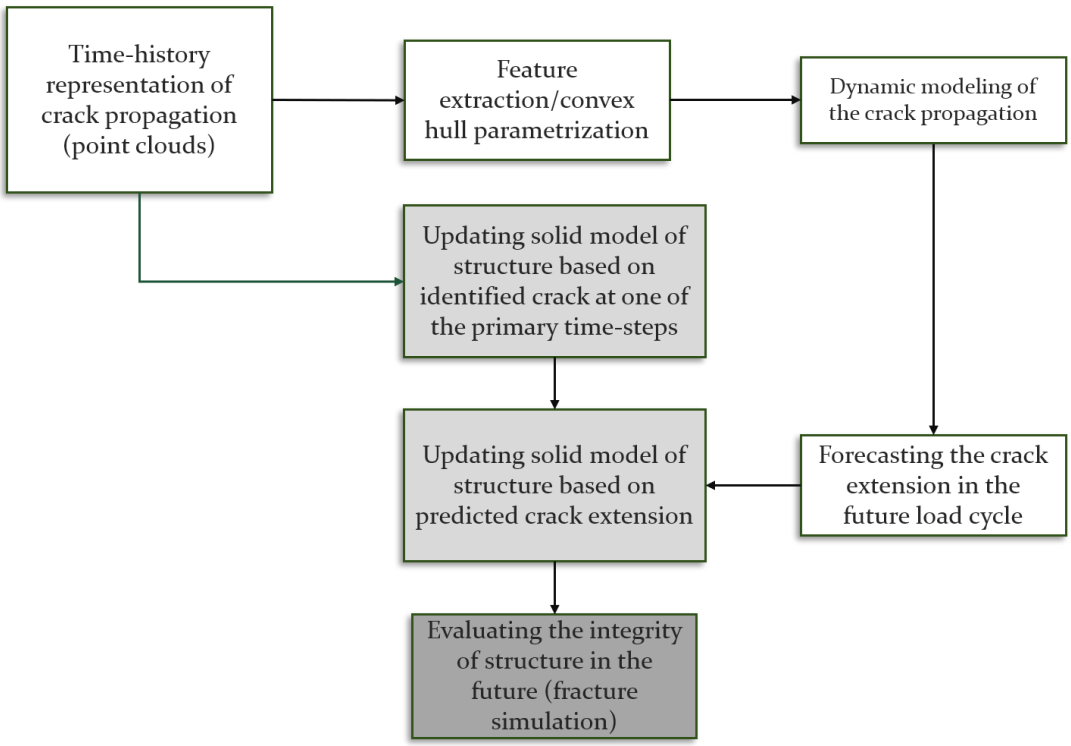

Figure 4.1. Proposed framework for finite element model updating of the structural component based on the future state of its existing crack.

Prediction of the Crack Extension

Remotely sensed cracks, once detected, are parametrized to model their dynamic evolution (Mohamadi and Lattanzi 2019). Parameterization is achieved with feature extraction from the point cloud through computational geometric modeling of the convex hull of the cloud, resulting in a combination of hull simplexes and vertices. These parameterizations are computed for multiple load steps over the life cycle of the structure. The evolution of features then is tracked over time by nearest neighbor search based on Euclidean distance and the resulting change in magnitude and orientation is used to

construct a dataset. Readers can refer to the authors' prior study (Mohamadi and Lattanzi 2019) for more detailed information.

Once the dataset representing the evolution of crack is constructed, a stochastic model can be fit to the dataset to model the dynamics of crack evolution and forecasting the future state of crack. Autoregressive integrated moving average (ARIMA) time series model is used in this study as a stochastic model. ARIMA model is used for capability of handling the non-stationary dataset and arbitrary defect evolution such as crack propagation problem (Mohamadi and Lattanzi 2019).

Once ARIMA is fitted to the crack evolution, the convex hull of the crack in the future load cycle is predicted. Once predicted, the future state of the crack can then be reconstructed by converting the feature vector into a hull shape. Subsequently the crack length is computed by calculating the distance between the predicted hull's extremes.

Finite Element Model Updating for Predictive Analysis

The focus of this step is to update the FE model of structures (structural component) with regard to the future state of remotely sensed cracks. The overall approach to FE model updating is composed of two main steps :1) updating the solid model, and 2) predictive simulation. Figure 4.2 illustrates the overall approach of solid model updating and FE meshing for predictive simulation.

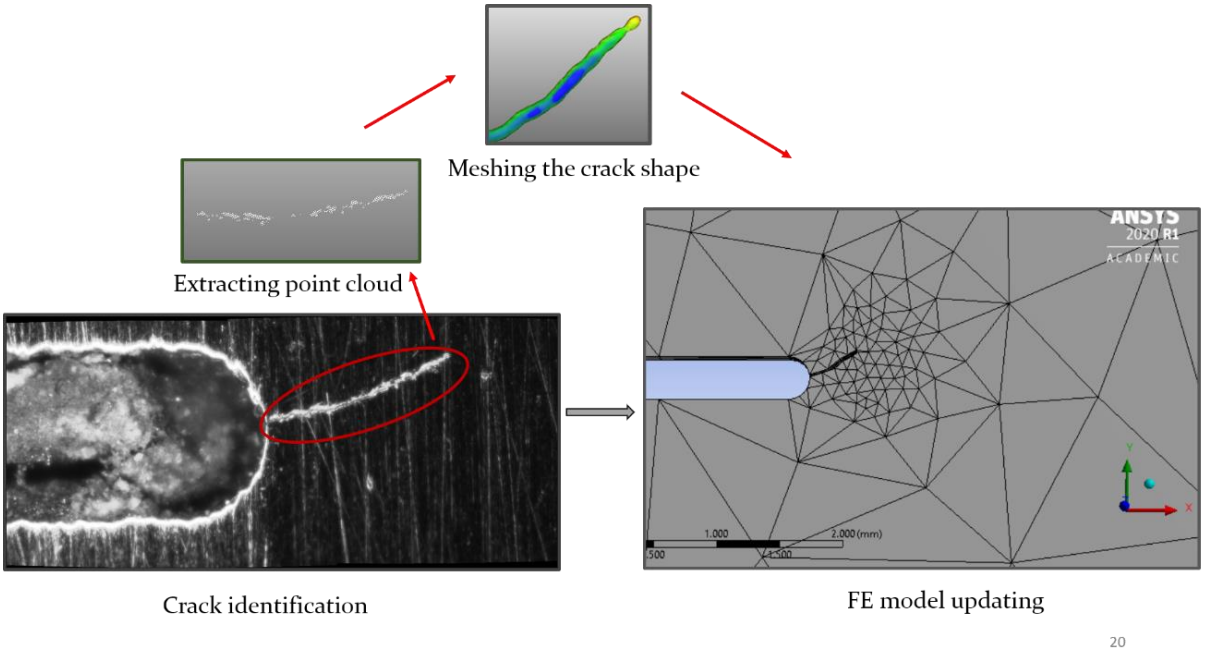

Figure 4.2. The overall approach of meshing the extracted point cloud and FE meshing for predictive simulation.

The identified crack represented as point cloud is meshed via surface reconstruction algorithm and 3D watertight surfaces of the crack is generated. Once generated, the 3D surface is used to update the solid model. Then the solid model is imported to a FE program and fatigue simulation is conducted. Crack propagation under cyclic loading can be studied for structure's performance forecasting.

Solid model updating

Solid models of structures can be updated with regard to the current state or future state of an identified crack. To do so, the solid model of the identified crack must be subtracted from an initial uncracked model (Ghahremani Kasra et al. 2018). In order to have more accurate solid model updating, the shape of the crack must be similar to the actual crack. The authors' previous study revealed that the predicted hull crack and ground

truth convex hull are more than 95% similar, however the reconstructed crack shape from the prediction algorithm does not mimic the actual crack shape (Figure 4.3), due to the process of parameterization (Mohamadi and Lattanzi 2019). In order to overcome the shortcoming of the parameterization method, a novel approach is presented here for model updating. Overall solid model updating consists of two steps: 1) reconstruction of the actual crack shape and 2) updating the crack extension.

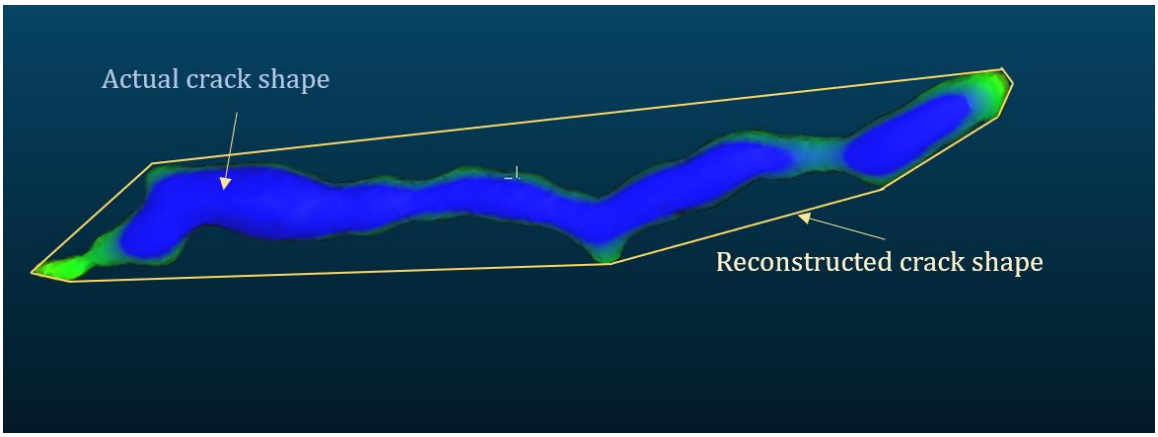

Figure 4.3. Comparison of the actual crack shape and the reconstructed crack shape.

Reconstruction of the actual crack shape

At this step, in order to capture the actual shape of the crack, the solid model of the structural component is updated with regard to an identified crack at one of the primary loading cycles. The identified crack is represented by a 3D point cloud. The point cloud is meshed and converted to watertight solid model (Ghahremani Kasra et al. 2018). The screened Poisson surface reconstruction developed by Kazhdan and Hoppe (Kazhdan and

Hoppe 2013) is used to generate 3D watertight surfaces of the crack. The created meshes are then converted into a solid model.

The baseline solid model is updated at this step. The initial or baseline solid model of the component is built from prior modeling experiences and provides a reference for the overall modeling strategy. In this case the initial model is the solid model of the structural component without any crack. The solid model of the quantified crack is then used to update the baseline solid model of the component via subtraction from initial model (Hoffmann 1989).

Updating the crack extension

As stated earlier, the previous study showed that though the predicted crack hull is very similar to the hull of ground truth crack, the reconstructed crack shape from the prediction algorithm is not mimicking the actual shape. While not discussed in the previous work, once the crack hull is predicted, the crack length and orientation can be computed from the prediction result. The distance between crack extremes representing the crack length can then be used to update the solid model of structural components once more. An assumption has been made in this study that the width of crack is constant under increasing loading cycles and crack propagation.

The other parameter that is taken into consideration is the orientation of the crack extension (aka the crack path). The orientation of the crack may change smoothly or suddenly under loading conditions and in order to compute crack propagation more accurately this fact should be taken into consideration. The crack orientation also can be computed from the dynamic modeling of the crack using the horizontal and vertical

distance between crack extremes as shown in Figure 4.4. Once the crack length and orientation are determined from the ARIMA model prediction, the extension of the crack length and change of the orientation is used to project a new crack tip location (Figure 4.5).

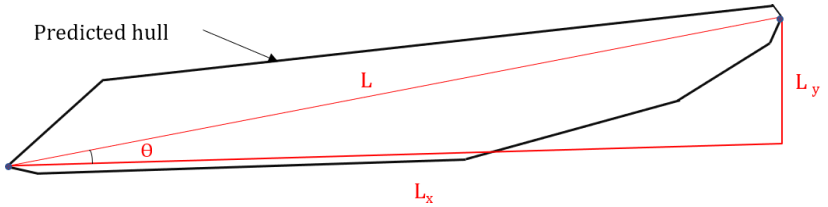

$$\Theta = arctan\frac{L_y}{L_x}$$

Figure 4.4. Computation of crack orientation.

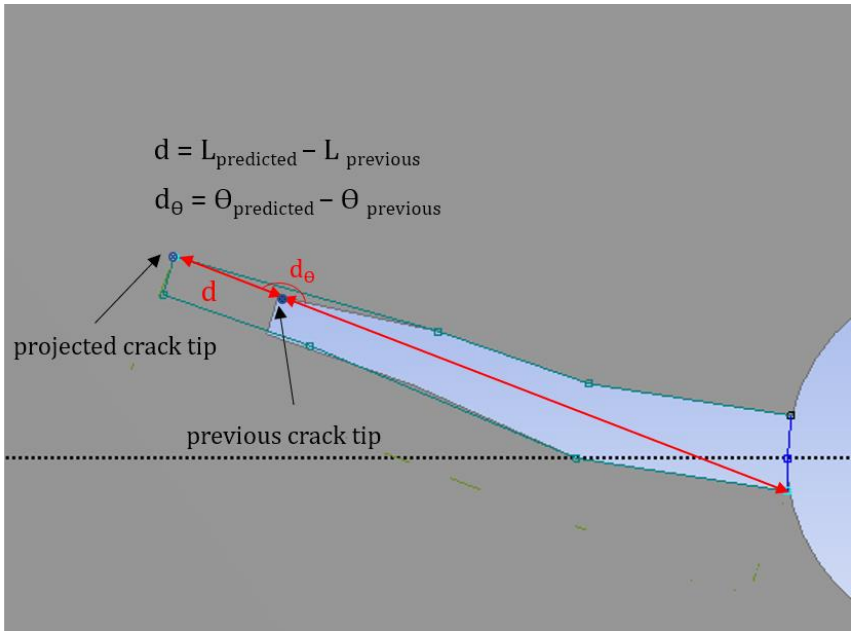

Figure 4.5. Projection of new crack tip location using extension of the crack and its orientation.

The updated solid model is then exported a FE analysis program for mesh generation and predictive analysis.

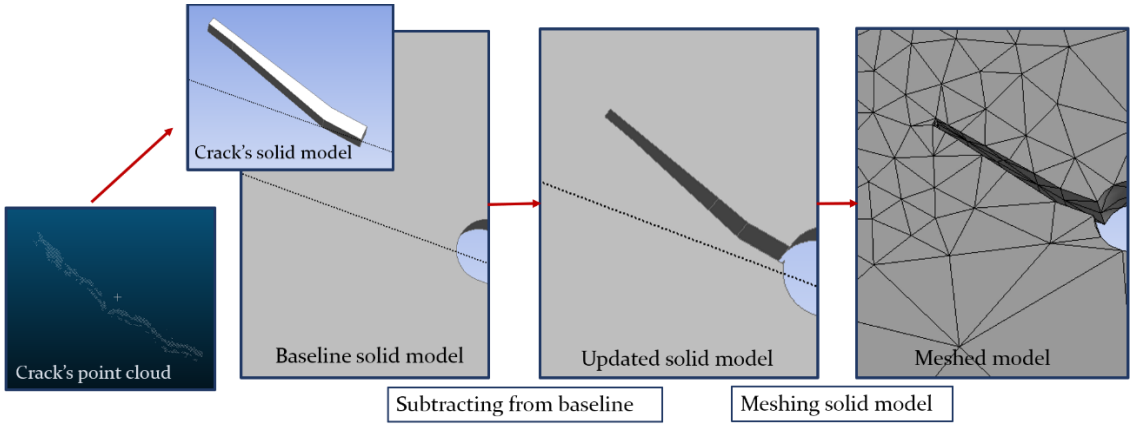

Figure 4.6. The overall approach of solid model updating and FE meshing for predictive simulation.

Predictive simulation

Once the solid model is updated with regards to the predicted crack topography, the model is meshed for FE fracture simulation. Once imported into the FE software program, the model is meshed using tetrahedral mesh elements as shown in Figure 4.6. Tetrahedral elements generally can fit better complex geometry such as curved geometry and acute angles and this makes it better fit for meshing the geometry of crack (Khoei et al. 2013). Consistent global element size is used for meshing the model except for around the crack tip for which a finer mesh is used to capture the induced stress concentration and crack

propagation effects. The mesh around the crack tip is refined using the sphere of influence method around the geometric edge going through thickness. This has the desired result of improving numerical accuracy in crack regions while maintaining computational efficiency and scalability for the overall model (Agathos, Chatzi, and Bordas 2018). Unstructured meshing method (UMM) is applied in this study for meshing process. UMM is more versatile and easier to use than any previous fracture simulation technology (Ayhan 2011) and has been used by many researchers mostly to determine the stress intensity factor (SIFs) for different kinds of crack shapes (Jones and Peng 2002; Kuang and Chen 2000; Broek 1972; R. A. Smith and Miller 1977; Tanaka and Akiniwa 1988). Applying the UMM and generating all-tetrahedral mesh for crack fronts, the same accurate results are achieved as simulation is run with the ideal hexahedron mesh configuration while this will reduce meshing time to a few minutes. Once the model is meshed then the fracture study is conducted.

After meshing the solid model, boundary conditions and loads are defined simulating the boundary conditions of the experimental fatigue test. To model crack propagation the linear elastic fracture mechanics (LEFM) is applied in this study. LEFM has been successfully used to model the fatigue crack growth behavior (Mach, Nelson, and Denny 2007; Alshoaibi and Fageehi 2020; Lesiuk et al. 2020). LEFM is the basic theory of fracture, originally developed by Griffith (Griffith and Taylor 1921) and completed in its essential form by Irwin (Irwin 1957) and Rice (Rice 1968). LEFM is a simplified, yet sophisticated, theory that deals with sharp cracks in elastic bodies. Based on experimental results, figure 4.7 shows schematically crack growth rate versus the stress intensity range.

Fatigue life can be divided into an initiation period (region I) and a crack growth period (region II, region III) (Schijve 1977).

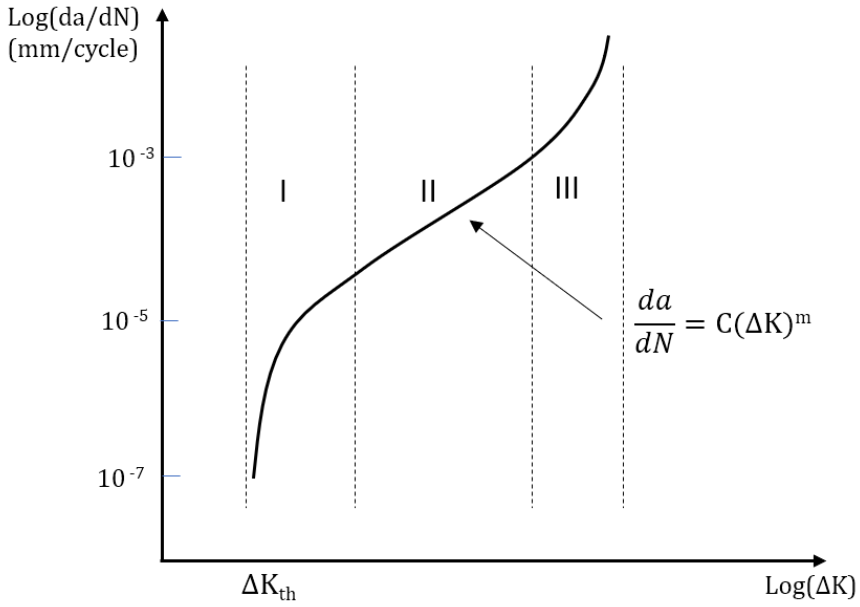

Figure 4.7. Crack growth rate versus the stress intensity range. The Paris' equation fits the central linear region (region II).

Crack growth equations are used to predict the crack size starting from a given initial crack and are typically based on experimental data obtained from fatigue tests. Region II representing the stable crack propagation region, suggests that the crack growth rate *da/dN* is a function of the stress intensity factor range ΔK in a log–log scale. The fatigue crack propagation can be modeled using Paris' law equation (Paris and Erdogan 1963):

Equation 4.1

$$\frac{da}{dN} = C(\Delta K)^m$$

Where C and m are material dependent constants (aka Paris constant), Δk is the Stress intensity factor range (based on maximum stress and minimum stress). Once the fracture analysis is conducted the crack growth rate and life cycle of the specimen can be computed under loading conditions.

Experimental Validation

This section presents and discusses an experimental study designed to demonstrate the potential capabilities of the proposed approach for accurate predictive simulation. The presented test in this section is derived from laboratory-scale test of fatigue crack propagation in aluminum tensile specimen. The experimental data has been used previously to evaluate the crack extension prediction by the authors and the results are reported and discussed in detail (Mohamadi and Lattanzi 2019). In this study as the continuation of the study, the proposed approach for finite element model updating is evaluated using the experimental data.

Experimental Dataset

Prior to this study, researchers at University of Maryland constructed a fatigue crack propagation experiment and assessed the result using microscopic images and DIC to capture strain fields around the crack tip (Lara, Bruck, and Fillafer 2020). Experiment set up and specimen dimension is shown in the Figure 4.8 and Figure 4.9 respectively.

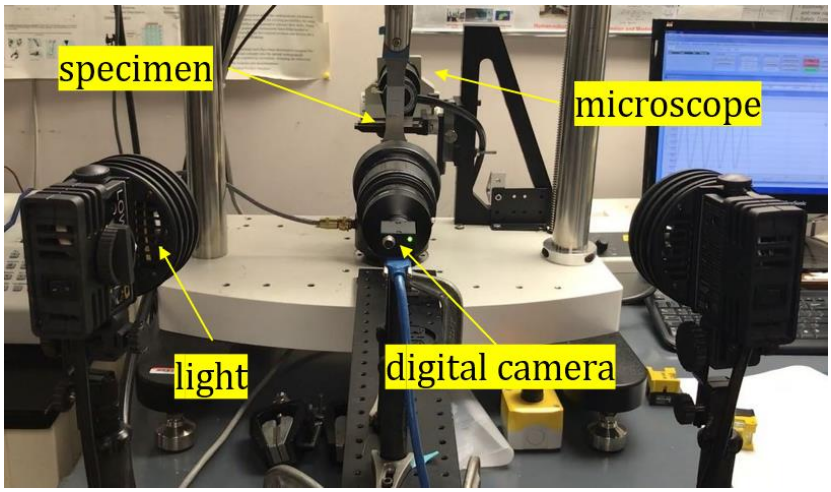

Figure 4.8. Fatigue experiment set up.

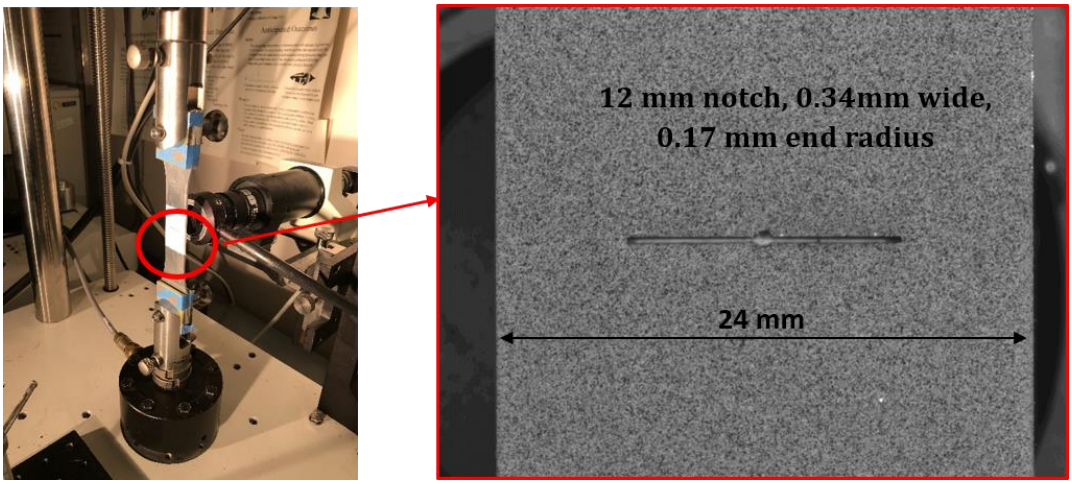

Figure 4.9. Specimen dimension.

In these laboratory tests, aluminum tensile coupons were tested to observe fatigue crack growth under cyclic fatigue loading. Marine-grade aluminum 5052-H32 with a nominal thickness of 2.29 mm was used. The specimen had a machined elliptical flaw in

the center, and increasing load caused initiation and growth of cracks on both the right and left sides of this notch. Cycling tension loading was performed over 80000 cycles. The state of the crack growth was captured at 30 intermediate intervals during the test, using an inspection microscope connected to a digital camera.

The captured images from the inspection microscope were then segmented to isolate the crack, and the crack patterns were transformed from pixels into point clouds through binarization and spatial point sampling. This resulted in 2D point clouds with between 6000 and 12,000 points, depending on the size of the crack. The point cloud data extracted from microscopic images were used to prototype and test crack prediction algorithms and updating finite element models discussed in the methodology (see methodology section).

The convex hulls of these point clouds were computed, then features evolution were exported as time series and future state of crack was predicted, per the methodology delineated in Section 2.1. The solid model was then updated with regard to the predicted crack extension. Two different tests are presented in this section to evaluate the proposed FE model updating methodology including single-step prediction and multiple-step prediction. For single-step prediction, ARIMA model was used to find the crack propagation and prediction of the future state of the crack. On the other hand, for multiple-step prediction, after cracks at multiple loading cycles were fit to ARIMA, prediction of a four time-steps into the future was computed. The solid model was then updated with regard to both predicted cracks and the updated finite element model was evaluated as results were compared against those from the experiment.

Metrics

The key metric for evaluating the FE model updating methodology was the crack extension. Once the fracture simulation was conducted, the crack extension during increasing loading cycles were compared against those from the experiment (aka ground truth). The crack growth rate (aka da/dn) also was evaluated through comparing the results against the ground truth. In addition, strain along the cross section and strain field at specific loading cycles were extracted from the simulation and were compared against the experimental data. Strain results from the experiment were computed using the DIC system which has been applied to the field measurement of displacement and strain of civil structures in the recent years (McCormick and Lord 2010; Yoneyama et al. 2007; Helfrick et al. 2011; Reagan, Sabato, and Niezrecki 2017).

Crack Propagation Modeling

As stated in the methodology section, in order to update the geometry of the model, first the solid model was updated based on the identified crack in one of the primary loading cycles (i.e. 30k cycles). To do so the solid model of defect must be subtracted from baseline model in an intermediate solid modeling software. Autodesk Inventor was used in this study for modeling purpose. Then the predicted crack length and orientation from the ARIMA forecasting model were used to update the crack tip location. Once the solid model was updated, the model was imported into ANSYS FE software program for meshing and crack propagation study.

Single-step prediction

Performance of the proposed FE model updating methodology based on the single-step prediction is evaluated in this section. 15 steps of the right and left cracks, corresponding to approximately 48k loading intervals were used to predict the crack length at 52k loading cycles. The true crack extension at time steps 16 corresponding to the 52k loading cycle was then held out as the ground truth. The crack extension was predicted using the ARIMA model. The predicted crack extension (length and orientation) was then used to update the solid model as explained earlier. Once the solid model was imported into ANSYS, the model was meshed with tetrahedron elements. Global element size was set to 3mm and around the crack tip on both sides 1/10 finer mesh was used in 0.5 mm circle and through thickness of the model. As cracks grew, the crack geometry changed, and the mesh was updated accordingly. Separating Morphing and Adaptive Remeshing Technology (SMART) in ANSYS software program which relies on the UMM process is applied for crack propagation study. Remeshing with tetrahedron elements was done automatically at a critical region around the crack tip at each iteration of the simulation process using Separating Morphing and Adaptive Remeshing Technology (SMART) crack growth simulation in ANSYS. Linear elastic behavior was assumed for aluminum and Paris constants C and m were set equal to 8.87E-08 and 3.14 respectively for modeling the crack propagation. The Paris constants were taken from the literature (Moreto et al. 2015). Once the loading and boundary condition were defined the fatigue crack simulation was conducted. Extension of the right and left side cracks, crack growth rate, strain at crack tip

under increasing loading cycles, the strain along the cross section at specific loading cycles were computed and compared against the ground truth.

Multiple step prediction

To further evaluate the capability of the proposed approach, the FE model was updated based on multiple step prediction. To do so, once ARIMA model fit to series of crack extension at multiple load cycle, rather than predicting the state of crack in the following load cycle, the crack extension at four load cycles into future was forecasted. Seven load steps of the right and left sides crack, corresponding to approximately 38k loading intervals used to predict the crack length at four load steps into the future corresponding to 46k loading cycles. The true convex hulls of the crack at 12^{th} load step corresponding to the 46k load cycle were then computed and held out as the ground truth. Previous study showed that the multiple step prediction has lower accuracy and there is also a sudden change in the direction of crack growth after 48k load cycles. It is expected that the predictive time-series models could not accurately forecast the length and orientation of the crack immediately after this event. This affects the crack propagation result as well. Once the crack at four load steps into the future was computed, the solid model was updated with regard to the predicted crack extension. Meshing and fracture simulation steps then were done similar to the previous section.

Results and Discussion

From the single step prediction algorithm, the right and left crack extensions were predicted with 5% and 3% relative error respectively and in both cases the predicted lengths were smaller than the ground truth.

Comparison of crack length vs number of load cycles for single step prediction is shown in Figure 4.10 for the right and the left crack from experiment and FE simulation. Also, crack propagation with increasing load cycle were computed from fatigue simulation and were compared against ground truth crack propagation. The relative error of crack extension is shown in Table 4.1. It can be observed that there is a slight difference between growth of the right and left crack in both experiment and simulation. However, in the experiment the extension of cracks on both sides of the notch converge as load cycles increases, where from the fracture simulation these two numbers do not converge. The predicted crack length on the left side differs less from the ground truth compared to the right crack as the left crack predicted from the ARIMA model had lower relative error initially. Table 4.1 shows that overall, the crack extension can be predicted with a relatively small relative error with minimum of 0.34% and maximum of 12%. Average relative error for the right and left side cracks were 6.25% and 5% respectively.

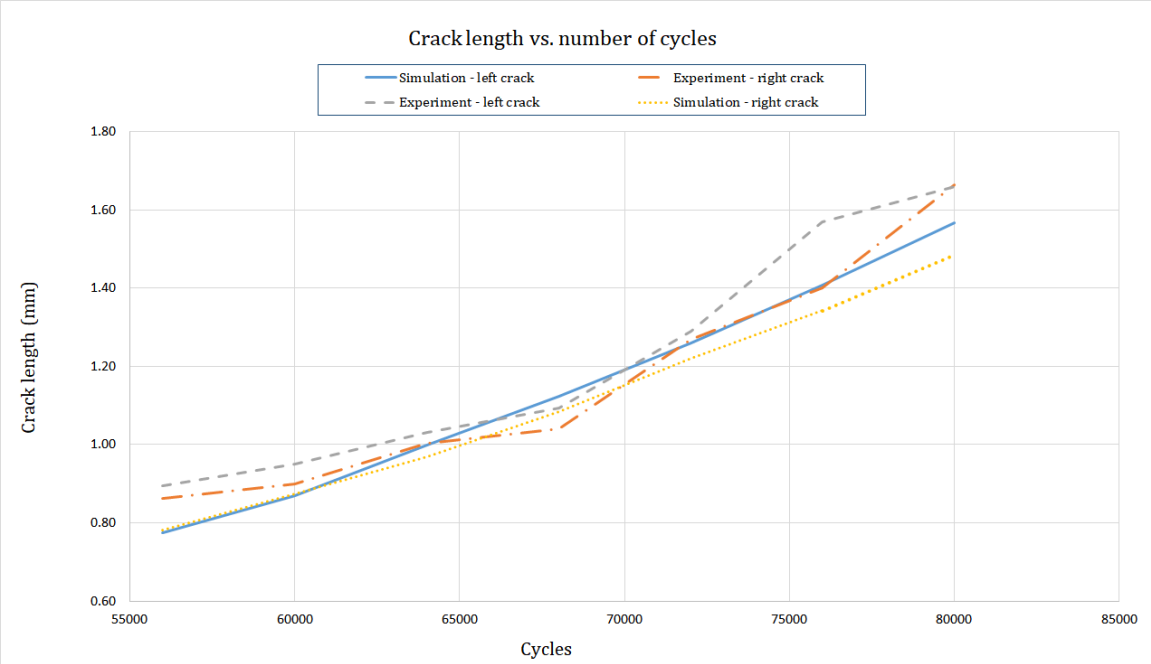

Figure 4.10. Comparison of crack length vs number of load cycles for the right and left crack from experiment and FE simulation through single step prediction.

Table 4.1. Relative error (%) of the right and left crack extension estimation.

Number of Cycles	Right Crack Error (%)	Left Crack Error (%)
56k	-12.61	-10.27
60k	-8.01	-3.30
64k	-6.16	-0.34
68k	-0.68	8.06
72k	-5.30	-0.67
76k	-0.54	6.56
80k	-10.45	-5.82

In addition, the comparison of the crack growth rate is shown in Figure 4.11. Results indicate that there is a large variation between crack growth rate from the experiment and FE simulation and at some cycles this error is about 50%. The error may come from the fracture simulation assumption. LEFM simulation directly affects the crack growth rate as it follows the Paris law, however in the experiment, the specimen may have entered the plastic zone in which the Paris equation is invalid.

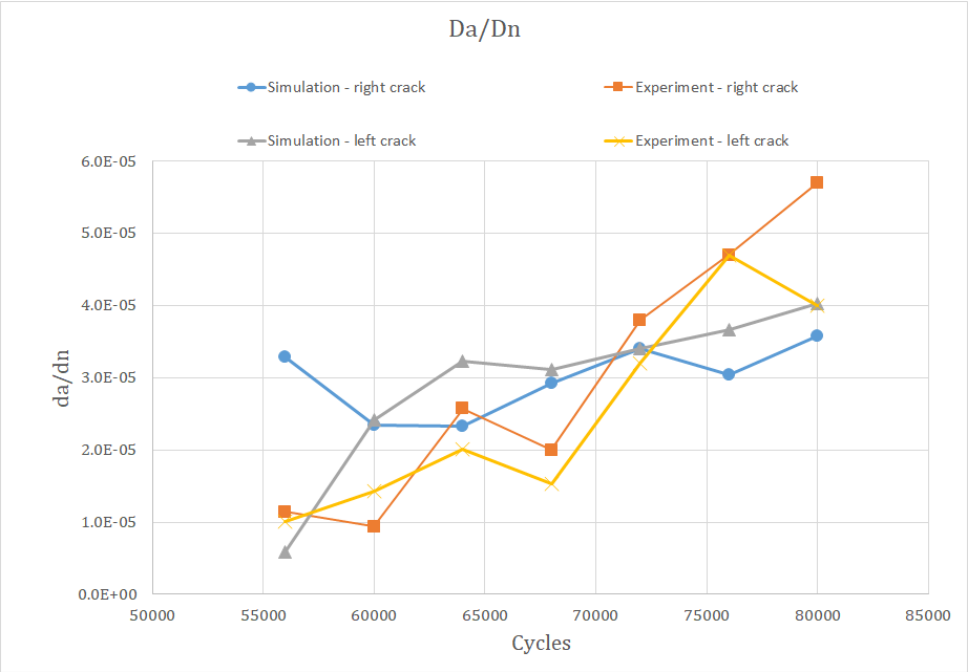

Figure 4.11. Comparison of crack growth rate vs number of load cycles for the right and left crack from experiment and FE simulation through single step prediction.

From multiple step prediction, the right and the left crack at 46k load cycles were predicted with 17% and 13% relative error respectively. Both the right and the left cracks were smaller than the ground truth. As mentioned earlier this hull estimation error comes from multiple step prediction. In addition, a nonlinear system behavior and sudden change of crack direction is another source of hull estimation error. Comparison of crack length vs number of load cycles for multiple steps ahead (4 steps) prediction is shown for the right and the left crack from experiment and FE simulation (Figure 4.12). Also, relative error of crack propagation from the simulation is shown in Table 4.2. It can be observed that the extension of cracks on the both sides of the notch unlike the experimental data diverge as the load cycle increases.

Also, it can be observed from both Figure 4.12 and Table 4.2 that the difference between experimental and simulation results reduces as the loading cycle increases. The relative error of the left crack extension at the beginning of the simulation is approximately 35% and after three loading intervals this error reduced to approximately 3%.

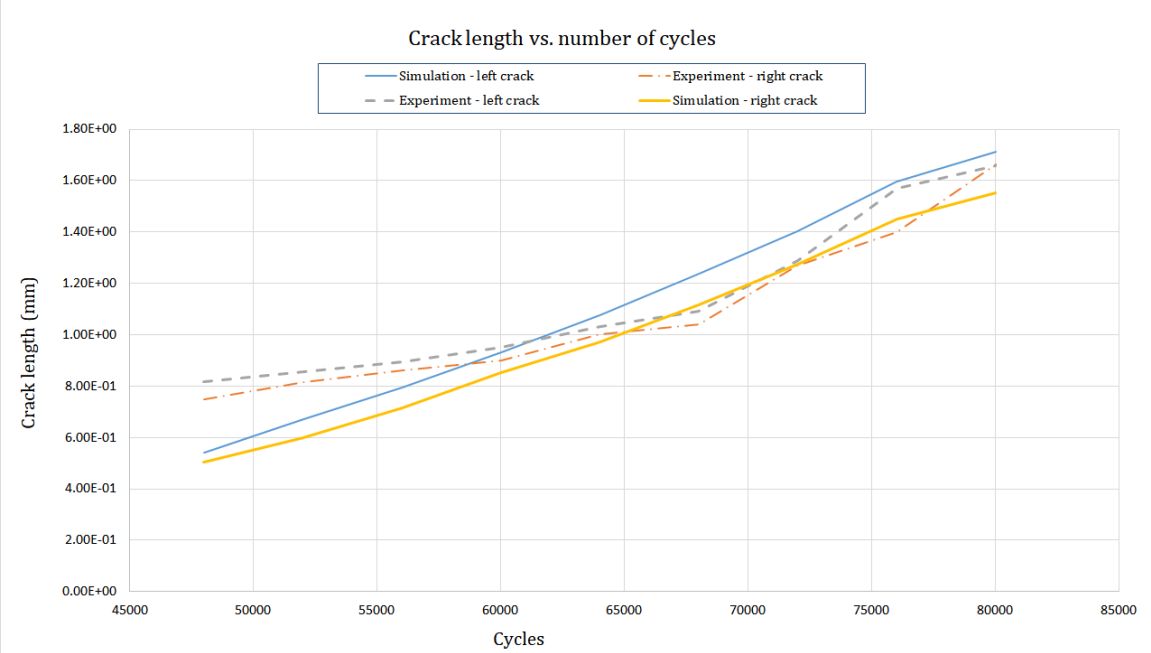

Figure 4.12. Comparison of crack length vs number of load cycles for the right and left crack from experiment and FE simulation through multiple step prediction.

Table 4.2. Relative error (%) of the right and left crack extension estimation.

Number of Cycles	Right Crack Error (%)	Left Crack Error (%)
48k	-32.56	-34.02
52k	-26.77	-21.6
56k	-17.07	-11.23
60k	-5.43	-2.26
64k	-2.98	4.38
68k	7.29	13.31
72k	0.43	8.89
76k	9.78	18.19
80k	-6.73	3.15

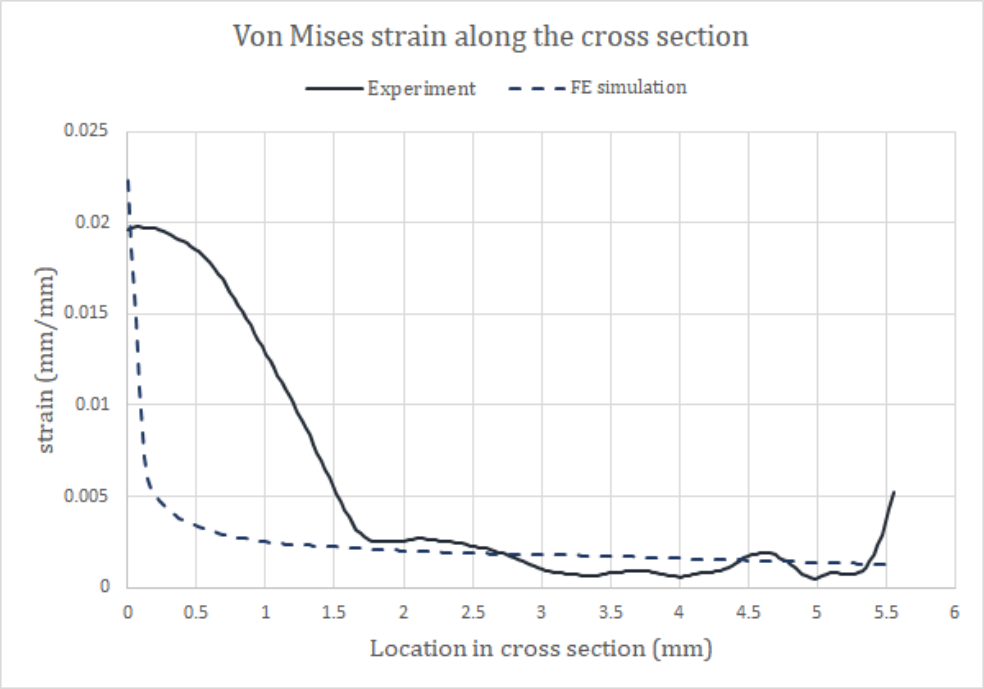

Figure 4.13. Comparison of Von Mises strain along the cross section of the specimen under 1100 N load from experiment and FE simulation.

Figure 4.13 shows the comparison of Von Mises strain along the cross section of the specimen under 1100 N load from experiment and FE simulation. The cross section is defined on the left side of the notch from the crack tip till the edge of the specimen and strain results were extracted from both experiment (DIC) and FE simulation. The predicted strain at the crack tip is very close to the experiment however, from the crack tip up until 1.5 mm away from it, discrepancies from the experiment measurements are apparent. This is due to localized plasticity and generating the plastic zone around the crack tip which was not captured in FE simulation. The strain field during increasing loading cycles shown in

Figure 4.14 for visualization purpose. It can be observed that strain around the crack tip expands in the circular region as loading cycle increases.

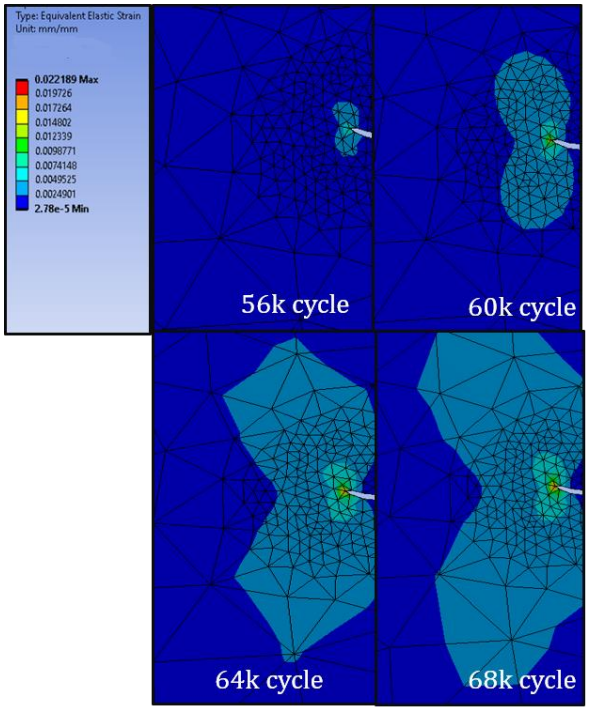

Figure 4.14. Strain field during increasing loading cycles.

Sources of error

There are several potential sources of error in this FE model updating methodology. Some errors stem from the crack identification and Poisson meshing process itself and also the crack extension prediction which tended to underpredict crack length and resulted in systematic underprediction of crack length in the FE fracture models consequently. Second, the linear behavior assumption used in the fracture simulation may have resulted in producing some error in strain computation. Finally, the Paris constants were taken from

the literature and it should be noted that the specification of the aluminum alloy, the processing condition such as temperature and air humidity, all affect the fatigue growth rate. In order to have more accurate constants, the fatigue crack growth rate (FCGR) experiments must be conducted following the ASTM E647 standard (ASTM, E08 Committee n.d.), the crack growth rate (da/dN) vs stress intensity factor range (ΔK) must be plotted to calculate the Paris constants.

Limitation of the method

While the developed FE model updating approach was shown to be effective under the experimental conditions described here, it is important to recognize the limitations of this approach. The presented fatigue test was performed under controlled laboratory conditions and was not subject to environmental variations which increase measurement uncertainty. How the fracture simulation approach performs under unpredictable loading such as varying amplitude cyclic loading and thermal conditions remains an unstudied problem. Also, more complex materials such as concrete cause highly random crack propagation and will degrade the accuracy of the crack identification and prediction consequently. Undoubtedly, field conditions are likely to degrade both the crack prediction and the FE model updating performance.

Conclusion and Future Work

In this work, a methodology to update the finite element model of structural components with regard to the future state of the crack based on the computer vision technique is introduced. Solid model of the structural component was updated in two steps to overcome the limitation of parameterization approach. 2D experimental point clouds

representing crack growth with increasing loading cycles were used to predict the crack extension in the future cycle. The future crack extension (i.e. length and orientation) was predicted via time-series model. The solid model of structural components was updated once again based on the predicted crack extension. Once updated, the solid model was meshed and LEFM was conducted.

The results indicate that linking the future state of the crack to FE model of structures provides a basis for future predictive simulation. The proposed methodology has several advantages over current practices. Firstly, it provides engineers a basis to study the crack propagation involving the geometry and location of crack. Secondly, it is capable of linking the FE model of structures to the future state of the crack and capturing the actual shape of the crack. Linking the FE model to the evolution of crack and evaluating the structural performance also results in more reliable forecasting capabilities and a more complete understanding of structural performance. This will lead to better system asset management decision-making, with apparent safety and financial benefits.

This study was part of an ongoing research program, and various parts of the presented methodology is being considered for further improvement.

The limitations discussed in section *Sources of error* highlight potential avenues for future work. The performance of the FE model updating approach under environment uncertainty and material variability should be investigated. More datasets from other crack scenarios should also be considered, for instance, concrete or asphalt cracking in civil infrastructure. Such studies may provide insight into how particular algorithmic aspects, such as crack identification, prediction and projection (see methodology section), behave

under complex material phenomena. Effect of varying amplitude cyclic loading also must be evaluated as it reflects the real-world scenarios. One notable avenue for future work is to adapt the algorithm to more complex fracture mechanics study such as Elastic Plastic Fracture Mechanics (EPFM) to estimate the crack growth rate.

CHAPTER FIVE: FUSION AND VISUALIZATION OF BRIDGE DECK NONDESTRUCTIVE EVALUATION DATA VIA MACHINE LEARNING

Introduction

To preserve infrastructure safety and integrity, reliable and effective damage detection techniques need to be established. Increasingly, nondestructive evaluation (NDE) technologies are used for the detection of surface and subsurface defects, evaluation of the extent of defects, and as a critical aspect of holistic asset management. A key challenge with NDE is that the accuracy of the data from a single source is dependent on operator training and environmental conditions that can add considerable uncertainty to defect detection and quantification (McCann and Forde 2001). From a practical standpoint, this measurement uncertainty has inhibited the adoption of NDE across many application domains.

To reduce measurement uncertainty, researchers have explored the concept of using multiple NDE methods in conjunction with data fusion algorithms. Recent advances in sensing and data analytics have led to the adoption of data fusion in fields such as computer vision and image analysis (F.-C. Chen et al. 2017), transportation systems (Faouzi, Leung, and Kurian 2011; Faouzi and Klein 2016), biometrics (Haghighat, Abdel-Mottaleb, and Alhalabi 2016), and structural health monitoring (Sun, Lee, and Lu 2016; R.-T. Wu and Jahanshahi 2018; Ramos et al. 2015; F.-C. Chen et al. 2017; Habib et al. 2016; Kralovec and Schagerl 2020). In these cases, the use of data fusion was shown to provide a better interpretation of observed information by decreasing the measurement uncertainty present in individual source data (Faouzi and Klein 2016).

Data fusion encompasses a vast array of analytical methods ranging from Bayesian probabilistic approaches, Dempster–Shafer (DS) evidence approaches, fuzzy reasoning, and machine learning (R.-T. Wu and Jahanshahi 2018; Khan and Anwar 2019). These methods have been used for damage identification, quantification, and system response estimates (D. Hall and Llinas 2001; Chair and Varshney 1986; Liu et al. 1999; Vanik M. W., Beck J. L., and Au S. K. 2000). For example, a recursive Bayesian framework was used to update the parameters of a crack growth model, as well as the probability distribution of the crack size and crack growth rate (Rabiei and Modarres 2013), and a neural network and fuzzy inference were combined to evaluate the structural condition of a cable bridge (Sun, Lee, and Lu 2016).

Data fusion can generally be carried out at various "levels" of data processing ranging from combinations of raw data to a fusion of individual operational decisions (Steinberg and Bowman 2017). Data-level fusion refers to combining raw data directly and it is possible only if the sensors measure the same physical quantities. On the other hand, if the survey observations are heterogeneous, then the data must be fused at the feature-level or decision-level. For feature-level fusion, a vector of data descriptors is extracted from the raw measurements of individual NDE results and the features are then combined together into a single concatenated descriptor vector (S.-L. Chen and Jen 2000). This combined vector can be further processed through machine learning techniques based on neural networks or clustering algorithms (Kittler 1975; Sun, Lee, and Lu 2016). Once features are fused through machine learning, the resulting output reflects the correlations in data content and reduces the uncertainty of results. Decision-level fusion is the blending

of operational decisions derived from individual data streams considered in isolation. Decision-level fusion naturally leads to loss of performance, but this type of fusion represents a feasible fusion approach when fusion at lower levels is not practical or advisable.

Frequently applied fusion methods in structural health monitoring include: Bayesian probabilistic approaches including techniques such as Kalman filtering (Vanik M. W., Beck J. L., and Au S. K. 2000; Rabiei and Modarres 2013; Ramos et al. 2015), Dempster–Shafer (DS) evidential reasoning (H. Wu 2004; Huang, Liu, and Sun 2014), and machine learning algorithms such as artificial neural networks (ANN) (F. Chen and Jahanshahi 2018; Jiang, Zhang, and Zhang 2011) or support vector machines (SVM) (Q. Zhou et al. 2015). SHM applications tend to focus on the fusion of time-series sensor data, such as from accelerometers, to reduce measurement and state-estimation uncertainty.

In this work, the application of machine learning driven data fusion to the NDE assessment of concrete bridge decks is considered. Bridge deck deterioration plays a critical role in highway asset management due to the costs and traffic disruptions associated with deck repair and replacement. While pattern analysis and machine learning have been studied for use with individual concrete NDE methods, they have not been considered as a basis for data fusion. Furthermore, how the results of NDE data fusion can be intuitively visualized and assessed holistically by engineers remains an under-studied problem.

The primary contributions of this work are:

• A wavelet-based approach to extracting statistically relevant features from NDE Waveforms

• A non-parametric machine learning approach to the fusion of NDE data features

• A novel visualization schema for representing the fused results and measurement uncertainty

In order to best illustrate the benefits of NDE fusion, the machine learning models developed in this work were trained and evaluated for the detection of single defect classes (binary classification). As such, they do not provide defect diagnosis across a range of observed defects. Such considerations may lead to different conclusions regarding fusion efficacy and are an avenue for future work.

The remainder of this paper is structured as follows. First, the overall methodological framework is presented. This is followed by an experimental case study to illustrate the behavior and performance of the approach, based on laboratory scale data collected at the Turner-Fairbank Highway Research Center (TFHRC). The NDE data for this case study was captured in a manner that mimicked the NDE systems available onboard an inspection robot developed at TFHRC, illustrating a potential practical application for the proposed framework. The following NDE methods were considered (see Experimental Validation for more details): ultrasonic surface waves (USW), impact echo (IE), ground penetrating radar (GPR), electrical resistivity (ER), ultrasonic tomography (UT), half-cell potential (HCP), infrared thermography (IRT), and impulse response (IR). The paper concludes with a discussion of outstanding research efforts that must be considered prior to practical implementation.

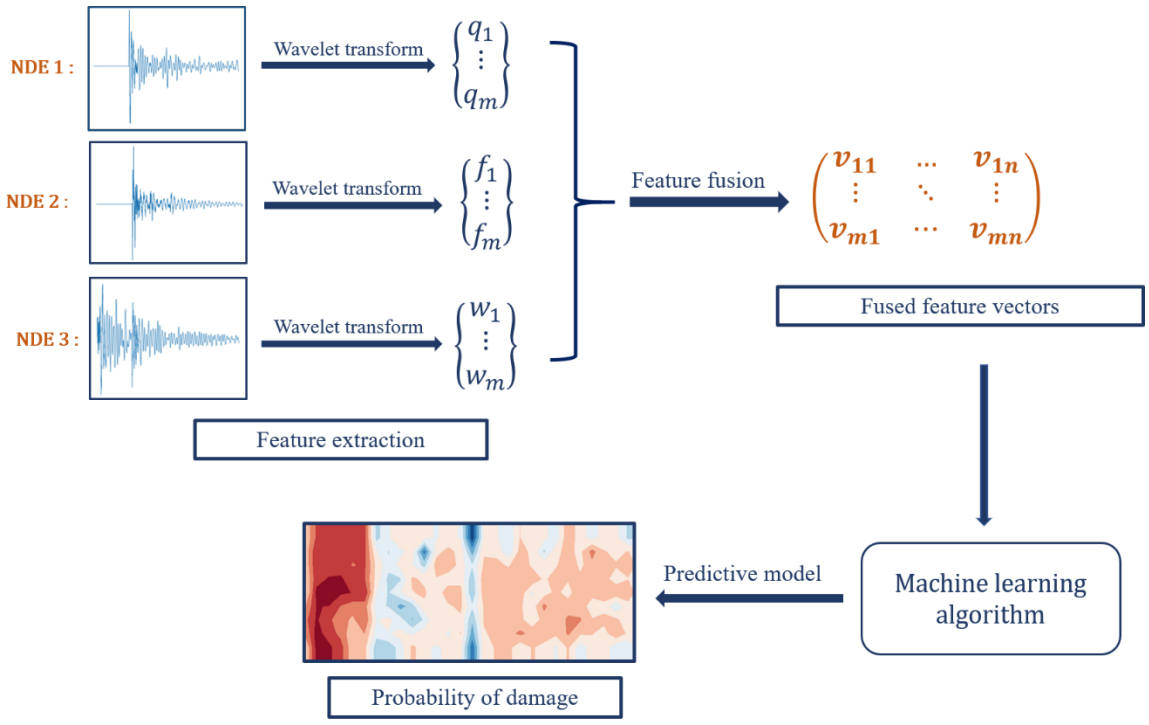

Figure 5.1. Schematic overview of the proposed methodology for multiple NDE feature fusion.

Methodology

The primary focus of this study was on the development of a feature-level fusion approach (Figure 5.1). A decision-level fusion approach was also developed for comparative purposes and is discussed in Decision Fusion. First, data from multiple NDE sources are preprocessed for spatial registration and salient numerical features are extracted from each NDE data source. Feature extraction is achieved through the discrete wavelet transform (DWT). Once extracted, features are combined into a concatenated feature (descriptor) vector. This feature vector then serves as input to a supervised machine learning classifier trained to detect subsurface defects in the concrete specimen. For model training, features extracted from test data were manually labeled to generate a ground truth.

Once the machine learning model assesses the likelihood of a defect at each location along a bridge deck, the probability of occurrence of damage across the deck is visualized as a red-blue heatmap.

Data Preprocessing

Data preprocessing encompasses a range of tasks such as data cleaning, data transformation, and feature extraction (Nantasenamat et al. 2009). In this work, the emphasis for data preprocessing is on making heterogeneous NDE datasets spatially compatible followed by feature extraction. Even for robotic multi-NDE systems, discrepancies in the location of measurements is inevitable. To accommodate, measurements are linearly interpolated onto a consistent 2D grid spacing. Incomplete data is also an inevitable problem in handling most real-world data sources and is interpolated as well.

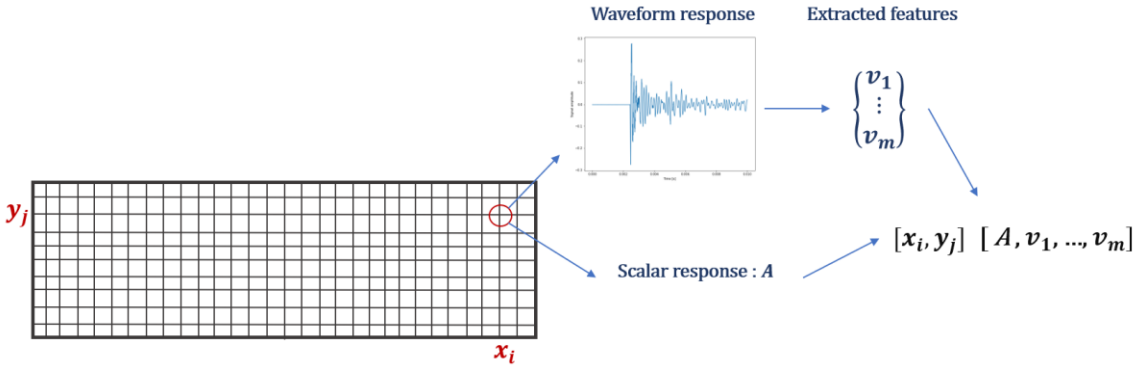

Figure 5.2. Combining scalar and waveform responses of interpolated data.

Some NDE techniques provide scalar valued measurements at each test point (e.g., HCP or ER) while others produce a waveform result (e.g., IE or GPR). This data heterogeneity necessitates fusion at either the feature or decision-level. To fuse at the feature-level, numerical feature must first be extracted from waveform measurements. These descriptors are then concatenated with scalar response data (Figure 5.2).

Waveform feature extraction

Feature extraction refers to the process of extracting statistically salient numerical descriptors from the original data. In most conventional approaches to NDE data analysis, feature extraction has focused on reducing an NDE waveform measurement to a single scalar-valued representation. For data fusion, such approaches dramatically reduce the amount of relevant information. The wavelet transform is a time-frequency analysis technique that is commonly used for advanced signal processing (Daubechies 1992). It was developed as an alternative to the short time Fourier (S. G. Mallat 1989; Nouri Shirazi, Mollamahmoudi, and Seyedpoor 2014) to overcome problems related to the simultaneous representation of frequency and time resolution properties. Compared to a traditional Fourier analysis, a wavelet transformation has the ability to simultaneously reproduce temporal and scale data, making it better suited for analyzing signals that are periodic, transient (or nonstationary), and noisy. As a result, wavelet transforms are increasingly employed in numerous applications for feature extraction (Epinat et al. 2001; Ghazali et al. 2007; Luk et al. 2008; Al Ghayab et al. 2019). In particular, wavelet transforms have recently seen use in SHM and NDE analysis, for instance in the assessment of acoustic IE

measurements of concrete slabs (Saadat et al. 2004; Khatam et al. 2007; Yeh and Liu 2008; Hou, Jankowski, and Ou 2015).

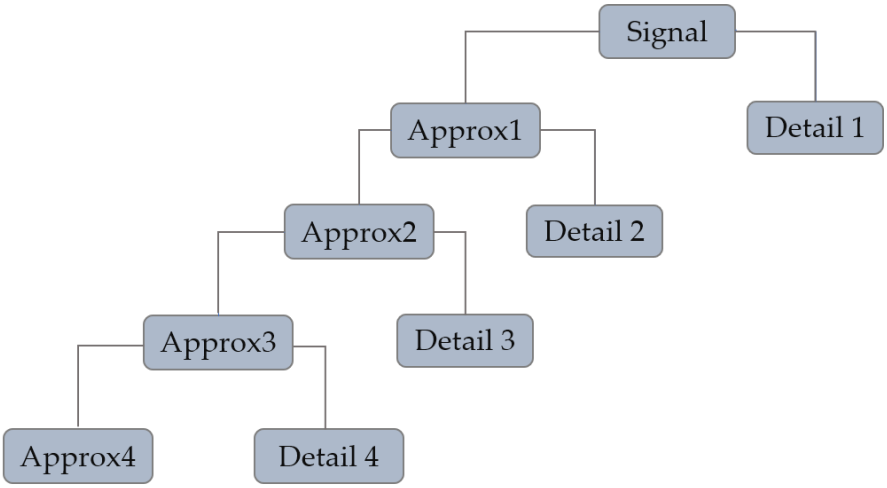

Figure 5.3. Schematic discrete wavelet transforms for the four-level Symlet wavelet decomposition used in this work.

Wavelets can be considered as a family of functions constructed from translations and dilations of a single function called the "mother wavelet" $\psi(t)$ (S. Mallat 2009). They are defined by the following equation:

Equation 5.1

$$\Psi_{a,b}(t) = \frac{1}{\sqrt{|a|}} \Psi \left(\frac{t-b}{a}\right) \qquad a, b \in R, a \neq 0$$

The parameter a is the scale, and it measures the degree of compression. The parameter b is the translation parameter that determines the time location of the wavelet and t is time (Debnath and Shah 2014). For a signal $s(t)$, the transformed wavelet representation of the signal, W_s , at scale a, position b is defined as an inner product:

Equation 5.2

$$W_s(b,a) = \int_{-\infty}^{\infty} s(t) \frac{1}{\sqrt{|a|}} \Psi \left(\frac{t-b}{a}\right) dt$$

The wavelet transform can be implemented in either a continuous or discrete form. The widely used DWT is employed in this study. DWT is an adaptive decomposition which decomposes a signal with high- and low-pass filters and increases the frequency resolution in lower frequency bands (G. Zhang et al. 2018). The DWT decomposes a signal onto a set of bases that correspond to different time and frequency scales or resolutions (Figure 5.3). At the first stage of decomposition, the initial signal is decomposed into approximation and detail coefficients. The first level approximation coefficients are further decomposed into second-level approximation and detail coefficients, and the process is repeated, resulting in levels of approximation and detail that capture both frequency and time domain information about a signal (J.-K. Zhang, Yan, and Cui 2016). The approximations are the high-scale, low-frequency components of the signal, while the details are low-scale, high frequency. This wavelet decomposition also suppresses signal noise, effectively serving to denoise the signals prior to data fusion.

In this work, a fourth order variant of the Daubechies wavelet, known as the Symlet wavelet, is used in conjunction with the DWT. This particular wavelet feature extraction approach was first developed in (J.-K. Zhang, Yan, and Cui 2016) for the analysis of IE data. In this study, this wavelet extraction approach is applied to both IE and GPR signals. Both IE and GPR signals are considered transient in nature with nonstationary noise characteristics, indicating that they are well suited for wavelet representation (X. Zhang et al. 2018).

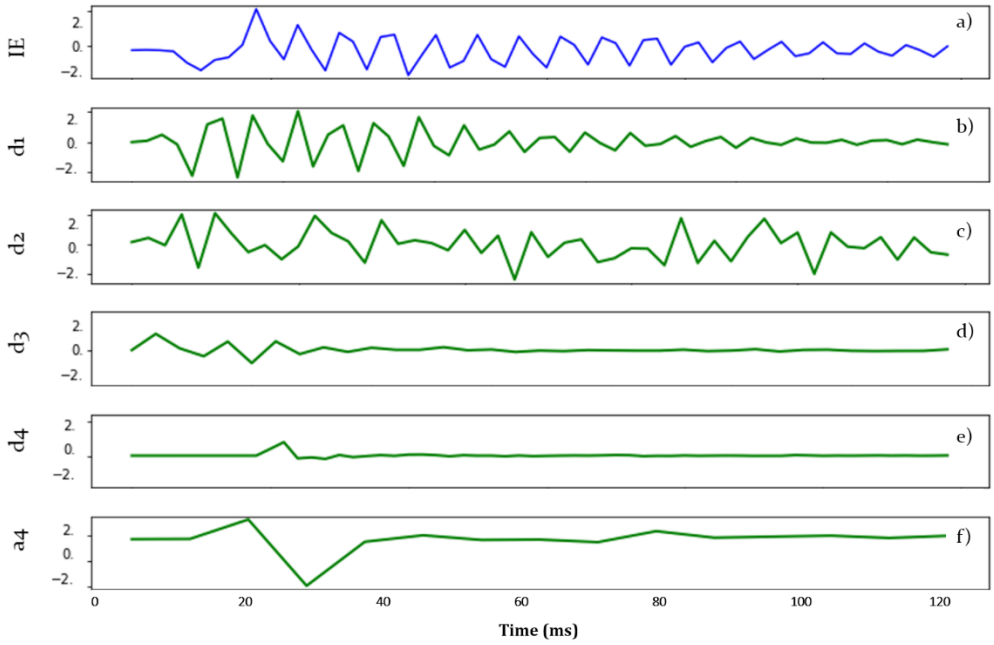

Figure 5.4. A) Original IE signal; (B–E) reconstructed detail coefficients at level 1(B), level 2 (C), level 3(D), level 4(E); (F) reconstructed approximation coefficients at level 4.

Based on prior studies and empirical analysis by the authors, a four-level decomposition is adopted for both IE and GPR signals and decomposition, as illustrated in Figure 5.4. After decomposition and reconstruction of sub-signals, four features are extracted from each wavelet basis. The root mean square (i.e., average power of signal), standard deviation (i.e., Second spectral moment), kurtosis (i.e., Third spectral moment) and skewness (i.e., Fourth spectral moment). Overall, this results in 20 features for each original measurement signal. These features extracted from IE and GPR signals are later

combined into a vector as an input to a given statistical model. The functions for feature calculation are defined as follows: Let x_n, n =1, 2, . . ., N be the time domain signals and $[p_i, f_i]$, i = 1, 2, . . ., M be its corresponding spectrum, where p_i and f_i are the amplitude and the frequency at i_{th} frequency bin, respectively.

$$Total\ Power: TP = \sum_{i=1}^{M} p_i\ ,\ \ Centroid: M_1 = \sum_{i=1}^{M} p_i \,.\, f_i / TP$$

Equation 5.3

$$Root\ Mean\ Square = \sqrt{1/M \sum_{i=1}^{M} p_i^2}$$

Equation 5.4

$$Standard\ Deviation: M_2 = \sqrt{\sum_{i=1}^{M} (f_i - M_1)^2 . p_i / TP}$$

Equation 5.5

$$Skewness: M_3 = \frac{\sum_{i=1}^{M} (f_i - M_1)^3 . p_i}{{M_2}^3 . TP}$$

Equation 5.6

$$Kurtosis:\ M_4 = \frac{\sum_{i=1}^{M} (f_i - M_1)^4 . p_i}{{M_2}^4 . TP}$$

Data interpolation

In a multi-NDE assessment scenario, the goal is to capture measurements at identical locations across an assessment area. However, the practicalities of NDE mean that it is typically not possible to achieve this goal. For instance, in the experimental study of this work, NDE measurement spacing was not consistent across NDE techniques and

there were intermittent missing measurements. Prior to data fusion, NDE values must be interpolated onto a consistent grid spacing. In the example shown in Figure 5.5, the grid spacings of measurements NDE 1 and NDE 2 are different. Features from NDE 2 are measured at grid points x_0, x, and x_1, resulting in measurements u_0, u, and u_1. Features extracted from NDE 1 are only measured at grid points x_0 and x_1 (measurements f_0 and f_1). The features f at location x is linearly interpolated via first order polynomial. The relationship between spatially distributed NDE measurements is not well-defined, and more complex interpolation approaches could prove more suitable. This is one potential avenue for future study.

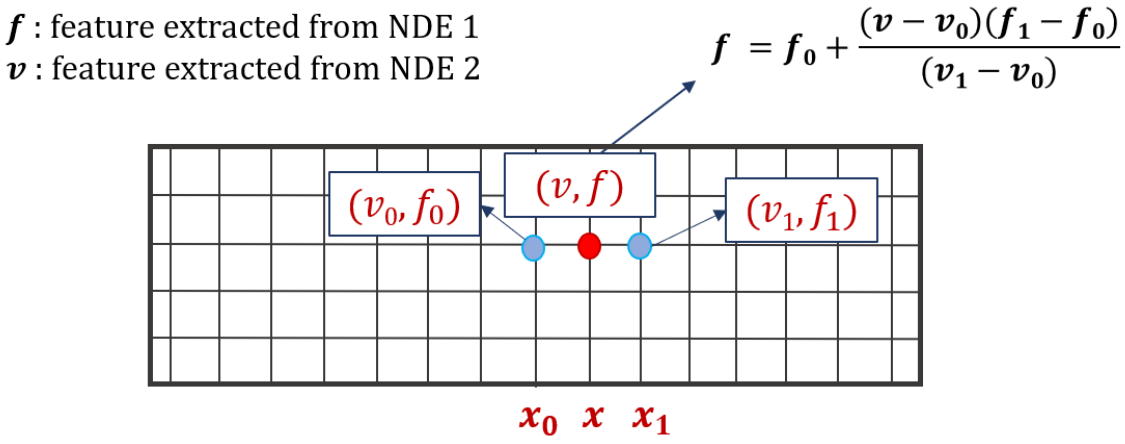

Figure 5.5. Linear interpolation of NDE data.

Data Fusion

As discussed previously, feature and decision-level fusion are considered in this study because the heterogeneity of bridge deck NDE data prohibits the use of data level

fusion. In general, the "higher up" in the fusion ontology from data to decision-level, the greater the loss of information. As such, it is generally advisable to fuse data at the lowest possible level, motivating the focus on feature-level fusion in this work.

The general concept is to take the concatenated set of wavelet features extracted from each NDE measurement (Waveform Feature Extraction) at each location and use the combined vector of features as the inputs into a statistical model that associates the vector with a statistical assessment of material condition. Here this statistical model takes the form of a statistical classification problem, one that classifies a feature vector as being a member of either a "detected defect" or "sound concrete" assessment class. Multiclass classifications are also possible, though they were not extensively studied here due to limited data availability (see Experimental Validation for more details). Ultimately, the end result is that the raw data from each NDE source is effectively fused together to provide an enhanced assessment.

There are a broad range of classification algorithms that can be used such purposes. Generally, they can be divided into parametric and nonparametric methods. Parametric techniques make assumptions about the underlying statistical distribution or the measurement uncertainty of observations in order to enable inference. Implicitly, such techniques often require statistical stationarity, as well as consistent and quantifiable measurement uncertainty. The alternative are nonparametric fusion methods. Nonparametric methods relax assumptions regarding underlying statistical distributions and instead construct a model of measurement states from sets of existing data (Tsiliki and Kossida 2011). Such approaches have the advantage of being applicable to highly complex

and nonlinear statistical problems. Machine learning approaches have become the dominant paradigm for nonparametric data fusion, with ANN and SVM as the most widely used approaches. ANN have the advantage of being more flexible with respect to data input and can be highly tuned for optimization to a specific problem domain. SVM have fewer user parameters (hyperparameters), making them more suitable for rapid prototyping and problems with less data available for model training (Dong et al. 2009). Given the limited size of the available data sets for prototyping, the focus here is on the use of SVM. The behavior of several other methods are presented as well for comparative purposes. These methods included: logistic regression, decision tree-based models and ANN. The weighted decision-level fusion is also studied and is briefly discussed (Lu and Michaels 2009; Heideklang and Shokouhi 2013).

Conventional machine learning performance metrics are used to assess data fusion capabilities, including confusion matrices, ROC curves and F1 scores (Fawcett 2006). While classifiers typically produce a discrete classification, statistical probabilities are used for class separation. This statistical probability provides a more nuanced representation of classifier performance and can be used for holistic assessment and visualization purposes (see Holistic Visualization for details).

Feature fusion – SVM

SVM are a group of algorithms that were originally designed for binary classification and gained popularity due to promising performance in a wide range of applications (Cortes and Vapnik 1995; Cristianini and Shawe-Taylor 2000; A. Ruiz and Lopez-de-Teruel 2001). SVMs attempt to discriminate between classes of data by finding

the optimal high-dimensional hyperplanes that bisect the data, and then combining these hyperplane bi-sections to enable more complex reasoning. The original data points from an input feature vector is projected by a kernel function into a higher dimension feature space (Figure 5.6). In this space, SVM tends to find the hyperplane that separates the data with the largest margin. The method places class-separating hyperplanes in the original or transformed feature space, and the new sample is labeled with the class label that maximizes the decision function—the distance between support vectors (Boser, Guyon, and Vapnik 1992, 199; Vapnik 2000).

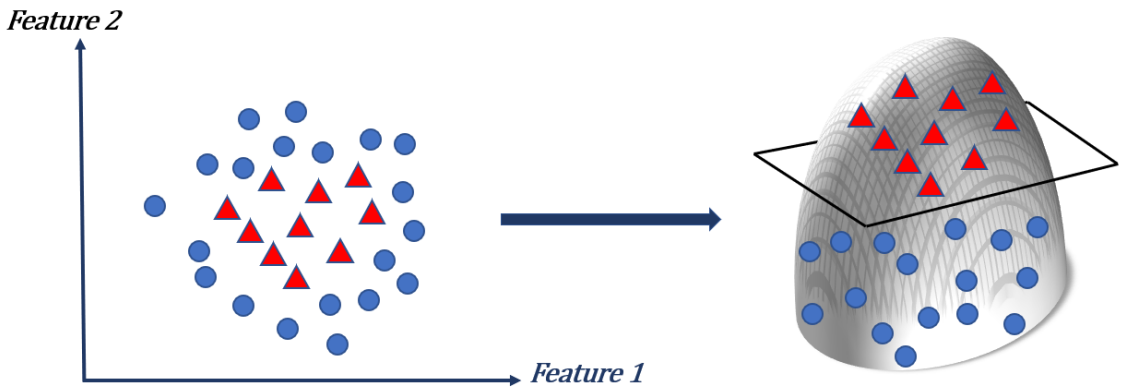

Figure 5.6. Support Vector Machine illustration of projection of 2D data into a higher dimension through kernel function projection.

The SVM is especially suited for scenarios with smaller sample sizes, as is the case for many NDE assessment scenarios (Luts et al. 2012). In contrast to other algorithms, SVM tends to use all available features, even if they are not of real statistical

importance, and therefore requires more care regarding cleaning and preprocessing of the input data.

SVM standardization

Standardization (i.e., feature scaling) refers to the process of rescaling the values of the input variables so that they share a common scale, in order to reduce classifier biasing. Standardization is an important step for SVM classifiers. For instance, many elements used in the RBF kernel of Support Vector Machines assume that all features are centered around 0 and have variance in the same order. If a feature has a variance that is orders of magnitude larger than others, it can potentially dominate the objective function and make the estimator unable to learn from other features. Data standardization also can speed up training time of SVM by starting the training process for each feature within the same scale (Kotsiantis, Zaharakis, and Pintelas 2006). Here, features are standardized by removing the mean and scaling to a unit variance. The standard score of a sample x is calculated as:

Equation 5.7

$$Z = \frac{(x - u)}{s}$$

where u is the mean of the training samples and s is the standard deviation of the training samples (Shanker, Hu, and Hung 1996). Centering and scaling happen independently on each feature by computing the relevant statistics from samples in the training set. These scaling parameters are then applied to the test data.

Hyperparameter identification

Prior to model training and fitting, the model hyperparameters must be optimized (T. Wang et al. 2010). Good model selection is the key to getting good performance from any machine learning algorithm. Also, if the hyperparameters are not selected appropriately, an SVM may take an unduly long time to train (Nalepa, Kawulok, and Dudzik 2018). The SVM model contains two main parameters that must be optimized: the kernel function used for dimensional reprojection, and the regularization parameter (c). SVM algorithms can use different types of kernel functions such as linear, polynomial, sigmoid, and radial basis functions (RBF). The regularization parameter (c) is used to prevent overfitting. In this study, a hyperparameter search (grid search) is performed across combinations of different kernel functions and regularization parameters. The performance of the selected hyperparameters and resulting trained model is then measured on a dedicated evaluation set that was not used during formal model selection and training. Different combinations of hyperparameters are compared against each other based on model predictive performance. For the experimental data set discussed in Experimental Validation, a combination of the Radial Based Function and regularization parameter, c, equal to unity showed the best performance among all combinations.

Other considered classifiers

To provide a point of comparison with SVM data fusion, logistic regression, decision trees, and ANN are presented and evaluated here as well. Logistic regression is a simple, parametric machine learning algorithm which assumes a linear mapping function between input data and output classification and has been used extensively in the data

fusion literature (Pigeon, Druyts, and Verlinde 2000). Generally, this function is a linear combination of the input variables. The benefit of the algorithm is that it does not require as much training data as methods such as methods such as SVM and ANN, however it is constrained to the specified logistic functional form, which may or may not be sufficiently accurate. As will be shown in Experimental Validation, since logistic regression is only suitable for linear problems, its performance was strongly biased to one of the technique's results and did not provide a true fusion of information for NDE data.

Tree-based learning models such as the Decision tree (DT) classifier are nonparametric algorithms that first select the best feature for an initial separation of the data (root node) using the concept of information gain ratio. It then builds subtrees and nodes in a recursive manner that splits the data into classes based on an evaluation of each feature in an input vector (Demirbas 1989). Decision trees generally work better for larger datasets and are prone to overfitting.

An ANN employs a complex network of nonlinear response functions, with the value of each function in the network weighted based on an optimized fitting to training data (A. Zhang et al. 2017). The input "layer" of the network can range from combinations of raw data to a set of extracted data features to a numerical representation of a set of decisions. The output can be a layer of the same size and type as the input, or smaller. Increasing the complexity of an ANN architecture allows for more nonlinear and sophisticated representations and fusions and is the basis for modern deep learning strategies. However, such increases in complexity typically require even larger increases in the amount of training data used to find network weights. Similarly, SVM outperformed

the ANN in the preliminary analysis. The reason is that unlike ANNs, the computational complexity of SVMs does not depend on the dimensionality of the input space. ANNs use empirical risk minimization, while SVMs use structural risk minimization. The reason that SVMs often outperform ANNs in practice, particularly for smaller data sets, is that SVMs are less prone to overfitting (Olson and Delen 2008). In recent years, deep learning–based approaches have become popular across research fields due to their ability to automatically learn meaningful feature representations from the raw data (Hinton, Osindero, and Teh 2006, 200; Najafabadi et al. 2015). However, for smaller dataset sizes, such as those in this study, deep learning algorithms do not perform well and become prone to overfitting (Brownlee 2017).

Decision fusion

Decision-level fusion combines information after each sensor source has been independently processed to make a preliminary determination of the existence of damage. Such fusions are valuable when an effective workflow for using a single data source in decision making already exists. Decision-level fusion then allows those existing workflows to be integrated and combined. As a point of comparison, the weighted decision algorithm (D. Hall and Llinas 2001) was used in this study.

Weighted decision makes assumption that each individual assessment has its own weight with respect to accuracy or validity. These weights can be assumed equal for simplicity, however usually the decision from a data source with less precision and confidence is assigned a smaller weight contribution prior to the fusion. For classification tasks, the selection of appropriate thresholds is needed to assign the predicted damage

pattern. This method therefore requires a priori assumptions regarding statistical distributions or the uncertainty of any given measurement.

It should be noted that many data fusion techniques can be used for decision-level fusion as easily as they can for feature or data-level fusions. What differs across these levels is the simplicity of the inputs to the algorithms, with data-level fusion requiring the largest and most complex inputs and decision-level requiring the simplest, with correlated requirements for the size of the data necessary for training and testing. Feature-level stands as a flexible compromise between the two extremes.

Holistic Visualization

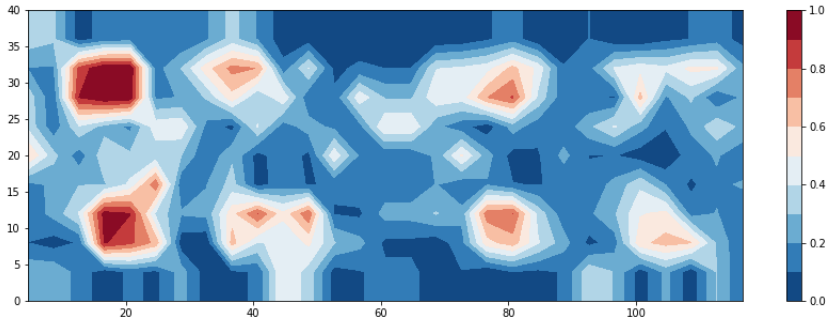

Figure 5.7. Heat map showing confidence of defect prediction.

The developed approach to visualization stemmed from a series of interviews the authors performed with NDE end-users, as well as recent advances in data visualization (Rangwala, Kauffman, and Karypis 2009; Choo et al. 2012). Rather than present the discrete output classification of the machine learner at each measurement location, the model's statistical confidence in its prediction is presented (Figure 5.7). To accomplish

this, the aggregated detection results across the deck slab are shown as a contour heat map, as is common practice. But rather than indicate a discretized detection, what is shown is in fact the machine learning model's classification confidence at each location, represented by a probability score ranging from 0.0 (confident in no defect) to 1.0 (confident in a detected defect). Once the probability of a defect's existence is estimated by the fusion algorithm for each measurement grid location, the grids with the same probability value range are then connected through polygonization. Further polygons are filled with varying shades of color corresponding to their probability score (Figure 5.8). The heat map uses a two-color diverging heat map scale, with varying shades of blue if no defect is more likely, and varying shades of red for a likely detected defect (Moreland 2009). Lighter color intensity indicates lower model confidence, with a white midpoint suggesting no confidence in an assessment. The resulting heatmap provides end users with a data product that is familiar to them while presenting nuanced information in an intuitive and comprehensible format. Moreover, the confidence thresholds can potentially be tuned and controlled by the end user, as several interview participants requested.

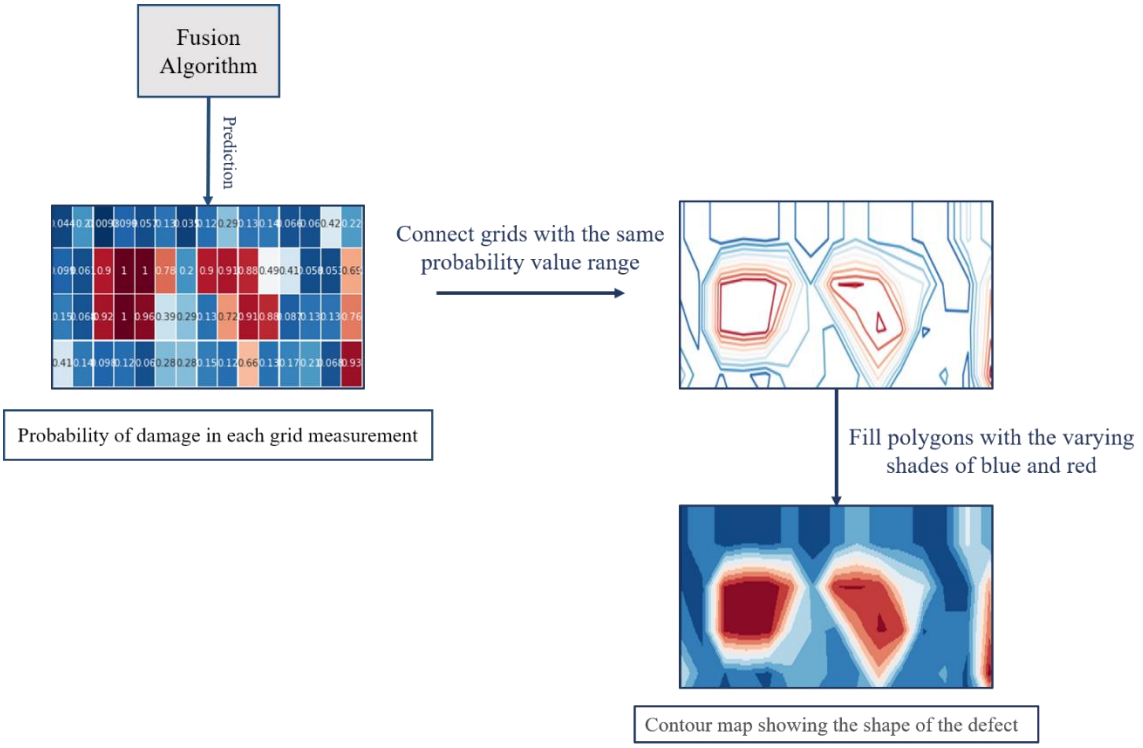

Figure 5.8. Flowchart of the process for generating fusion confidence visualizations.

Experimental Validation

This section presents an experimental study designed to illustrate the potential capabilities of a machine-learning approach to data fusion. Prior to this study, researchers at Turner-Fairbank Highway Research Center (TFHRC) constructed a series of laboratory-scale bridge decks and performed a set of NDE assessments on those decks. Overall, eight NDE techniques were used to collect synchronous data from the specimens. Four of these NDE measurements simulate measurements from the Federal Highway Administration (FHWA) Robotics Assisted Bridge Inspection Tool (RABIT), a robot designed to perform synchronous multi-NDE assessments of bridge decks (Gucunski et al. 2017; Gibb et al.

2018; Ahmed, La, and Gucunski 2020; La et al. 2017). The other four are commonly used techniques for bridge deck NDE.

The data from these NDE assessments was used to prototype and test the data fusion algorithms discussed in Methodology. The performance of the data fusion algorithm was tested for two different types of defects and NDE methods. The first set of tests focused on deck corrosion detection, while the second sets of tests explored algorithm performance for sub-surface delamination detection.

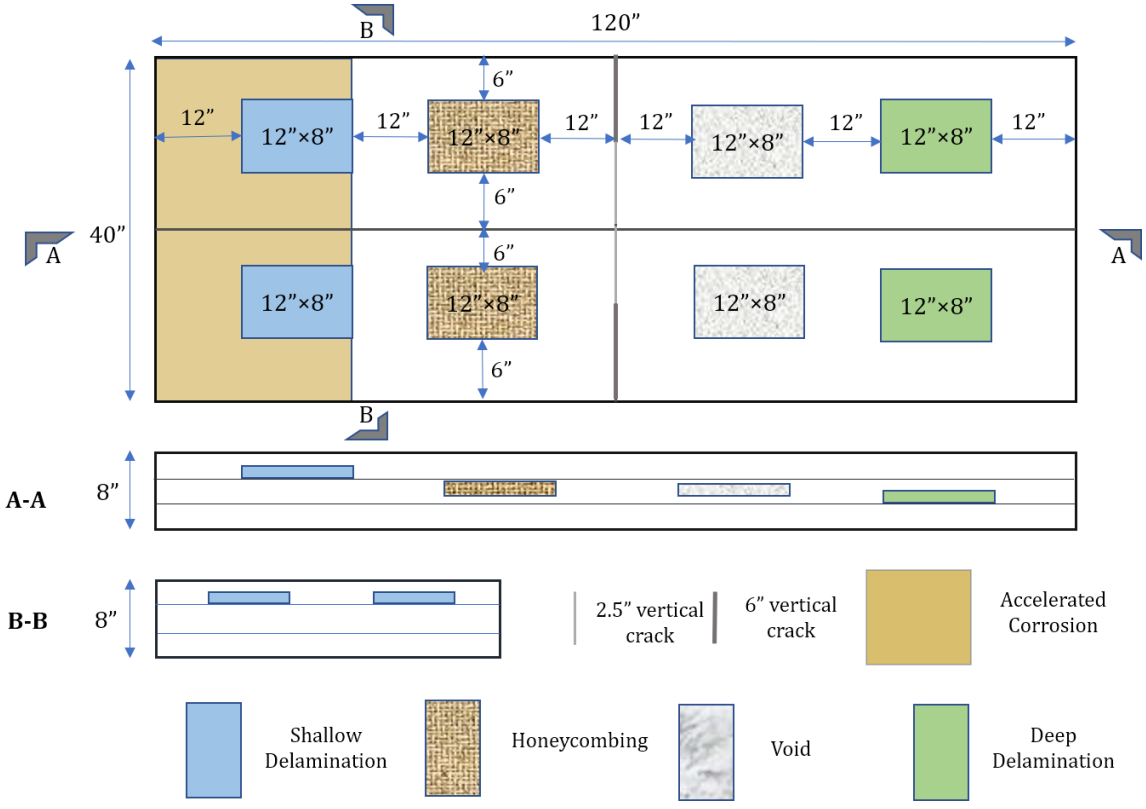

Figure 5.9. Laboratory-scale bridge deck specimen design. Section **(A-A)** shows the location for each defect type with respect to slab depth. Section **(B-B)** shows defect placement for shallow delaminations. The placement of other defects in the cross-section is similar, accounting for variations in depth.

It is important to note that these experiments were all performed under idealized laboratory conditions. While the test specimens and data are representative of real-world scenarios, environmental conditions and the practicalities of full-scale field assessments will inevitably degrade algorithm behavior. Still, the results of these experiments illustrate the potential benefits of data fusion and serve as motivation for larger-scale testing under field conditions.

Table 5.1. Details of NDE measurements used for data fusion.

Method	Measurement spacing	Number of samples prior to interpolation
IE	4 inches - data was not collected at centerline vertical crack	2016
GPR (A- scan)	9 longitudinal scan lines at 4 inches spacing–GPR was set to 36 scans/foot	2898
HCP	4 inches	2088
ER	4 inches	2088

Nondestructive Evaluation Data Generation

Researchers at TFHRC constructed eight geometrically identical concrete decks with a series of controlled subsurface defects (Figure 5.9). These defects included deep and shallow delamination, honeycombing, voids and vertical cracks and accelerated corrosion. The 12 × 8 inch artificial delamination were built using plexiglass and plastic gutter guards. Two plexiglass sheets with a thickness of 0.093 inches were cut to size, and two layers of

plastic gutter guard were placed between the sheets to create an air gap, then the edges were sealed with duct tape. This artificial delamination was used to simulate shallow and deep delaminations at the top and bottom rebar levels. The artificial honeycombing was simulated with a bag of loose aggregates. For each honeycomb defect, 12 lbs of aggregate were placed into mesh bags and the edges were stitched with wire. The mesh bags were then placed in wood molds and secured to the rebar cage. The 23 × 8 × 2 inch voids were simulated with Styrofoam boards, Corrugated plastic sheets with a height of either 6 inches or 2.5 inches, a thickness of 0.16 inch, and a length of 10 inches were used to simulate vertical cracks within the concrete structure. Then the RC decks were then constructed using normal-weight concrete mix with a water-to-cement ratio of 0.37.

After the RC decks were fully cured, prior to data collection, accelerated corrosion was employed to create a corrosive environment with elevated chloride content in the concrete and active corrosion in the pre-corroded rebar. Different levels and uneven distribution of chloride content were introduced by a sponge saturated with NaCl solution. The reader should consult (Meng, Lin, and Azari 2020) for more details on deck construction and the development of the corrosive environment. Of the eight specimens, four also had an overlay. After construction of the test specimens, 8 NDE techniques were used to collect synchronous data from the specimens. Employed technologies included ultrasonic surface waves (USW), IE, GPR, ER (RABIT-based techniques), ultrasonic tomography (UT), HCP, infrared thermography (IRT) and impulse response (IR).

Of all eight NDE techniques, HCP, ER and GPR A-scan data were used in this research for corrosion detection: HCP for detection of corrosion activity, ER for detection of corrosive environment, and GPR for condition assessment. Previous nondestructive testing (NDT) applications on RC decks have demonstrated that ER and GPR can detect corrosive environments in concrete (elevated chloride content in this study), and HCP can detect active corrosion in the reinforcement (Gucunski et al. 2011; 2012). For delamination detection, GPR, IE and ER were used for condition assessment. For each specimen, nine gridlines were established with a spacing of 4 inches in the transverse direction, and 29 gridlines with a spacing of 4 inches were set in the longitudinal direction. For all techniques, data was collected on a specific grid spacing across the deck surface, though that spacing varied based on the specific NDE method used. ER, HCP and IE data were collected at grid points, and GPR A-scans were collected along each gridline. The GPR was set to 36 scan/foot, resulting 322 scans along the longitudinal direction. As discussed in Data Interpolation, the data from each NDE method was linearly interpolated to generate approximate measurements on a consistent grid spacing. The specifics of the data set are shown in Table 5.1.

Data Fusion for Corrosion Detection

There are various electrochemical and physical methods for the detection of corrosion in concrete and the advantages and disadvantages of each respective method is well explained in the literature (Alonso, Andrade, and González 1988). The study concludes that there is no optimal method, and usually a combination of several techniques is used. For this study, three different NDE methods were chosen for corrosion detection:

HCP, GPR, and ER. The HCP technique is a generally accepted method for identifying active corrosion in reinforced concrete bridge decks. The method is supported by an American Society for Testing Materials C876–09 standard (ASTM C876–09, 1999) with well-defined thresholds distinguishing actively corroded and non-corroded areas. GPR data has been shown to correlate reasonably well with HCP data on bridge decks (Martino et al. 2014). ER probes are also frequently used in corrosion monitoring systems in various industrial fields, especially in the Petro-chemical industry (Legat 2007). In previous study (Legat, Leban, and Bajt 2004) it was shown that measurements with ER probes are efficient for measuring the corrosion of steel in concrete.

The HCP and ER data sources provided scalar values (voltage and resistivity value respectively) at each measurement location, whereas the GPR data was a waveform. Wavelet features were extracted from the GPR signal (including mean power of reconstructed waveform and second, third, and fourth spectral moment of spectrum of reconstructed waveform from each wavelet basis, see Waveform Feature Extraction) and combined with the scalar-valued HCP and ER data for model training and testing. All the values were standardized and hyperparameters were identified prior to training, as discussed in Methodology. Classifiers were then trained using 70% of the data and tested on the remaining 30%. Using the training dataset, the classifier automatically determines an optimal decision boundary, a hypersurface that partitions data into defect and no defect classes. The classifier then classifies all the points on one side of the decision boundary as belonging to one class and all those on the other side as belonging to the other class.

Unfortunately, direct interpretation of this hypersurface is challenging, and is a significant downside to machine learning driven analysis.

Corrosion detection: results and discussion

Once the scalar values from ER and HCP data sources and extracted features from GPR waveform are combined into a concatenated vector, this vector is then an input to a statistical model. In this study, as explained in Feature fusion – SVM (Other Considered Classifiers), ANN, decision tree, and logistic regression algorithms are considered to provide a point of comparison to SVM fusion. The performance of all mentioned algorithms are shown in Table 5.2. The results of this comparative analysis show that the SVM and ANN fusion algorithms produced relatively similar results. Accuracy for the decision tree model was slightly degraded, mostly due to a loss of precision. The logistic regression approach yielded by far the worst results, indicating that the statistical relationships between NDE measurements and corrosion are sufficiently nonlinear in nature to warrant more sophisticated machine learning approaches. Given the comparably performance of the SVM and ANN classifiers, the SVM approach is preferable due to the fewer hyperparameters and reduced risk of model overfitting.

Table 5.2. Comparison of fusion algorithm performance for corrosion detection.

Fusion Algorithm	Accuracy	Precision	Recall	F1- score
SVM	0.96	0.92	0.91	0.91
ANN	0.95	0.92	0.89	0.90
Decision tree	0.91	0.89	0.89	0.89
Logistic regression	0.89	0.82	0.82	0.82

Decision fusion for corrosion detection

As a point of comparison, a decision-level fusion approach was also developed. This approach combined the independent detection assessments of various different NDE methods, weighting them based on their statistical significance, a technique referred to as a Weighted-Sum Model (D. Hall and Llinas 2001). Each NDE technique was used to generate an independent decision based on its own features and an SVM classifier, with a binary declaration of either "corrosion" or "no corrosion." The weight of each decision was then determined. Several metrics for weighting were considered, including false positive rate, probability of detection (recall), and precision (Lu and Michaels 2009). Using precision as the criterion, the order of weights was GPR > HCP > ER. Considering recall, the order of weights changed to HCP > GPR > ER. For the false positive rate, the resulting weight order was GPR > HCP > ER. The resulting weighted decisions were then combined and compared against the SVM classifier (Table 5.3). As is shown, the accuracy never reached the level of feature-level fusion via SVM. Similar results were found for decision fusion of delamination defects.

Table 5.3. Comparison of weighted decision combination with various weight order in corrosion detection.

Techniques	HCP>GPR>ER	GPR>ER>HCP	GPR>HCP>ER	SVM
Overall accuracy (%)	94.0	88.5	85.65	96.0

SVM fusion analysis

Once SVM was identified as the preferred machine learning method for corrosion detection, a more in-depth analysis of SVM model behavior was performed. In addition to a fusion of all the techniques, different fusion combinations were studied. The goal was to understand the effect of adding an NDE data source to fusion models and identify the best combination of techniques for deck assessment. The following data fusion combinations were tested: ER + HCP, ER + GPR, HCP + GPR, and ER + HCP + GPR. SVM classifiers were also constructed for each NDE type separately. For scalar-valued HCP and ER data a linear function was fit to the data, whereas for the waveform GPR data, wavelet-based features were fit to an SVM model with a RBF function, similar to the model used for the fused case.

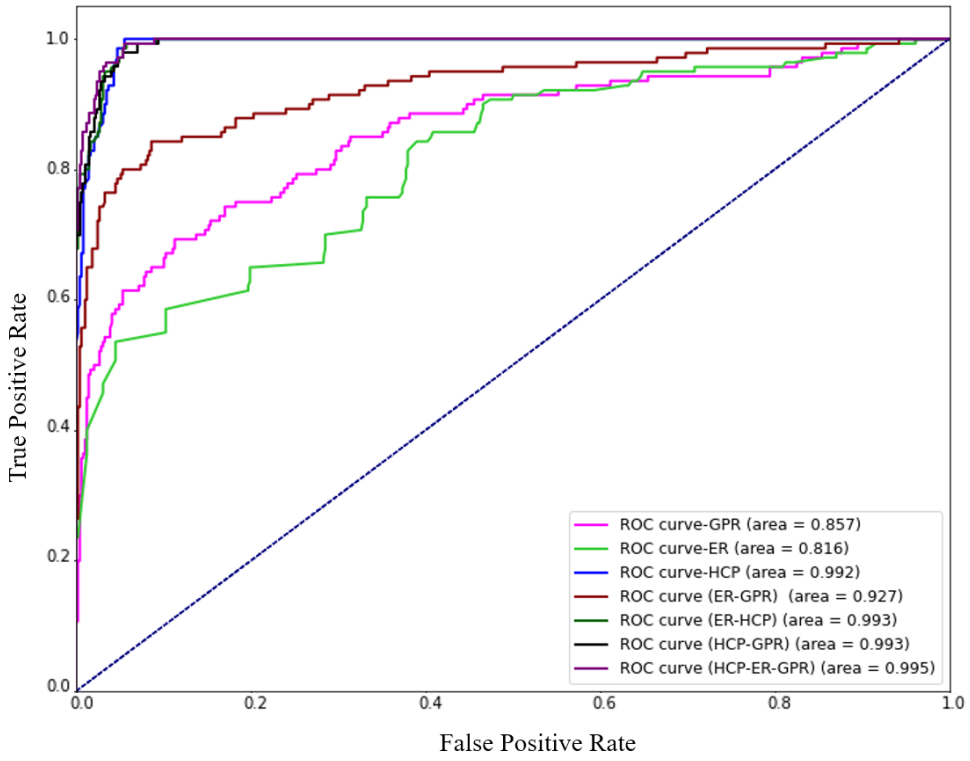

Figure 5.10. Receiver Operating Characteristic curve of Support Vector Machine for corrosion detection.

Some of these algorithms didn't increase the corrosion detection accuracy in compare with individual techniques, also their underperformance in comparison with SVM was more for delamination detection.

The resulting Receiver-Operator-Characteristic (ROC) curves from each fusion combination for corrosion detection is shown in Figure 5.10. The area under a ROC curve is an effective measure of the sensitivity of a classifier to variations in classification thresholds, with a larger area indicating a more robust classifier. What can clearly be seen is that HCP on its own is a highly effective method of quantifying corrosion, whereas ER and GPR perform relatively poorly in isolation. In fact, GPR serves to degrade classifier

accuracy when fused with HCP data. This behavior is due to the nature of laboratory conditions for the HCP measurements that were idealized and may not be representative of performance under field conditions. After the RC decks were fully cured, accelerated corrosion was employed with elevated chloride content in the concrete and active corrosion in the pre-corroded rebar. This caused corrosion to occur much faster compared to natural conditions (Meng, Lin, and Azari 2020). This type of accelerated corrosion is ideal for HCP measurements and led to high detection accuracy for HCP (Yuan, Ji, and Shah 2007). Such a result reflects the potential for model biasing that can occur in machine learning. The fusion of all three data sources is slightly better than for HCP or HCP + ER, but these differences are statistically negligible. The most notable result is that the fusion of ER + GPR is measurably better than either measurement on its own and highlights the value of statistical data fusion.

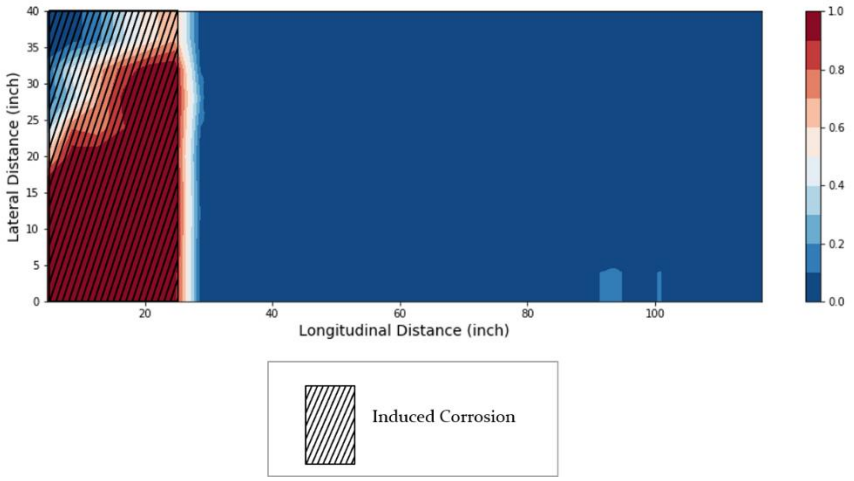

Figure 5.11. Fusion heat map based on Support Vector Machine indicating existence of corrosion in slab.

A visualization heat map for the complete fusion (HCP + ER + GPR) is shown in Figure 5.11. An analysis of the visualization shows that the certainty of corrosion was degraded near the upper left corner of the slab. Again, the reasons for this loss in detection certainty are likely due to experimental testing conditions.

Data Fusion for Delamination and Crack Detection

To evaluate the impact of data fusion for detecting subsurface delamination and cracks, three NDE methods were considered: GPR, ER and IE. Similar to the procedure for corrosion detection, data from these techniques were combined into a unified dataset. Like GPR, IE produces a waveform signal at each grid location, and wavelet features were extracted from IE and GPR (Waveform Feature Extraction). Once salient features were extracted using wavelet transform, a series of classifiers were prototyped. As with the corrosion tests, the SVM classifier produced the most accurate and robust classifications. Results for the ANN, decision tree, and logistic regression classifiers, as well as the decision-level fusions were similar to the corrosion tests and are not reported here.

Delamination detection: results and discussion

The resulting ROC curves for SVM classifiers for delamination and crack detection are shown in Figure 5.12, and the resulting heat map is shown in Figure 5.13. For this set of tests, no single NDE method dominated classifier performance and single source NDE assessments were consistently poor performers. In all cases, fusions produced substantially improved assessments, and the complete data fusion was substantially better than any other combination. These results not only show that the fusion algorithm significantly improve

delamination detection capabilities on their own, but the fusion of any combination of techniques results in a substantial improvement in detection accuracy compared individual techniques. This was most notable for IE data. For example, IE + GPR fusion improved detection accuracy by +50% compared to IE and GPR detection. These results show the most dramatic improvements from data fusion observed in this study and should be the focus of future data fusion efforts.

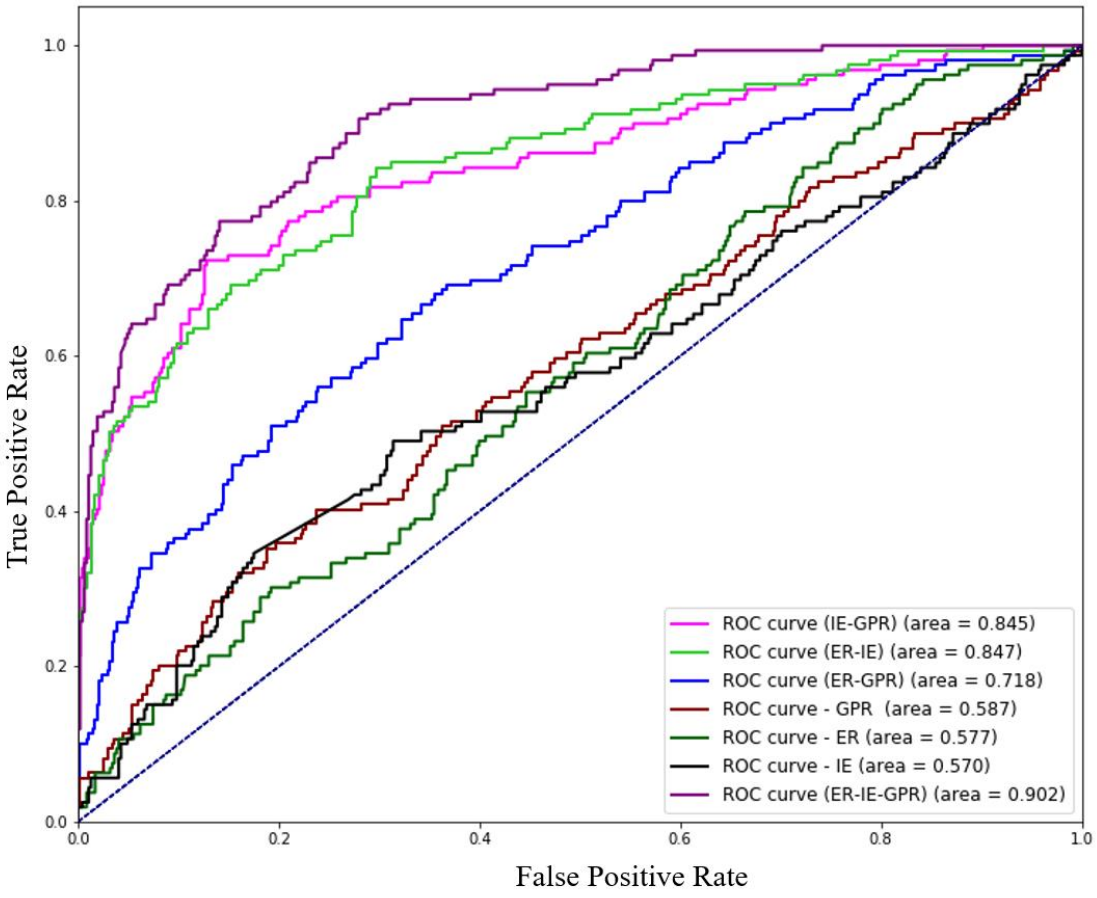

Figure 5.12. Receiver Operating Characteristic curve of Support Vector Machine classifiers for delamination detection.

The results for the ER data warrant additional discussion. ER measurements are not designed to explicitly detect delamination in concrete, but rather the associated rebar corrosion, and the artificial delamination of this test were not corroded to simulate this relationship. Yet adding ER data to the fusion of IR and GPR had a measurable beneficial impact on detection accuracy and served to reduce measurement uncertainty across the slab. An analysis of the results indicates that this benefit is not isolated to the corroded left-hand portion of the slab or any particular type of defect within the slab. While not conclusive, the authors believe that this result may be related to how the artificial defects are installed within the test slabs and may not be representative of field conditions. Further investigation is warranted and highlights the need for physics-driven understanding of machine learning analysis.

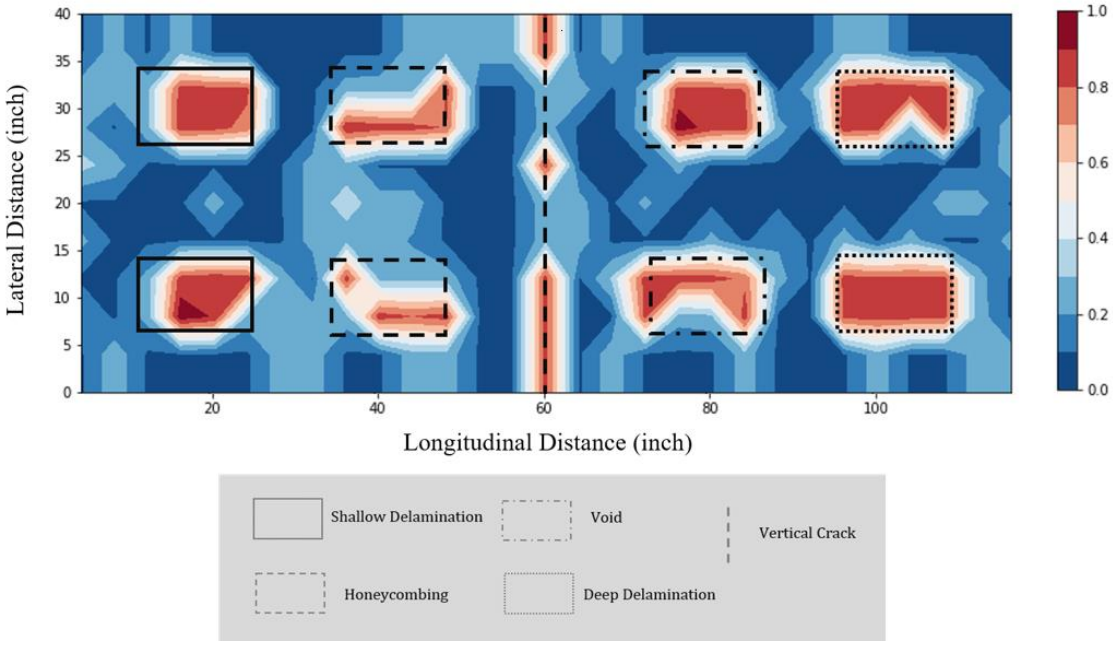

Figure 5.13. Support Vector Machine fusion heat map indicating the existence and extents of delamination and cracking.

While not shown here for clarity, an initial series of tests utilized scalar-valued measurements extracted from the IE waveform results, as was done in (Hsiao et al. 2008). Single source classifications were comparable between waveform and scalar valued NDE data. The benefits of data fusion without the complete waveform response were negligible. What this suggests is that components of an NDE signal that are not relevant for single-source assessments can be of high value for a data fusion scenario.

The behavior of the fused SVM classifier is more clearly seen in the heatmap visualization of Figure 5.12. The upper and lower part of the crack in the middle of the slab was detected while the middle part was not detected because of the shallower crack depth (2” vs. 6”). While not every defect was perfectly identified, a large portion of each of the eight defects was classified as a delamination by the SVM. The worst performance was seen for the honeycombing defect, where a smaller portion of the defect was detected. The other six defects were more clearly detected. For a holistic assessment, this kind of visualization goes beyond defect detection and illustrates both the extents of a defect and NDE detection confidence in an intuitive context that is familiar to engineers and inspectors.

Conclusion and Future Work

In this work, a methodology to process and fuse multiple NDE data sources for bridge deck defect detection is developed. This approach leverages a wavelet transform

(DWT) to extract numerical features from waveform NDE responses. Using the DWT provides consistent feature extraction that is well suited to signals that are periodic, transient (or nonstationary), and noisy. In conjunction with scalar-valued NDE measurements, these data sources are used as input in a machine learning classifier to provide a feature-level data fusion of NDE measurements. Support vector machine methods showed demonstrably better detection accuracy than other machine learning algorithms, most noticeably when compared to linear classification methods that more closely mirror conventional assessment methods. The benefits of data fusion were most significant for the detection of delaminations and cracks, while the results from the corrosion analysis were likely biased by how HCP data was collected in the laboratory and may not be representative of realistic field performance. Overall, the findings of this study show that data fusion has a measurable and positive impact on defect detection performance for both corrosion assessment and generalized defect detection. The visualization approach developed in this study is capable of intuitively representing the classifiers detection confidence—a key criterion for inspectors and engineers managed as part of this study—and provides a more nuanced representation of NDE assessments that help to quantify the geometric extents of a defect. As stated before, the laboratory conditions for the test data likely overestimate classifier accuracy under field conditions, but they do reflect the relative benefits of data fusion over single-source NDE assessments. It is also important to emphasize that the data fusion processes developed in this work do not allow direct insight into the capabilities of any single NDE method to detect defects

such as delaminations. Creating fusion approaches that provide such insights is a compelling avenue for future work.

This study was part of an on-going research program and various part of the presented methodology are being considered for further improvement. The goal of this study was to fundamentally explore fusion viability, leveraging NDE data relevant to the FHWA RABIT inspection system. While the results show the promise of data fusion, there are many unanswered questions. For instance, this study only considered a small subset of possible data fusion combinations and defect classes, and the results showed that data fusion was more beneficial for delamination detection than corrosion. This suggests the need for additional studies that consider a broader range of NDE methods and defect types, and that the benefits of fusion for any given scenario cannot be easily generalized to other scenarios. However, the framework and evaluative methodology presented here are generalizable enough to be effective for a diverse range of experimental scenarios. As stated earlier, the statistical learning models developed here are not capable of distinguishing between defect classes, a simplification that aided illustration of the impact of NDE fusion. Future work could include expanding the work to include defect diagnosis, rather than detection, for instance the distinction between shallow and deep defects for a given data fusion. Based on these initial findings, additional studies on the wavelet decomposition-based feature extraction methods are warranted as well. There is also a need to evaluate these approaches under realistic field conditions. Lastly, the probability score of damage in the structural component can be modeled as stochastic process and tracked over time and using time series modeling their

future states can be predicted. Tracking the fused data for prognostic purposes would be highly beneficial to engineers and managers attempting to do portfolio-level asset management.

CHAPTER SIX: CONCLUSIONS AND AVENUES FOR FUTURE RESEARCH

Conclusions

The primary outcome of this doctoral dissertation is a framework to support digital twin modeling of structures that addresses two main problems of digital twin modeling : 1. life cycle modeling of time-dependent defects and linking such defects' evolution to the numerical model of structures and 2. fusion of multiple data sources to increase accuracy of defect detection in digital twin systems.

A methodology to parametrize and model the dynamics of defect evolution based on convex hull parametrization and time-series modeling is introduced in the first part of study. Using convex hull parametrization, 2D synthetic and experimental point clouds representing various defect shapes and stochastic evolutions were parametrized, and their evolutions were modeled using time-series forecasting models. The future state of defects was then forecasted and evaluated against ground truth. The results indicated that this convex hull approach provides consistent and accurate representations of defect evolution across a range of defect topologies and is reasonably robust to noisy measurements.

Next, a study was conducted to link the time dependent defects to numerical simulation of structure to perform predictive simulation. A methodology to update the finite element model of structural components with regard to the future state of the crack based on the computer vision technique was introduced. 2D experimental point clouds representing crack growth with increasing loading cycles were used to predict the crack extension in the future cycle. The future crack extension (i.e. length and orientation) was

predicted via time-series models. The solid model of structural components was updated first based on an identified crack at one of the primary loading cycles and once again was updated based on the predicted crack extension. Once updated, the solid model was meshed and LEFM was conducted. The results indicated that linking the future state of the crack to the FE model of structures provides a basis for future predictive simulation. While the proposed methodology for FE model updating was applied for fatigue crack propagation, this study can be expanded to other time dependent defects with different dynamics of evolution.

Finally, to improve the accuracy and robustness of the NDE results in digital twin systems, a methodology to process and fuse multiple NDE data sources for bridge deck defect detection was developed. This approach leveraged a wavelet transform (DWT) to extract numerical features from waveform NDE responses. In conjunction with scalar-valued NDE measurements, these data sources were used as input in a machine learning classifier to provide a feature-level data fusion of NDE measurements. A novel visualization approach was introduced which provides inspectors and engineer with an intuitive representing of confidence of detected defect. Overall, the findings of this study showed that data fusion has a measurable and positive impact on defect detection performance for both corrosion assessment and generalized defect detection in digital twin systems.

Overall, the presented methods will lead to a new structural assessment framework that supports decision-making on the necessary maintenance of the structure. The main contributions of the developed framework include:

• Providing engineers with an intuitive and consistent representation of remotely sensed information over a structure's life cycle.

• Providing more reliable forecasting capabilities and a more complete understanding of structural performance.

• Providing a more nuanced representation of NDE assessments that help to quantify the geometric extents of a defect.

• Improvements in how engineers and inspectors interact with detected defect data through a visualization approach.

Due to the complex and challenging nature of each of the developed algorithms, further research exists for extending and expanding different steps within the introduced computational framework. The following future avenues can be investigated for each of the presented studies.

Future Work In Life Cycle Modeling of Structural Defects

Study showed that the behavior of the underlying dynamical process plays a significant role in predictive accuracy and predictive accuracy degrades as defect evolution becomes increasingly nonlinear.

The behavior of the algorithm under higher degrees of statistical uncertainty and material variability should be investigated. More datasets from other crack scenarios should also be considered, for instance, concrete cracking in civil infrastructure. Such studies may provide insight into how particular algorithmic aspects, such as the nearest neighbor matching aspects of hull tracking, behave under complex material phenomena

such as crazing or alkali–silica reactions in concrete. In such cases, the cracks may branch and split, creating unforeseen modeling challenges.

The parametrizations and hull modeling are being studied for temporal tracking of non-geometric changes such as color change in structures. The hull parametrization method is also being extended to high-dimensional feature space analyses, supporting the fusion of multiple sensors and survey information for holistic life-cycle modeling. One notable avenue for future work is to adapt the algorithm to parameterize defect shapes using a combination of a convex and concave hull algorithm more realistically [68]. Such an approach would allow for more accurate depiction of complex geometric topologies similar to the fatigue cracks evaluated in this work. In addition, nonlinear time-series modeling methods such as recurrent neural networks may be studied for more complex defect evolutions; however, such machine-learning-driven approaches need much larger datasets to be employed.

Future Work in Finite Element Model Updating

The performance of the FE model updating approach under environment uncertainty and material variability should be investigated. More datasets from other crack scenarios should also be considered, for instance, concrete or asphalt cracking in civil infrastructure. Such studies may provide insight into how particular algorithmic aspects, such as crack identification, prediction and projection (Section 2), behave under complex material phenomena. The effect of varying amplitude cyclic loading also must be evaluated as it reflects the real-world scenarios. One notable avenue for future work is to adapt the

algorithm to more complex fracture mechanic studies such as Elastic Plastic Fracture Mechanics (EPFM) to estimate the crack growth rate.

Future Work In Data Fusion

The proposed approach reflected the relative benefits of data fusion over single-source NDE assessments, however the laboratory conditions for the test data likely overestimate classifier accuracy under field conditions. It is also important to emphasize that the data fusion processes developed in this work do not allow direct insight into the capabilities of any single NDE method to detect defects such as delamination. Creating fusion approaches that provide such insights is a compelling avenue for future work.

While the results show the promise of data fusion, there are many unanswered questions. For instance, this study only considered a small subset of possible data fusion combinations and defect classes, and the results showed that data fusion was more beneficial for delamination detection than corrosion. This suggests the need for additional studies that consider a broader range of NDE methods and defect types, and that the benefits of fusion for any given scenario cannot be easily generalized to other scenarios. However, the framework and evaluative methodology presented here are generalizable enough to be effective for a diverse range of experimental scenarios. As stated earlier, the statistical learning models developed here are not capable of distinguishing between defect classes, a simplification that aided illustration of the impact of NDE fusion. Future work could include expanding the work to include defect diagnosis, rather than detection, for instance the distinction between shallow and deep defects for a given data fusion. Based

on these initial findings, additional studies on the wavelet decomposition-based feature extraction methods are warranted as well. There is also a need to evaluate these approaches under realistic field conditions. Lastly, the probability score of damage in the structural component can be modeled as stochastic process and tracked over time and using time series modeling their future states can be predicted. Tracking the fused data for prognostic purposes would be highly beneficial to engineers and managers attempting to do portfolio-level asset management.

REFERENCES

Abdel-Qader Ikhlas, Abudayyeh Osama, and Kelly Michael E. 2003. “Analysis of Edge-Detection Techniques for Crack Identification in Bridges.” *Journal of Computing in Civil Engineering* 17 (4): 255–63. https://doi.org/10.1061/(ASCE)0887-3801(2003)17:4(255).

Agathos, Konstantinos, Eleni Chatzi, and Stéphane P. A. Bordas. 2018. “Multiple Crack Detection in 3D Using a Stable XFEM and Global Optimization.” *Computational Mechanics* 62 (4): 835–52. https://doi.org/10.1007/s00466-017-1532-y.

Aggelis, Dimitrios G. 2011. “Classification of Cracking Mode in Concrete by Acoustic Emission Parameters.” *Mechanics Research Communications* 38 (3): 153–57. https://doi.org/10.1016/j.mechrescom.2011.03.007.

Aghagholizadeh, Mehrdad, and Necati Catbas. 2015. “A Review of Model Updating Methods for Civil Infrastructure Systems.” In , 83–99. https://doi.org/10.4203/csets.38.4.

Ahmed, Habib, Hung Manh La, and Nenad Gucunski. 2020. “Review of Non-Destructive Civil Infrastructure Evaluation for Bridges: State-of-the-Art Robotic Platforms, Sensors and Algorithms.” *Sensors* 20 (14): 3954. https://doi.org/10.3390/s20143954.

Akl, Selim G., and Godfried T. Toussaint. 1979. “EFFICIENT CONVEX HULL ALGORITHMS FOR PATTERN RECOGNITION APPLICATIONS.” In . https://nyu-staging.pure.elsevier.com/en/publications/efficient-convex-hull-algorithms-for-pattern-recognition-applicat.

Al Ghayab, Hadi Ratham, Yan Li, S. Siuly, and Shahab Abdulla. 2019. “A Feature Extraction Technique Based on Tunable Q-Factor Wavelet Transform for Brain Signal Classification.” *Journal of Neuroscience Methods* 312 (January): 43–52. https://doi.org/10.1016/j.jneumeth.2018.11.014.

Alonso, C., C. Andrade, and J. A. González. 1988. “Relation between Resistivity and Corrosion Rate of Reinforcements in Carbonated Mortar Made with Several Cement Types.” *Cement and Concrete Research* 18 (5): 687–98. https://doi.org/10.1016/0008-8846(88)90091-9.

Alshoaibi, Abdulnaser M., and Yahya Ali Fageehi. 2020. “Numerical Analysis of Fatigue Crack Growth Path and Life Predictions for Linear Elastic Material.” *Materials* 13 (15). https://doi.org/10.3390/ma13153380.

ASTM C876-09 (1999). Standard test method for half cell potentials of reinforcing steel in concrete. West Conshohocken, PA: ASTM

ASTM. (2014) Measurement of fatigue crack growth rates. ASTM E647-13a, USA. https://doi.org/10.1520/E0647-15E01

Aranguren, G., P. M. Monje, Valerijan Cokonaj, Eduardo Barrera, and Mariano Ruiz. 2013. “Ultrasonic Wave-Based Structural Health Monitoring Embedded Instrument.” *Review of Scientific Instruments* 84 (12): 125106. https://doi.org/10.1063/1.4834175.

Atkinson, C. 1977. “On Stress Singularities and Interfaces in Linear Elastic Fracture Mechanics.” *International Journal of Fracture* 13 (6): 807–20. https://doi.org/10.1007/BF00034324.

Ayhan, Ali O. 2011. “Three-Dimensional Fracture Analysis Using Tetrahedral Enriched Elements and Fully Unstructured Mesh.” *International Journal of Solids and Structures* 48 (3): 492–505. https://doi.org/10.1016/j.ijsolstr.2010.10.012.

Banks-Sills, Leslie. 1991. “Application of the Finite Element Method to Linear Elastic Fracture Mechanics.” *Applied Mechanics Reviews* 44 (10): 447–61. https://doi.org/10.1115/1.3119488.

Barber, C. Bradford, David P. Dobkin, David P. Dobkin, and Hannu Huhdanpaa. 1996. “The Quickhull Algorithm for Convex Hulls.” *ACM Trans. Math. Softw.* 22 (4): 469–83. https://doi.org/10.1145/235815.235821.

Barenblatt, G. I. 1962. “The Mathematical Theory of Equilibrium Cracks in Brittle Fracture.” In *Advances in Applied Mechanics*, edited by H. L. Dryden, Th. von Kármán, G. Kuerti, F. H. van den Dungen, and L. Howarth, 7:55–129. Elsevier. https://doi.org/10.1016/S0065-2156(08)70121-2.

Baydoun, M., and T. P. Fries. 2012. “Crack Propagation Criteria in Three Dimensions Using the XFEM and an Explicit–Implicit Crack Description.” *International Journal of Fracture* 178 (1): 51–70. https://doi.org/10.1007/s10704-012-9762-7.

Behnia, Arash, Hwa Kian Chai, and Tomoki Shiotani. 2014. “Advanced Structural Health Monitoring of Concrete Structures with the Aid of Acoustic Emission.” *Construction and Building Materials* 65 (August): 282–302. https://doi.org/10.1016/j.conbuildmat.2014.04.103.

Belytschko, T., and T. Black. 1999. “Elastic Crack Growth in Finite Elements with Minimal Remeshing.” *International Journal for Numerical Methods in Engineering* 45 (5): 601–20. https://doi.org/10.1002/(SICI)1097-0207(19990620)45:5<601::AID-NME598>3.0.CO;2-S.

Berg, Mark de, ed. 2008. *Computational Geometry: Algorithms and Applications*. 3rd ed. Berlin: Springer.

Besl, P. J., and N. D. McKay. 1992. “A Method for Registration of 3-D Shapes.” *IEEE Transactions on Pattern Analysis and Machine Intelligence* 14 (2): 239–56. https://doi.org/10.1109/34.121791.

Boser, Bernhard E., Isabelle M. Guyon, and Vladimir N. Vapnik. 1992. “A Training Algorithm for Optimal Margin Classifiers.” In *Proceedings of the Fifth Annual Workshop on Computational Learning Theory*, 144–52. COLT ’92. Pittsburgh, Pennsylvania, USA: Association for Computing Machinery. https://doi.org/10.1145/130385.130401.

Box, George E. P., and Gwilym M. Jenkins. 1976. *Time Series Analysis: Forecasting and Control*. Holden-Day.

Box, George Edward Pelham, and Gwilym Jenkins. 1990. *Time Series Analysis, Forecasting and Control*. San Francisco, CA, USA: Holden-Day, Inc.

Brandon, J A. 1998. “Some Insights into the Dynamics of Defective Structures.” *Proceedings of the Institution of Mechanical Engineers, Part C: Journal of*

Mechanical Engineering Science 212 (6): 441–54. https://doi.org/10.1243/0954406981521358.

Broek, D. 1972. "The Propagation of Fatigue Cracks Emanating from Holes." *NLR-TR 72134 U*. https://repository.tudelft.nl/islandora/object/uuid%3A471ede30-ca26-4419-a0ae-3497c214d465.

Brownlee, Jason. 2017. "Autoregression Models for Time Series Forecasting With Python." *Machine Learning Mastery* (blog). January 2, 2017. https://machinelearningmastery.com/autoregression-models-time-series-forecasting-python/.

Cabaleiro, M., B. Riveiro, P. Arias, and J. C. Caamaño. 2015. "Algorithm for the Analysis of Deformations and Stresses Due to Torsion in a Metal Beam from LIDAR Data." *Structural Control and Health Monitoring*, January, n/a-n/a. https://doi.org/10.1002/stc.1824.

Cabaleiro, M., B. Riveiro, P. Arias, J. C. Caamaño, and J. A. Vilán. 2014. "Automatic 3D Modelling of Metal Frame Connections from LiDAR Data for Structural Engineering Purposes." *ISPRS Journal of Photogrammetry and Remote Sensing* 96 (October): 47–56. https://doi.org/10.1016/j.isprsjprs.2014.07.006.

Cadini, F., E. Zio, and D. Avram. 2009. "Monte Carlo-Based Filtering for Fatigue Crack Growth Estimation." *Probabilistic Engineering Mechanics* 24 (3): 367–73. https://doi.org/10.1016/j.probengmech.2008.10.002.

Caleyo, F., J.C. Velázquez, A. Valor, and J.M. Hallen. 2009. "Markov Chain Modelling of Pitting Corrosion in Underground Pipelines." *Corrosion Science* 51 (9): 2197–2207. https://doi.org/10.1016/j.corsci.2009.06.014.

Catbas, F Necati, Hasan B Gokce, and Mustafa Gul. 2012. "Nonparametric Analysis of Structural Health Monitoring Data for Identification and Localization of Changes: Concept, Lab, and Real-Life Studies." *Structural Health Monitoring* 11 (5): 613–26. https://doi.org/10.1177/1475921712451955.

Cerrone, Albert, Jacob Hochhalter, Gerd Heber, and Anthony Ingraffea. 2014. "On the Effects of Modeling As-Manufactured Geometry: Toward Digital Twin." Research article. International Journal of Aerospace Engineering. 2014. https://doi.org/10.1155/2014/439278.

Chair, Z., and P. K. Varshney. 1986. "Optimal Data Fusion in Multiple Sensor Detection Systems." *IEEE Transactions on Aerospace and Electronic Systems* AES-22 (1): 98–101. https://doi.org/10.1109/TAES.1986.310699.

Chang Peter C. and Liu S. Chi. 2003. "Recent Research in Nondestructive Evaluation of Civil Infrastructures." *Journal of Materials in Civil Engineering* 15 (3): 298–304. https://doi.org/10.1061/(ASCE)0899-1561(2003)15:3(298).

Chen Dar Hao and Wimsatt Andrew. 2010. "Inspection and Condition Assessment Using Ground Penetrating Radar." *Journal of Geotechnical and Geoenvironmental Engineering* 136 (1): 207–14. https://doi.org/10.1061/(ASCE)GT.1943-5606.0000190.

Chen, F., and M. R. Jahanshahi. 2018. "NB-CNN: Deep Learning-Based Crack Detection Using Convolutional Neural Network and Naïve Bayes Data Fusion." *IEEE*

Transactions on Industrial Electronics 65 (5): 4392–4400. https://doi.org/10.1109/TIE.2017.2764844.

Chen, Fu-Chen, Mohammad R. Jahanshahi, Rih-Teng Wu, and Chris Joffe. 2017. "A Texture-Based Video Processing Methodology Using Bayesian Data Fusion for Autonomous Crack Detection on Metallic Surfaces." *Computer-Aided Civil and Infrastructure Engineering* 32 (4): 271–87. https://doi.org/10.1111/mice.12256.

Chen, Shang-Liang, and Y. W. Jen. 2000. "Data Fusion Neural Network for Tool Condition Monitoring in CNC Milling Machining." *International Journal of Machine Tools and Manufacture* 40 (3): 381–400. https://doi.org/10.1016/S0890-6955(99)00066-8.

Choo, Jaegul, Fuxin Li, Keehyoung Joo, and Haesun Park. 2012. "A Visual Analytics Approach for Protein Disorder Prediction." In *Expanding the Frontiers of Visual Analytics and Visualization*, edited by John Dill, Rae Earnshaw, David Kasik, John Vince, and Pak Chung Wong, 163–74. London: Springer London. https://doi.org/10.1007/978-1-4471-2804-5_10.

Clifton, J. R., and N. J. Carino. 1982. *Nondestructive Evaluation Methods for Quality Acceptance of Installed Building Materials*. National Institute of Standards and Technology. http://archive.org/details/jresv87n5p407_A1b.

Colomina, I., and P. Molina. 2014. "Unmanned Aerial Systems for Photogrammetry and Remote Sensing: A Review." *ISPRS Journal of Photogrammetry and Remote Sensing* 92 (June): 79–97. https://doi.org/10.1016/j.isprsjprs.2014.02.013.

Comisu, Cristian-Claudiu, Nicolae Taranu, Gheorghita Boaca, and Maria-Cristina Scutaru. 2017. "Structural Health Monitoring System of Bridges." *Procedia Engineering* 199: 2054–59. https://doi.org/10.1016/j.proeng.2017.09.472.

Cortes, Corinna, and Vladimir Vapnik. 1995. "Support-Vector Networks." *Machine Learning* 20 (3): 273–97. https://doi.org/10.1007/BF00994018.

Cristianini, Nello, and John Shawe-Taylor. 2000. "An Introduction to Support Vector Machines and Other Kernel-Based Learning Methods." Cambridge Core. Cambridge University Press. March 2000. https://doi.org/10.1017/CBO9780511801389.

Daniels, J. I., L. K. Ha, T. Ochotta, and C. T. Silva. 2007. "Robust Smooth Feature Extraction from Point Clouds." In *IEEE International Conference on Shape Modeling and Applications 2007 (SMI '07)*, 123–36. https://doi.org/10.1109/SMI.2007.32.

Daubechies, I. 1992. *Ten Lectures on Wavelets*. CBMS-NSF Regional Conference Series in Applied Mathematics. Society for Industrial and Applied Mathematics. https://doi.org/10.1137/1.9781611970104.

Debnath, Lokenath, and Firdous Ahmad Shah. 2014. *Wavelet Transforms and Their Applications*. Springer.

Demirbas, K. 1989. "Distributed Sensor Data Fusion with Binary Decision Trees." *IEEE Transactions on Aerospace and Electronic Systems* 25 (5): 643–49. https://doi.org/10.1109/7.42081.

Dickey, David A., and Wayne A. Fuller. 1981. “Likelihood Ratio Statistics for Autoregressive Time Series with a Unit Root.” *Econometrica* 49 (4): 1057–72. https://doi.org/10.2307/1912517.

Dimarogonas, Andrew D. 1996. “Vibration of Cracked Structures: A State of the Art Review.” *Engineering Fracture Mechanics* 55 (5): 831–57. https://doi.org/10.1016/0013-7944(94)00175-8.

Ding, Lina, Hong Hao, Yong Xia, and Andrew J. Deeks. 2012. “Evaluation of Bridge Load Carrying Capacity Using Updated Finite Element Model and Nonlinear Analysis.” *Advances in Structural Engineering* 15 (10): 1739–50. https://doi.org/10.1260/1369-4332.15.10.1739.

Doebling, S. W., C. R. Farrar, M. B. Prime, and D. W. Shevitz. 1996. “Damage Identification and Health Monitoring of Structural and Mechanical Systems from Changes in Their Vibration Characteristics: A Literature Review.” Report. Other Information: PBD: May 1996. May 1, 1996. https://doi.org/10.2172/249299.

Dong, Jiang, Dafang Zhuang, Yaohuan Huang, and Jingying Fu. 2009. “Advances in Multi-Sensor Data Fusion: Algorithms and Applications.” *Sensors; Basel* 9 (10): 7771–84. http://dx.doi.org.mutex.gmu.edu/10.3390/s91007771.

Doucet, Arnaud. 1998. “On Sequential Simulation-Based Methods for Bayesian Filtering.”

Dugdale, D. S. 1960. “Yielding of Steel Sheets Containing Slits.” *Journal of the Mechanics and Physics of Solids* 8 (2): 100–104. https://doi.org/10.1016/0022-5096(60)90013-2.

Ebert, T., J. Belz, and O. Nelles. 2014. “Interpolation and Extrapolation: Comparison of Definitions and Survey of Algorithms for Convex and Concave Hulls.” In *2014 IEEE Symposium on Computational Intelligence and Data Mining (CIDM)*, 310–14. https://doi.org/10.1109/CIDM.2014.7008683.

Epinat, Virginie, Alfred Stein, Steven M de Jong, and Johan Bouma. 2001. “A Wavelet Characterization of High-Resolution NDVI Patterns for Precision Agriculture.” *International Journal of Applied Earth Observation and Geoinformation* 3 (2): 121–32. https://doi.org/10.1016/S0303-2434(01)85003-0.

Fan, Wei, and Pizhong Qiao. 2011. “Vibration-Based Damage Identification Methods: A Review and Comparative Study.” *Structural Health Monitoring* 10 (1): 83–111. https://doi.org/10.1177/1475921710365419.

Faouzi, Nour-Eddin El, and Lawrence A. Klein. 2016. “Data Fusion for ITS: Techniques and Research Needs.” *Transportation Research Procedia*, International Symposium on Enhancing Highway Performance (ISEHP), June 14-16, 2016, Berlin, 15 (January): 495–512. https://doi.org/10.1016/j.trpro.2016.06.042.

Faouzi, Nour-Eddin El, Henry Leung, and Ajeesh Kurian. 2011. “Data Fusion in Intelligent Transportation Systems: Progress and Challenges – A Survey.” *Information Fusion*, Special Issue on Intelligent Transportation Systems, 12 (1): 4–10. https://doi.org/10.1016/j.inffus.2010.06.001.

Fathi, Habib, Fei Dai, and Manolis Lourakis. 2015. “Automated As-Built 3D Reconstruction of Civil Infrastructure Using Computer Vision: Achievements, Opportunities, and Challenges.” *Advanced Engineering Informatics*,

Infrastructure Computer Vision, 29 (2): 149–61. https://doi.org/10.1016/j.aei.2015.01.012.
Fawcett, Tom. 2006. “An Introduction to ROC Analysis.” *Pattern Recognition Letters*, ROC Analysis in Pattern Recognition, 27 (8): 861–74. https://doi.org/10.1016/j.patrec.2005.10.010.
Feng, Yongcun, and K. E. Gray. 2019. “XFEM-Based Cohesive Zone Approach for Modeling near-Wellbore Hydraulic Fracture Complexity.” *Acta Geotechnica* 14 (2): 377–402. https://doi.org/10.1007/s11440-018-0645-6.
Fernandez, Ignasi, Jesús Miguel Bairán, and Antonio R. Marí. 2016. “3D FEM Model Development from 3D Optical Measurement Technique Applied to Corroded Steel Bars.” *Construction and Building Materials* 124 (October): 519–32. https://doi.org/10.1016/j.conbuildmat.2016.07.133.
Figueiredo, E., M. D. Todd, C. R. Farrar, and E. Flynn. 2010. “Autoregressive Modeling with State-Space Embedding Vectors for Damage Detection under Operational Variability.” *International Journal of Engineering Science*, Structural Health Monitoring in the Light of Inverse Problems of Mechanics, 48 (10): 822–34. https://doi.org/10.1016/j.ijengsci.2010.05.005.
Fleming, Roland W., Daniel Holtmann-Rice, and Heinrich H. Bülthoff. 2011. “Estimation of 3D Shape from Image Orientations.” *Proceedings of the National Academy of Sciences* 108 (51): 20438–43. https://doi.org/10.1073/pnas.1114619109.
Friswell, M. I., and J. E. T. Penny. 2002. “Crack Modeling for Structural Health Monitoring.” *Structural Health Monitoring* 1 (2): 139–48. https://doi.org/10.1177/1475921702001002002.
Ghahremani Kasra, Khaloo Ali, Mohamadi Sara, and Lattanzi David. 2018. “Damage Detection and Finite-Element Model Updating of Structural Components through Point Cloud Analysis.” *Journal of Aerospace Engineering* 31 (5): 04018068. https://doi.org/10.1061/(ASCE)AS.1943-5525.0000885.
Ghazali, K. H., M. F. Mansor, M. M. Mustafa, and A. Hussain. 2007. “Feature Extraction Technique Using Discrete Wavelet Transform for Image Classification.” In *2007 5th Student Conference on Research and Development*, 1–4. https://doi.org/10.1109/SCORED.2007.4451366.
Gibb, Spencer, Hung Manh La, Tuan Le, Luan Nguyen, Ryan Schmid, and Huy Pham. 2018. “Nondestructive Evaluation Sensor Fusion with Autonomous Robotic System for Civil Infrastructure Inspection.” *Journal of Field Robotics* 35 (6): 988–1004. https://doi.org/10.1002/rob.21791.
Glaessgen, Edward, and David Stargel. n.d. “The Digital Twin Paradigm for Future NASA and U.S. Air Force Vehicles.” In *53rd AIAA/ASME/ASCE/AHS/ASC Structures, Structural Dynamics and Materials Conference*. American Institute of Aeronautics and Astronautics. Accessed January 24, 2018. https://doi.org/10.2514/6.2012-1818.
Golewski, G. L., P. Golewski, and T. Sadowski. 2012. “Numerical Modelling Crack Propagation under Mode II Fracture in Plain Concretes Containing Siliceous Fly-

Ash Additive Using XFEM Method." *Computational Materials Science* 62 (September): 75–78. https://doi.org/10.1016/j.commatsci.2012.05.009.
Griffith, Alan Arnold, and Geoffrey Ingram Taylor. 1921. "VI. The Phenomena of Rupture and Flow in Solids." *Philosophical Transactions of the Royal Society of London. Series A, Containing Papers of a Mathematical or Physical Character* 221 (582–593): 163–98. https://doi.org/10.1098/rsta.1921.0006.
Grogan, D. M., C. M. Ó Brádaigh, and S. B. Leen. 2015. "A Combined XFEM and Cohesive Zone Model for Composite Laminate Microcracking and Permeability." *Composite Structures* 120 (February): 246–61. https://doi.org/10.1016/j.compstruct.2014.09.068.
Gucunski, Nenad, Basily Basily, Jinyoung Kim, Jingang Yi, Trung Duong, Kien Dinh, Seong-Hoon Kee, and Ali Maher. 2017. "RABIT: Implementation, Performance Validation and Integration with Other Robotic Platforms for Improved Management of Bridge Decks." *International Journal of Intelligent Robotics and Applications* 1 (3): 271–86. https://doi.org/10.1007/s41315-017-0027-5.
Gucunski, Nenad, Arezoo Imani, Francisco Romero, Soheil Nazarian, Deren Yuan, Herbert Wiggenhauser, Parisa Shokouhi, et al. 2012. *Nondestructive Testing to Identify Concrete Bridge Deck Deterioration*. Washington, D.C.: Transportation Research Board. https://doi.org/10.17226/22771.
Gucunski, Nenad, Francisco Romero, Sabine Kruschwitz, Ruediger Feldmann, and Hooman Parvardeh. 2011. "Comprehensive Bridge Deck Deterioration Mapping of Nine Bridges by Nondestructive Evaluation Technologies," January. https://trid.trb.org/view/1147508.
Gudmundson, P. 1982. "Eigenfrequency Changes of Structures Due to Cracks, Notches or Other Geometrical Changes." *Journal of the Mechanics and Physics of Solids* 30 (5): 339–53. https://doi.org/10.1016/0022-5096(82)90004-7.
Habib, Carol, Abdallah Makhoul, Rony Darazi, and Christian Salim. 2016. "Self-Adaptive Data Collection and Fusion for Health Monitoring Based on Body Sensor Networks." *IEEE Transactions on Industrial Informatics* 12 (6): 2342–52. https://doi.org/10.1109/TII.2016.2575800.
Haghighat, M., M. Abdel-Mottaleb, and W. Alhalabi. 2016. "Discriminant Correlation Analysis: Real-Time Feature Level Fusion for Multimodal Biometric Recognition." *IEEE Transactions on Information Forensics and Security* 11 (9): 1984–96. https://doi.org/10.1109/TIFS.2016.2569061.
Hall, D. L., and J. Llinas. 1997. "An Introduction to Multisensor Data Fusion." *Proceedings of the IEEE* 85 (1): 6–23. https://doi.org/10.1109/5.554205.
Hall, David Lee, and Sonya A. H. McMullen. 2004. *Mathematical Techniques in Multisensor Data Fusion*. Artech House.
Hall, David, and James Llinas. 2001. *Multisensor Data Fusion*. CRC press.
Hamilton, James Douglas. 1994. *Time Series Analysis*. Princeton University Press.
Hannan, E. J., and B. G. Quinn. 1979. "The Determination of the Order of an Autoregression." *Journal of the Royal Statistical Society. Series B (Methodological)* 41 (2): 190–95.

He, Xu-hui, Zhi-wu Yu, and Zheng-qing Chen. 2008. “Finite Element Model Updating of Existing Steel Bridge Based on Structural Health Monitoring.” *Journal of Central South University of Technology* 15 (3): 399–403. https://doi.org/10.1007/s11771-008-0075-y.

Heideklang, Rene, and Parisa Shokouhi. 2013. “Application of Data Fusion in Nondestructive Testing (NDT).” In *Proceedings of the 16th International Conference on Information Fusion, FUSION 2013,* 835–41. https://pennstate.pure.elsevier.com/en/publications/application-of-data-fusion-in-nondestructive-testing-ndt.

Helfrick, Mark, Christopher Niezrecki, Peter Avitabile, and Timothy Schmidt. 2011. “3D Digital Image Correlation Methods for Full-Field Vibration Measurement.” *Mechanical Systems and Signal Processing* 25 (April): 917–27. https://doi.org/10.1016/j.ymssp.2010.08.013.

Hellier, Charles. 2001. *Handbook of Nondestructive Evaluation*. McGraw-Hill.

Hinton, Geoffrey E., Simon Osindero, and Yee-Whye Teh. 2006. “A Fast Learning Algorithm for Deep Belief Nets.” *Neural Computation* 18 (7): 1527–54. https://doi.org/10.1162/neco.2006.18.7.1527.

Hoffmann, C. M. 1989. “The Problems of Accuracy and Robustness in Geometric Computation.” *Computer* 22 (3): 31–39. https://doi.org/10.1109/2.16223.

Hong, H. P. 1999. “Application of the Stochastic Process to Pitting Corrosion.” *Corrosion; Houston* 55 (1): 10.

Hou, Jilin, Łukasz Jankowski, and Jinping Ou. 2015. “Frequency-Domain Substructure Isolation for Local Damage Identification.” *Advances in Structural Engineering* 18 (1): 137–53. https://doi.org/10.1260/1369-4332.18.1.137.

Hsiao, Chiamen, Chia-Chi Cheng, Tzunghao Liou, and Yuanting Juang. 2008. “Detecting Flaws in Concrete Blocks Using the Impact-Echo Method.” *NDT and E International* 41 (2): 98–107. https://doi.org/10.1016/j.ndteint.2007.08.008.

Huang, Jianping, Wanyu Liu, and Xiaoming Sun. 2014. “A Pavement Crack Detection Method Combining 2D with 3D Information Based on Dempster-Shafer Theory.” *Computer-Aided Civil and Infrastructure Engineering* 29 (4): 299–313. https://doi.org/10.1111/mice.12041.

Irani, S., M. Mehri, and Z. Seifollahi. 2014. “CRACK GROWTH XFEM ANALYSIS USING PARALLEL PROCESSING AND OPTIMUM NUMERICAL METHODS.” Undefined. 2014. /paper/CRACK-GROWTH-XFEM-ANALYSIS-USING-PARALLEL-AND-Irani-Mehri/c9ef3c90e382bab079e91afb4e0d10360c81c4bd.

Irwin, G. R. 1957. “ANALYSIS OF STRESS AND STRAINS NEAR THE END OF A CRACK TRAVERSING A PLATE.” Undefined. 1957. /paper/ANALYSIS-OF-STRESS-AND-STRAINS-NEAR-THE-END-OF-A-A-Irwin/efe3290a3a750547e71269ea328d66ea8cb8e525.

Jafari, Bahman, Ali Khaloo, and David Lattanzi. 2016. “Long-Term Monitoring of Structures through Point Cloud Analysis.” In , 9805:98052K-98052K – 8. https://doi.org/10.1117/12.2217586.

Jahanshahi, Mohammad R., Jonathan S. Kelly, Sami F. Masri, and Gaurav S. Sukhatme. 2009. “A Survey and Evaluation of Promising Approaches for Automatic Image-Based Defect Detection of Bridge Structures.” *Structure and Infrastructure Engineering* 5 (6): 455–86. https://doi.org/10.1080/15732470801945930.

Jahanshahi, Mohammad R., and Sami F. Masri. 2012. “Adaptive Vision-Based Crack Detection Using 3D Scene Reconstruction for Condition Assessment of Structures.” *Automation in Construction* 22 (March): 567–76. https://doi.org/10.1016/j.autcon.2011.11.018.

Jahanshahi, Mohammad R., Sami F. Masri, Curtis W. Padgett, and Gaurav S. Sukhatme. 2013. “An Innovative Methodology for Detection and Quantification of Cracks through Incorporation of Depth Perception.” *Machine Vision and Applications* 24 (2): 227–41. https://doi.org/10.1007/s00138-011-0394-0.

Jain, Akash, Ankit Kathuria, Adarsh Kumar, Yogesh Verma, and Krishna Murari. 2013. “Combined Use of Non-Destructive Tests for Assessment of Strength of Concrete in Structure.” *Procedia Engineering*, The 2nd International Conference on Rehabilitation and Maintenance in Civil Engineering (ICRMCE), 54 (January): 241–51. https://doi.org/10.1016/j.proeng.2013.03.022.

Jiang, Shao-Fei, Chun-Ming Zhang, and Shuai Zhang. 2011. “Two-Stage Structural Damage Detection Using Fuzzy Neural Networks and Data Fusion Techniques.” *Expert Systems with Applications* 38 (1): 511–19. https://doi.org/10.1016/j.eswa.2010.06.093.

Jones, R., and D. Peng. 2002. “A Simple Method for Computing the Stress Intensity Factors for Cracks at Notches.” *Engineering Failure Analysis* 9 (6): 683–702. https://doi.org/10.1016/S1350-6307(02)00007-9.

KABE, A. M. 1985. “Stiffness Matrix Adjustment Using Mode Data.” *AIAA Journal* 23 (9): 1431–36. https://doi.org/10.2514/3.9103.

Kalogerakis, Evangelos, Melinos Averkiou, Subhransu Maji, and Siddhartha Chaudhuri. 2017. “3D Shape Segmentation With Projective Convolutional Networks.” In , 3779–88. http://openaccess.thecvf.com/content_cvpr_2017/html/Kalogerakis_3D_Shape_Segmentation_CVPR_2017_paper.html.

Kaseko Mohamed S., Lo Zhen-Ping, and Ritchie Stephen G. 1994. “Comparison of Traditional and Neural Classifiers for Pavement-Crack Detection.” *Journal of Transportation Engineering* 120 (4): 552–69. https://doi.org/10.1061/(ASCE)0733-947X(1994)120:4(552).

Kazhdan, Michael, and Hugues Hoppe. 2013. “Screened Poisson Surface Reconstruction.” *ACM Trans. Graph.* 32 (3): 29:1-29:13. https://doi.org/10.1145/2487228.2487237.

Khaloo, Ali, and David Lattanzi. 2019. “Automatic Detection of Structural Deficiencies Using 4D Hue-Assisted Analysis of Color Point Clouds.” In *Dynamics of Civil Structures, Volume 2*, edited by Shamim Pakzad, 197–205. Conference Proceedings of the Society for Experimental Mechanics Series. Springer International Publishing.

Khan, Md Nazmuzzaman, and Sohel Anwar. 2019. “Time-Domain Data Fusion Using Weighted Evidence and Dempster–Shafer Combination Rule: Application in Object Classification.” *Sensors* 19 (23): 5187. https://doi.org/10.3390/s19235187.

Khatam, Hamed, Ali Akbar Golafshani, S. B. Beheshti-Aval, and Mohammad Noori. 2007. “Harmonic Class Loading for Damage Identification in Beams Using Wavelet Analysis.” *Structural Health Monitoring* 6 (1): 67–80. https://doi.org/10.1177/1475921707072064.

Khoei, A. R., M. Eghbalian, H. Moslemi, and H. Azadi. 2013. “Crack Growth Modeling via 3D Automatic Adaptive Mesh Refinement Based on Modified-SPR Technique.” *Applied Mathematical Modelling* 37 (1): 357–83. https://doi.org/10.1016/j.apm.2012.02.040.

Kisa, Murat, and Brandon JA. 2000. “The Effects of Closure of Cracks on the Dynamics of a Cracked Cantilever Beam.” *Journal of Sound and Vibration* 238 (November): 1–18. https://doi.org/10.1006/jsvi.2000.3099.

Kittler, J. 1975. “Mathematical Methods of Feature Selection in Pattern Recognition.” *International Journal of Man-Machine Studies*.

Klein, Lawrence A. 1999. *Sensor and Data Fusion Concepts and Applications*. SPIE.

Kleinberg, Jon M. 1997. “Two Algorithms for Nearest-Neighbor Search in High Dimensions.” In *Proceedings of the Twenty-Ninth Annual ACM Symposium on Theory of Computing - STOC ’97*, 599–608. El Paso, Texas, United States: ACM Press. https://doi.org/10.1145/258533.258653.

Klikowicz, Piotr, Marek Salamak, and Grzegorz Poprawa. 2016. “Structural Health Monitoring of Urban Structures.” *Procedia Engineering* 161: 958–62. https://doi.org/10.1016/j.proeng.2016.08.833.

Kotsiantis, S. B., I. D. Zaharakis, and P. E. Pintelas. 2006. “Machine Learning: A Review of Classification and Combining Techniques.” *Artificial Intelligence Review* 26 (3): 159–90. https://doi.org/10.1007/s10462-007-9052-3.

Kralovec, Christoph, and Martin Schagerl. 2020. “Review of Structural Health Monitoring Methods Regarding a Multi-Sensor Approach for Damage Assessment of Metal and Composite Structures.” *Sensors* 20 (3): 826. https://doi.org/10.3390/s20030826.

Kuang, J. H., and C. K. Chen. 2000. “Use of Strip Yield Approach for Multiple-Site Damage Failure Scenarios.” *Journal of Aircraft* 37 (5): 887–91. https://doi.org/10.2514/2.2686.

La, Hung M., Nenad Gucunski, Kristin Dana, and Seong-Hoon Kee. 2017. “Development of an Autonomous Bridge Deck Inspection Robotic System.” *Journal of Field Robotics* 34 (8): 1489–1504. https://doi.org/10.1002/rob.21725.

Lara, Paul A., Hugh A. Bruck, and Felix J. Fillafer. 2020. “Experimental Measurements of Overload and Underloads on Fatigue Crack Growth Using Digital Image Correlation.” In *Challenges in Mechanics of Time Dependent Materials, Fracture, Fatigue, Failure and Damage Evolution, Volume 2*, edited by Meredith Silberstein, Alireza Amirkhizi, Xia Shuman, Allison Beese, Ryan B. Berke, and Garrett Pataky, 29–40. Conference Proceedings of the Society for Experimental

Mechanics Series. Cham: Springer International Publishing. https://doi.org/10.1007/978-3-030-29986-6_5.
Lee, Sam (Kwok Lun), and David Martin. 2016. “Application of XFEM to Model Stationary Crack and Crack Propagation for Pressure Containing Subsea Equipment.” In . American Society of Mechanical Engineers Digital Collection. https://doi.org/10.1115/PVP2016-63199.
Legat, A. 2007. “Monitoring of Steel Corrosion in Concrete by Electrode Arrays and Electrical Resistance Probes.” *Electrochimica Acta*, ELECTROCHEMICAL METHODS IN CORROSION RESEARCH Selection of papers from the 9th International Symposium (EMCR 2006) 18-23 June 2006, Dourdan, France, 52 (27): 7590–98. https://doi.org/10.1016/j.electacta.2007.06.060.
Legat, A, M Leban, and Ž Bajt. 2004. “Corrosion Processes of Steel in Concrete Characterized by Means of Electrochemical Noise.” *Electrochimica Acta*, Electrochemical Methods in Corrosion Research, 49 (17): 2741–51. https://doi.org/10.1016/j.electacta.2004.01.036.
Lesiuk, Grzegorz, Michał Smolnicki, Dariusz Rozumek, Halyna Krechkovska, Oleksandra Student, José Correia, Rafał Mech, and Abílio De Jesus. 2020. “Study of the Fatigue Crack Growth in Long-Term Operated Mild Steel under Mixed-Mode (I + II, I + III) Loading Conditions.” *Materials* 13 (1). https://doi.org/10.3390/ma13010160.
Liu, Z., K. Tsukada, K. Hanasaki, and M. Kurisu. 1999. “Two-Dimensional Eddy Current Signal Enhancement via Multifrequency Data Fusion.” *Research in Nondestructive Evaluation* 11 (3): 165–77. https://doi.org/10.1007/PL00003919.
Lu, Y., and J. E. Michaels. 2009. “Feature Extraction and Sensor Fusion for Ultrasonic Structural Health Monitoring Under Changing Environmental Conditions.” *IEEE Sensors Journal* 9 (11): 1462–71. https://doi.org/10.1109/JSEN.2009.2019339.
Luk, Bing L, Z D Jiang, Louis K P Liu, and F Tong. 2008. “Impact Acoustic Non-Destructive Evaluation in Noisy Environment Based on Wavelet Packet Decomposition.” *Hong Kong*, 4.
Lütkepohl, Helmut. 2005. *New Introduction to Multiple Time Series Analysis*. Berlin: New York : Springer.
Luts, Jan, Geert Molenberghs, Geert Verbeke, Sabine Van Huffel, and Johan A. K. Suykens. 2012. “A Mixed Effects Least Squares Support Vector Machine Model for Classification of Longitudinal Data.” *Computational Statistics and Data Analysis* 56 (3): 611–28. https://doi.org/10.1016/j.csda.2011.09.008.
Mach, Katharine J., Drew V. Nelson, and Mark W. Denny. 2007. “Techniques for Predicting the Lifetimes of Wave-Swept Macroalgae: A Primer on Fracture Mechanics and Crack Growth.” *Journal of Experimental Biology* 210 (13): 2213–30. https://doi.org/10.1242/jeb.001560.
Mallat, S.G. 1989. “A Theory for Multiresolution Signal Decomposition: The Wavelet Representation.” *IEEE Transactions on Pattern Analysis and Machine Intelligence* 11 (7): 674–93. https://doi.org/10.1109/34.192463.
Mallat, Stéphane. 2009. *A Wavelet Tour of Signal Processing: The Sparse Way*. Vol. xx.

Martino, Nicole, Ralf Birken, Kenneth Maser, and Ming Wang. 2014. “Developing a Deterioration Threshold Model for the Assessment of Concrete Bridge Decks Using Ground Penetrating Radar.” In . https://trid.trb.org/view/1289060.

McCann, D. M, and M. C Forde. 2001. “Review of NDT Methods in the Assessment of Concrete and Masonry Structures.” *NDT & E International* 34 (2): 71–84. https://doi.org/10.1016/S0963-8695(00)00032-3.

McCormick, Nick, and Jerry Lord. 2010. “Digital Image Correlation.” *Materials Today* 13 (12): 52–54. https://doi.org/10.1016/S1369-7021(10)70235-2.

McDowall, David. 1980. *Interrupted Time Series Analysis*. SAGE.

Meng, Dewei, Shibin Lin, and Hoda Azari. 2020. “Nondestructive Corrosion Evaluation of Reinforced Concrete Bridge Decks with Overlays: An Experimental Study.” *Journal of Testing and Evaluation* 48 (1): 20180388. https://doi.org/10.1520/JTE20180388.

Mi, Bao, Jennifer E. Michaels, and Thomas E. Michaels. 2006. “An Ultrasonic Method for Dynamic Monitoring of Fatigue Crack Initiation and Growth.” *The Journal of the Acoustical Society of America* 119 (1): 74–85. https://doi.org/10.1121/1.2139647.

Modak, S. V., T. K. Kundra, and B. C. Nakra. 2002. “Comparative Study of Model Updating Methods Using Simulated Experimental Data.” *Computers & Structures* 80 (5): 437–47. https://doi.org/10.1016/S0045-7949(02)00017-2.

Mohamadi, Sara, and David Lattanzi. 2019. “Life-Cycle Modeling of Structural Defects via Computational Geometry and Time-Series Forecasting.” *Sensors* 19 (20): 4571. https://doi.org/10.3390/s19204571.

Mohamadi, Sara, David Lattanzi, and Hoda Azari. 2020. “Fusion and Visualization of Bridge Deck Nondestructive Evaluation Data via Machine Learning.” *Frontiers in Materials* 7. https://doi.org/10.3389/fmats.2020.576918.

Moreland, Kenneth. 2009. “Diverging Color Maps for Scientific Visualization.” In *Advances in Visual Computing*, edited by George Bebis, Richard Boyle, Bahram Parvin, Darko Koracin, Yoshinori Kuno, Junxian Wang, Renato Pajarola, et al., 92–103. Lecture Notes in Computer Science. Berlin, Heidelberg: Springer. https://doi.org/10.1007/978-3-642-10520-3_9.

Moreto, J., Fernando Júnior, Carla Maciel, Luís Bonazzi, José Júnior, Cassius Ruchert, and Waldek Filho. 2015. “Environmentally-Assisted Fatigue Crack Growth in AA7050-T73511 al Alloy and AA2050-T84 Al-Cu-Li Alloy.” *Materials Research* 18 (November). https://doi.org/10.1590/1516-1439.018915.

Mosalam, Khalid M., and Glaucio H. Paulino. 1997. “Evolutionary Characteristic Length Method for Smeared Cracking Finite Element Models.” *Finite Elements in Analysis and Design* 27 (1): 99–108. https://doi.org/10.1016/S0168-874X(97)00007-3.

Mottershead, J. E., and M. I. Friswell. 1993. “Model Updating In Structural Dynamics: A Survey.” *Journal of Sound and Vibration* 167 (2): 347–75. https://doi.org/10.1006/jsvi.1993.1340.

Myötyri, E., U. Pulkkinen, and K. Simola. 2006. “Application of Stochastic Filtering for Lifetime Prediction.” *Reliability Engineering & System Safety* 91 (2): 200–208. https://doi.org/10.1016/j.ress.2005.01.002.

Najafabadi, Maryam M., Flavio Villanustre, Taghi M. Khoshgoftaar, Naeem Seliya, Randall Wald, and Edin Muharemagic. 2015. “Deep Learning Applications and Challenges in Big Data Analytics.” *Journal of Big Data* 2 (1): 1. https://doi.org/10.1186/s40537-014-0007-7.

Nalepa, Jakub, Michal Kawulok, and Wojciech Dudzik. 2018. “Tuning and Evolving Support Vector Machine Models.” In *Man-Machine Interactions 5*, edited by Aleksandra Gruca, Tadeusz Czachórski, Katarzyna Harezlak, Stanisław Kozielski, and Agnieszka Piotrowska, 418–28. Advances in Intelligent Systems and Computing. Cham: Springer International Publishing. https://doi.org/10.1007/978-3-319-67792-7_41.

Nantasenamat, Chanin, Chartchalerm Isarankura-Na-Ayudhya, Thanakorn Naenna, and Virapong Prachayasittikul. 2009. “A Practical Overview of Quantitative Structure-Activity Relationship.” *EXCLI Journal* 8 (May): 74–88. https://doi.org/10.17877/DE290R-690.

Nassr Amr A. and El-Dakhakhni Wael W. 2009. “Damage Detection of FRP-Strengthened Concrete Structures Using Capacitance Measurements.” *Journal of Composites for Construction* 13 (6): 486–97. https://doi.org/10.1061/(ASCE)CC.1943-5614.0000042.

Nouri Shirazi, M., H. Mollamahmoudi, and S. Seyedpoor. 2014. “Structural Damage Identification Using an Adaptive Multi-Stage Optimization Method Based on a Modified Particle Swarm Algorithm.” *Journal of Optimization Theory and Applications* 160 (3): 1009–19. https://doi.org/10.1007/s10957-013-0316-6.

Ohno, Kentaro, and Masayasu Ohtsu. 2010. “Crack Classification in Concrete Based on Acoustic Emission.” *Construction and Building Materials*, Special Issue on Fracture, Acoustic Emission and NDE in Concrete (KIFA-5), 24 (12): 2339–46. https://doi.org/10.1016/j.conbuildmat.2010.05.004.

Ohtsu, Masayasu, Masakatsu Uchida, Takahisa Okamoto, and Shigenori Yuyama. 2002. “Damage Assessment of Reinforced Concrete Beams Qualified by Acoustic Emission.” *Structural Journal* 99 (4): 411–17. https://doi.org/10.14359/12109.

Olson, David L., and Dursun Delen. 2008. *Advanced Data Mining Techniques*. Springer Science & Business Media.

Ostachowicz, Wiesław M., and Marek Krawczuk. 2001. “On Modelling of Structural Stiffness Loss Due to Damage.” Key Engineering Materials. Trans Tech Publications Ltd. 2001. https://doi.org/10.4028/www.scientific.net/KEM.204-205.185.

Pak, Y. E. 1992. “Linear Electro-Elastic Fracture Mechanics of Piezoelectric Materials.” *International Journal of Fracture* 54 (1): 79–100. https://doi.org/10.1007/BF00040857.

Pal, Nikhil R, and Sankar K Pal. 1993. “A Review on Image Segmentation Techniques.” *Pattern Recognition* 26 (9): 1277–94. https://doi.org/10.1016/0031-3203(93)90135-J.

Pan, Ernian. 1997. “A General Boundary Element Analysis of 2-D Linear Elastic Fracture Mechanics.” *International Journal of Fracture* 88 (1): 41–59. https://doi.org/10.1023/A:1007462319811.

Pankratz, Alan, ed. 1983. *Forecasting with Univariate Box-Jenkins Models*. Wiley Series in Probability and Statistics. Hoboken, NJ, USA: John Wiley & Sons, Inc. https://doi.org/10.1002/9780470316566.

Paris, P., and F. Erdogan. 1963. “A Critical Analysis of Crack Propagation Laws.” *Journal of Basic Engineering* 85 (4): 528–33. https://doi.org/10.1115/1.3656900.

Pauly, Mark, Richard Keiser, and Markus Gross. 2003. “Multi-Scale Feature Extraction on Point-Sampled Surfaces.” *Computer Graphics Forum* 22 (3): 281–89. https://doi.org/10.1111/1467-8659.00675.

Perera, Ricardo, Sheng-En Fang, and C. Huerta. 2009. “Structural Crack Detection without Updated Baseline Model by Single and Multiobjective Optimization.” *Mechanical Systems and Signal Processing* 23 (3): 752–68. https://doi.org/10.1016/j.ymssp.2008.06.010.

Pigeon, Stéphane, Pascal Druyts, and Patrick Verlinde. 2000. “Applying Logistic Regression to the Fusion of the NIST’99 1-Speaker Submissions.” *Digital Signal Processing* 10 (1): 237–48. https://doi.org/10.1006/dspr.1999.0358.

Rabiei, Masoud, and Mohammad Modarres. 2013. “A Recursive Bayesian Framework for Structural Health Management Using Online Monitoring and Periodic Inspections.” *Reliability Engineering & System Safety* 112 (April): 154–64. https://doi.org/10.1016/j.ress.2012.11.020.

Rahulkumar, P., Anand Jagota, S.J. Bennison, and Sunil Saigal. 2000. “Cohesive Element Modeling of Viscoelastic Fracture: Application to Peel Testing of Polymers.” *International Journal of Solids and Structures* 37 (March): 1873–97. https://doi.org/10.1016/S0020-7683(98)00339-4.

Ramos, Luís F., Tiago Miranda, Mayank Mishra, Francisco M. Fernandes, and Elizabeth Manning. 2015. “A Bayesian Approach for NDT Data Fusion: The Saint Torcato Church Case Study.” *Engineering Structures* 84 (February): 120–29. https://doi.org/10.1016/j.engstruct.2014.11.015.

Rangwala, Huzefa, Christopher Kauffman, and George Karypis. 2009. “SvmPRAT: SVM-Based Protein Residue Annotation Toolkit.” *BMC Bioinformatics* 10 (December): 439. https://doi.org/10.1186/1471-2105-10-439.

Reagan, Daniel, Alessandro Sabato, and Christopher Niezrecki. 2017. “Unmanned Aerial Vehicle Acquisition of Three-Dimensional Digital Image Correlation Measurements for Structural Health Monitoring of Bridges.” In *Nondestructive Characterization and Monitoring of Advanced Materials, Aerospace, and Civil Infrastructure 2017*, 10169:1016909. International Society for Optics and Photonics. https://doi.org/10.1117/12.2259985.

Ren, Wei-Xin, and Guido De Roeck. 2002. “Structural Damage Identification Using Modal Data. II: Test Verification.” *Journal of Structural Engineering* 128 (1): 96–104. https://doi.org/10.1061/(ASCE)0733-9445(2002)128:1(96).

Rens Kevin L. and Greimann Lowell F. 1997. “Ultrasonic Approach for Nondestructive Testing of Civil Infrastructure.” *Journal of Performance of Constructed Facilities* 11 (3): 97–104. https://doi.org/10.1061/(ASCE)0887-3828(1997)11:3(97).

Rice, J. R. 1968. “A Path Independent Integral and the Approximate Analysis of Strain Concentration by Notches and Cracks.” *Journal of Applied Mechanics* 35 (2): 379–86. https://doi.org/10.1115/1.3601206.

Rosenfeld, Azriel. 1969. “Picture Processing by Computer.” *ACM Comput. Surv.* 1 (3): 147–76. https://doi.org/10.1145/356551.356554.

Ruiz, A., and P.E. Lopez-de-Teruel. 2001. “Nonlinear Kernel-Based Statistical Pattern Analysis.” *IEEE Transactions on Neural Networks* 12 (1): 16–32. https://doi.org/10.1109/72.896793.

Ruiz, Gonzalo, Anna Pandolfi, and Michael Ortiz. 2001. “Three-dimensional cohesive modeling of dynamic mixed-mode fracture.” *International Journal for Numerical Methods in Engineering* 52 (1–2): 97–120. https://doi.org/10.1002/nme.273.

Ryan, Thomas W, Raymond A Hartle, United States, Federal Highway Administration, National Highway Institute (U.S.), Michael Baker Jr, and Inc. 2012. *Bridge Inspector’s Reference Manual: BIRM*. Washington, D.C.]; [Arlington, Va.]; [Springfield, VA: U.S. Federal Highway Administration ; National Highway Institute ; [Available through the National Technical Information Service.

Saadat, Soheil, Mohammad N Noori, Gregory D Buckner, Tadatoshi Furukawa, and Yoshiyuki Suzuki. 2004. “Structural Health Monitoring and Damage Detection Using an Intelligent Parameter Varying (IPV) Technique.” *International Journal of Non-Linear Mechanics* 39 (10): 1687–97. https://doi.org/10.1016/j.ijnonlinmec.2004.03.001.

Sagar, R. Vidya, and B. K. Raghu Prasad. 2012. “A Review of Recent Developments in Parametric Based Acoustic Emission Techniques Applied to Concrete Structures.” *Nondestructive Testing and Evaluation* 27 (1): 47–68. https://doi.org/10.1080/10589759.2011.589029.

Sartor Richard R., Culmo Michael P., and DeWolf John T. 1999. “Short-Term Strain Monitoring of Bridge Structures.” *Journal of Bridge Engineering* 4 (3): 157–64. https://doi.org/10.1061/(ASCE)1084-0702(1999)4:3(157).

Schijve, J. 1977. “Four Lectures on Fatigue Crack Growth.” *Delft University of Technology, Department of Aerospace Engineering, Report LR-254*. https://repository.tudelft.nl/islandora/object/uuid%3A704226c6-658f-46b8-8cf4-68eeb56fb45a.

Shanker, M., M. Y. Hu, and M. S. Hung. 1996. “Effect of Data Standardization on Neural Network Training.” *Omega* 24 (4): 385–97. https://doi.org/10.1016/0305-0483(96)00010-2.

Sharma Shruti and Mukherjee Abhijit. 2011. “Monitoring Corrosion in Oxide and Chloride Environments Using Ultrasonic Guided Waves.” *Journal of Materials in Civil Engineering* 23 (2): 207–11. https://doi.org/10.1061/(ASCE)MT.1943-5533.0000144.

Shull, Peter. 2002. *Nondestructive Evaluation: Theory, Techniques, and Applications*. Dekker Mechanical Engineering. CRC Press. https://doi.org/10.1201/9780203911068.

Siegel, Mel, and Priyan Gunatilake. 1998. *Remote Enhanced Visual Inspection of Aircraft by a Mobile Robot*.

Siegmund, T., N.A. Fleck, and A. Needleman. 1997. "Dynamic Crack Growth across an Interface." *International Journal of Fracture* 85 (4): 381–402. https://doi.org/10.1023/A:1007460509387.

Smith, R. A., and K. J. Miller. 1977. "Fatigue Cracks at Notches." *International Journal of Mechanical Sciences* 19 (1): 11–22. https://doi.org/10.1016/0020-7403(77)90011-X.

Smith, Suzanne Weaver, and Christopher A. Beattie. 1991. "Secant-Method Adjustment for Structural Models." *AIAA Journal* 29 (1): 119–26. https://doi.org/10.2514/3.10553.

Sohn, H. (Hoon), C. R. (Charles R.) Farrar, F. M. (François M.) Hemez, and J. J. (Jerry J.) Czarnecki. 2002. "A Review of Structural Health Review of Structural Health Monitoring Literature 1996-2001." Article. Submitted to: Third World Conference on Structural Control, Como, Italy, April 7-12, 2002. January 1, 2002. https://digital.library.unt.edu/ark:/67531/metadc927238/.

Song, Seong Hyeok, Glaucio H. Paulino, and William G. Buttlar. 2006. "Simulation of Crack Propagation in Asphalt Concrete Using an Intrinsic Cohesive Zone Model." *Journal of Engineering Mechanics* 132 (11): 1215–23. https://doi.org/10.1061/(ASCE)0733-9399(2006)132:11(1215).

Song, Seong, Glaucio Paulino, and William Buttlar. 2008. "Influence of the Cohesive Zone Model Shape Parameter on Asphalt Concrete Fracture Behavior." *AIP Conference Proceedings* 973 (February). https://doi.org/10.1063/1.2896872.

Spencer, Billie F., Vedhus Hoskere, and Yasutaka Narazaki. 2019. "Advances in Computer Vision-Based Civil Infrastructure Inspection and Monitoring." *Engineering* 5 (2): 199–222. https://doi.org/10.1016/j.eng.2018.11.030.

Steinberg, Alan N., and Christopher L. Bowman. 2017. "Revisions to the JDL Data Fusion Model." Handbook of Multisensor Data Fusion. January 6, 2017. https://doi.org/10.1201/9781420053098-8.

Su, Hang, Subhransu Maji, Evangelos Kalogerakis, and Erik Learned-Miller. 2015. "Multi-View Convolutional Neural Networks for 3D Shape Recognition." In , 945–53. https://www.cv-foundation.org/openaccess/content_iccv_2015/html/Su_Multi-View_Convolutional_Neural_ICCV_2015_paper.html.

Sukumar, N., and J. -H. Prévost. 2003. "Modeling Quasi-Static Crack Growth with the Extended Finite Element Method Part I: Computer Implementation." *International Journal of Solids and Structures* 40 (26): 7513–37. https://doi.org/10.1016/j.ijsolstr.2003.08.002.

Sun, D., V. C. S. Lee, and Y. Lu. 2016. "An Intelligent Data Fusion Framework for Structural Health Monitoring." In *2016 IEEE 11th Conference on Industrial*

Electronics and Applications (ICIEA), 49–54. https://doi.org/10.1109/ICIEA.2016.7603550.

Tanaka, K., and Y. Akiniwa. 1988. "Resistance-Curve Method for Predicting Propagation Threshold of Short Fatigue Cracks at Notches." *Engineering Fracture Mechanics* 30 (6): 863–76. https://doi.org/10.1016/0013-7944(88)90146-4.

Tarancón, J. E., A. Vercher, E. Giner, and F. J. Fuenmayor. 2009. "Enhanced blending elements for XFEM applied to linear elastic fracture mechanics." *International Journal for Numerical Methods in Engineering* 77 (1): 126–48. https://doi.org/10.1002/nme.2402.

Teughels, Anne, and Guido De Roeck. 2005. "Damage Detection and Parameter Identification by Finite Element Model Updating." *Archives of Computational Methods in Engineering* 12 (2): 123–64. https://doi.org/10.1007/BF03044517.

Tsao Stephen, Kehtarnavaz Nasser, Chan Paul, and Lytton Robert. 1994. "Image-Based Expert-System Approach to Distress Detection on CRC Pavement." *Journal of Transportation Engineering* 120 (1): 52–64. https://doi.org/10.1061/(ASCE)0733-947X(1994)120:1(52).

Tsiliki, Georgia, and Sophia Kossida. 2011. "Fusion Methodologies for Biomedical Data." *Journal of Proteomics* 74 (12): 2774–85. https://doi.org/10.1016/j.jprot.2011.07.001.

Tuegel, Eric J., Anthony R. Ingraffea, Thomas G. Eason, and S. Michael Spottswood. 2011. "Reengineering Aircraft Structural Life Prediction Using a Digital Twin." Research article. International Journal of Aerospace Engineering. 2011. https://doi.org/10.1155/2011/154798.

Valor, A., F. Caleyo, L. Alfonso, D. Rivas, and J. M. Hallen. 2007. "Stochastic Modeling of Pitting Corrosion: A New Model for Initiation and Growth of Multiple Corrosion Pits." *Corrosion Science* 49 (2): 559–79. https://doi.org/10.1016/j.corsci.2006.05.049.

Vandaele, Walter. 1983. *Applied Time Series and Box-Jenkins Models*. Academic Press.

Vanik M. W., Beck J. L., and Au S. K. 2000. "Bayesian Probabilistic Approach to Structural Health Monitoring." *Journal of Engineering Mechanics* 126 (7): 738–45. https://doi.org/10.1061/(ASCE)0733-9399(2000)126:7(738).

Vapnik, Vladimir. 2000. *The Nature of Statistical Learning Theory*. 2nd ed. Information Science and Statistics. New York: Springer-Verlag. https://doi.org/10.1007/978-1-4757-3264-1.

Verma, Sanjeev Kumar, Sudhir Singh Bhadauria, and Saleem Akhtar. 2013. "Review of Nondestructive Testing Methods for Condition Monitoring of Concrete Structures." Research article. Journal of Construction Engineering. 2013. https://doi.org/10.1155/2013/834572.

Vu, Kim, Mark G. Stewart, and John Mullard. 2005. "Corrosion-Induced Cracking: Experimental Data and Predictive Models." *ACI Structural Journal; Farmington Hills* 102 (5): 719–26.

Wang, Tinghua, Houkuan Huang, Shengfeng Tian, and Jianfeng Xu. 2010. "Feature Selection for SVM via Optimization of Kernel Polarization with Gaussian ARD

Kernels." *Expert Systems with Applications* 37 (9): 6663–68. https://doi.org/10.1016/j.eswa.2010.03.054.
Wang, Weizhuo, John E. Mottershead, Alexander Ihle, Thorsten Siebert, and Hans Reinhard Schubach. 2011. "Finite Element Model Updating from Full-Field Vibration Measurement Using Digital Image Correlation." *Journal of Sound and Vibration* 330 (8): 1599–1620. https://doi.org/10.1016/j.jsv.2010.10.036.
Wang, Ying, Suiyang Khoo, An-jui Li, and Hong Hao. 2013. "FEM Calibrated ARMAX Model Updating Method for Time Domain Damage Identification." *Advances in Structural Engineering* 16 (1): 51–60. https://doi.org/10.1260/1369-4332.16.1.51.
Wu, Huadong. 2004. "Sensor Data Fusion for Context -Aware Computing Using Dempster -Shafer Theory." Ph.D., United States -- Pennsylvania: Carnegie Mellon University. http://search.proquest.com/docview/305207449/abstract/D39940116B7F47EEPQ/1.
Wu, Rih-Teng, and Mohammad Reza Jahanshahi. 2018. "Data Fusion Approaches for Structural Health Monitoring and System Identification: Past, Present, and Future." *Structural Health Monitoring*, September, 1475921718798769. https://doi.org/10.1177/1475921718798769.
Yan, Xiangqiao. 2007. "Automated Simulation of Fatigue Crack Propagation for Two-Dimensional Linear Elastic Fracture Mechanics Problems by Boundary Element Method." *Engineering Fracture Mechanics* 74 (14): 2225–46. https://doi.org/10.1016/j.engfracmech.2006.10.020.
Yan, Yujie, Burcu Guldur, and Jerome F. Hajjar. 2017. "Automated Structural Modelling of Bridges from Laser Scanning," April, 457–68. https://doi.org/10.1061/9780784480403.039.
Yao, Ruigen, and Shamim N. Pakzad. 2012. "Autoregressive Statistical Pattern Recognition Algorithms for Damage Detection in Civil Structures." *Mechanical Systems and Signal Processing* 31 (August): 355–68. https://doi.org/10.1016/j.ymssp.2012.02.014.
Yeh, Po-Liang, and Pei-Ling Liu. 2008. "Application of the Wavelet Transform and the Enhanced Fourier Spectrum in the Impact Echo Test." *NDT & E International* 41 (5): 382–94. https://doi.org/10.1016/j.ndteint.2008.01.002.
Yoneyama, S., A. Kitagawa, S. Iwata, K. Tani, and H. Kikuta. 2007. "Bridge Deflection Measurement Using Digital Image Correlation." *Experimental Techniques* 31 (1): 34–40. https://doi.org/10.1111/j.1747-1567.2006.00132.x.
Yoon Dong-Jin, Weiss W. Jason, and Shah Surendra P. 2000. "Assessing Damage in Corroded Reinforced Concrete Using Acoustic Emission." *Journal of Engineering Mechanics* 126 (3): 273–83. https://doi.org/10.1061/(ASCE)0733-9399(2000)126:3(273).
Yuan, Yingshu, Yongsheng Ji, and Surendra P. Shah. 2007. "Comparison of Two Accelerated Corrosion Techniques for Concrete Structures." *ACI Structural Journal; Farmington Hills* 104 (3): 344–47.
Zaki, Ahmad, Hwa Kian Chai, Dimitrios G. Aggelis, and Ninel Alver. 2015. "Non-Destructive Evaluation for Corrosion Monitoring in Concrete: A Review and

Capability of Acoustic Emission Technique." *Sensors* 15 (8): 19069–101. https://doi.org/10.3390/s150819069.
Zhang, Allen, Kelvin C. P. Wang, Baoxian Li, Enhui Yang, Xianxing Dai, Yi Peng, Yue Fei, Yang Liu, Joshua Q. Li, and Cheng Chen. 2017. "Automated Pixel-Level Pavement Crack Detection on 3D Asphalt Surfaces Using a Deep-Learning Network." *Computer-Aided Civil and Infrastructure Engineering* 32 (10): 805–19. https://doi.org/10.1111/mice.12297.
Zhang, G. Peter. 2003. "Time Series Forecasting Using a Hybrid ARIMA and Neural Network Model." *Neurocomputing* 50 (January): 159–75. https://doi.org/10.1016/S0925-2312(01)00702-0.
Zhang, Guicai, Changle Li, Haitao Zhou, and Timothy Wagner. 2018. "Punching Process Monitoring Using Wavelet Transform Based Feature Extraction and Semi-Supervised Clustering." *Procedia Manufacturing* 26: 1204–12. https://doi.org/10.1016/j.promfg.2018.07.156.
Zhang, Jing-Kui, Weizhong Yan, and De-Mi Cui. 2016. "Concrete Condition Assessment Using Impact-Echo Method and Extreme Learning Machines." *Sensors* 16 (4): 447. https://doi.org/10.3390/s16040447.
Zhang, Q. W., C. C. Chang, and T. Y. P. Chang. 2000. "Finite Element Model Updating for Structures with Parametric Constraints." *Earthquake Engineering & Structural Dynamics* 29 (7): 927–44. https://doi.org/10.1002/1096-9845(200007)29:7<927::AID-EQE955>3.0.CO;2-4.
Zhang, Shilei, Shaofeng Chen, Huanding Wang, Wei Wang, and Zaixian Chen. 2013. "Model Updating with a Neural Network Method Based on Uniform Design." *Advances in Structural Engineering* 16 (7): 1207–21. https://doi.org/10.1260/1369-4332.16.7.1207.
Zhang, Xuebing, Enhedelihai Nilot, Xuan Feng, Qianci Ren, and Zhijia Zhang. 2018. "IMF-Slices for GPR Data Processing Using Variational Mode Decomposition Method." *Remote Sensing* 10 (3): 476. https://doi.org/10.3390/rs10030476.
Zhang, Zhengyou. 1994. "Iterative Point Matching for Registration of Free-Form Curves and Surfaces." *International Journal of Computer Vision* 13 (2): 119–52. https://doi.org/10.1007/BF01427149.
Zhou, Bing Hai, and Zi Qing Zhai. 2010. "Lifetime Distribution Model of Port Facilities with Pitting Corrosion of Stochastic Processes." *Applied Mechanics and Materials; Zurich* 44–47 (December): 46. http://dx.doi.org.mutex.gmu.edu/10.4028/www.scientific.net/AMM.44-47.46.
Zhou, Qifeng, Hao Zhou, Qingqing Zhou, Fan Yang, Linkai Luo, and Tao Li. 2015. "Structural Damage Detection Based on Posteriori Probability Support Vector Machine and Dempster-Shafer Evidence Theory." *Appl. Soft Comput.* 36 (C): 368–74. https://doi.org/10.1016/j.asoc.2015.06.057.
Zhou, Xiao-Ping, Jun-Wei Chen, and Filippo Berto. 2020. "XFEM Based Node Scheme for the Frictional Contact Crack Problem." *Computers & Structures* 231 (April): 106221. https://doi.org/10.1016/j.compstruc.2020.106221.

BIOGRAPHY

Sara Mohamadi graduated from Fairfax High School, Fairfax, Virginia, in 1983. She received her Bachelor of Arts from George Mason University in 1987. She was employed as a teacher in Fairfax County for two years and received her Master of Arts in English from George Mason University in 1987.